FUNCTIONAL AND BIOCHEMICAL CHARACTERIZATION OF ZIP4 EXTRACELLULAR DOMAIN – IMPLICATIONS ON ACRODERMATITIS ENTEROPATHICA, A LIFE-THREATENING GENETIC DISORDER

By

Eziz Kuliyev

A DISSERTATION

Submitted to
Michigan State University
in partial fulfillment of the requirements
for the degree of

Chemistry – Doctor of Philosophy

2020

ABSTRACT

FUNCTIONAL AND BIOCHEMICAL CHARACTERIZATION OF ZIP4 EXTRACELLULAR DOMAIN – IMPLICATIONS ON ACRODERMATITIS ENTEROPATHICA, A LIFE-THREATENING GENETIC DISORDER

By

Eziz Kuliyev

Zinc is essential for any living organism and the second most abundant transition metal element in human after iron. Zinc is thought to bind nearly 3000 human proteins. Neither excessive zinc nor zinc deficiency is good for human health, and therefore zinc homeostasis must be regulated in delicate balance. The Zrt-/Irt- like protein (ZIP) family is responsible for zinc influx from either extracellular space or intracellular vesicles into the cytoplasm.

Dietary food is the primary zinc supply for humans. ZIP4 is highly expressed on apical surface of gastrointestinal tract, responsible for zinc uptake from diet. ZIP4 is a transporter with a large extracellular domain (ECD). Apo form pZIP4-ECD from *Pteropus Alecto* (black fruit bat) crystal structure revealed homodimerization and two subdomains. Previous studies have shown ZIP4-ECD is crucial for optimal zinc uptake. However, underlying mechanism has not been clarified. We examined zinc binding to the isolated pZIP4–ECD using a zinc competing fluorescent dye FluoZin-1, and then located the primary zinc-binding sites with a low micromolar affinity within a histidine-rich loop ubiquitously present in ZIP4 proteins through mutagenesis. Zinc binding to this protease-susceptible loop induces local conformational change, whereas global structure remains unchanged. Mutagenesis and functional study on human ZIP4 by using a cell-based zinc uptake assay indicated that the histidine residues within this loop are not involved in preselection of metal substrate but play a role in promoting zinc transport. The results allowed us to propose the roles of the histidine-rich loop in an efficient zinc uptake.

Missense mutations of ZIP4 lead to a life-threatening genetic disorder, Acrodermatitis enteropathica (AE), which causes severe zinc deficiency. Seven out of the reported fifteen mutations are located within ZIP4-ECD, but the impacts of these mutations on protein structure and function have not been systematically studied. Here we characterized these AE-causing mutant variants individually both *in vivo* and *in vitro*. Immunostaining, functional assay and biophysical studies suggest that AE is likely to be a protein misfolding disease. Due to defects in protein trafficking, the mutant proteins seem to be retained in the ER and cannot be presented at cell surface, which explains total loss of zinc uptake activity. Mutagenesis and biophysical study on pZIP4-ECD by using circular dichroism revealed secondary structure changes and/or reduction in thermal stability caused by these mutations. Overall, this work revealed the molecular basis of ZIP4 dysfunction in AE-carrying patients and is deemed to be helpful for better therapeutics.

This thesis is dedicated to my mom, dad, sister, fiancée. Thank you for always being my driving force.

ACKNOWLEDGMENTS

Foremost, I want to thank Dr. Jian Hu for his unconditional support morally, financially and as an academician in my graduate student life during these past five years. Dr. Hu is an outstanding scientist himself and what I admire the most is his perspective about digesting any sort of scientific problems and addressing them with very clever ways of experimental set ups, those left me amazed at times. I always look up to him as an exemplary mentor of highest level and try molding myself to become a professional scientist. I have no doubt that I'll be following how his research story unfolds even long after my graduation just because it has become integral part of my scientific curiosity. I cannot thank Dr. Hu enough for picking up my gloomy moods when I thought I had "bad" results and humbling me during my ups. I feel very privileged and honored to be the first graduate student under his mentorship and I will be looking forward to our future scientific dialogues.

I want to thank Dr. Tuo Zhang for teaching me first ropes of laboratory techniques those become fundamental basis of my research. Dr. Zhang was an incredibly productive postdoc and was able to juggle multiple projects simultaneously. He was an exemplary character for everyone in the lab with his hard-working ethics. I want to thank him for laying good basis for my research before I joined the Hu's lab and collaborating with me to achieve first goal of my thesis project.

I want to thank Mr. Dexin Sui for passing his life-long experienced wisdom in scientific aspect. Mr. Sui has been working at our Biochemistry and Molecular Biology department as a research technician since even before I was born. He is the man whom everybody goes to when

they have any kind of issues in their research projects just because he is that skilled. I feel very lucky to have him by my side during my entire grad school and I want to thank him for his unreserved contribution for my thesis projects.

I want to thank Dr. Chi Zhang for her contribution in second part of my thesis project. Chi is a mother to a baby daughter and very hard-working professionally resilient postdoc herself. I remember her picking me up at 6 a.m. morning for our microscopy facility bookings just because she would not want me to wait for a bus in snowy Michigan winter. I can't thank Chi enough for her benevolence and bottom of my heart I wish her the best whatever she decides to pursue in the next stage of her life.

I want to thank my mom and dad for their unwavering support and bearing my absence past six years since last time I visited home. I am thankful for having such amazing parents and for their understanding that I could not visit them for many sorts of reasons. I am thankful for having my sister, brother-in-law, niece and nephews close by in Ohio and not making me feel like a stranger in a foreigner country. I want to thank my fiancée for her moral support, and I am very excited about our future in the next chapter of my life.

Last but not least, I would like to thank my friends Debarshi, Saeedeh, Daniel and all others who I had acquaintance with at MSU community. At MSU, I have met all sorts of people with those each had their unique success story. For me MSU is institution of collective people with great ambitions and I feel very honored and privileged to be receiving doctorate degree from such an amazing academic establishment.

TABLE OF CONTENTS

LIST OF TABLES

LIST OF FIGURES

KEY TO ABBREVIATIONS

AE	Acrodermatitis enteropathica
Bb	*Bordetella bronchiseptica*
BMC	Binuclear metal center
CD	Circular Dichroism
CDF	Cation diffusion facilitator
CLSM	Confocal laser scanning microscope
CTD	C-terminal domain
DMEM	Dulbecco's modified eagle medium
DPBS	Dulbecco's phosphate buffered saline
ECD	Extracellular domain
ER	Endoplasmic reticulum
ESI	Electrospray ionization
ESI-TOF-MS	Time-of-flight mass spectrometer using electrospray ionization
FcεRI	Fc epsilon receptor I
His	Histidine
HRD	Helix-rich domain
hZIP4	Human ZIP4
Irt	Iron-regulated transporter
LOF	Loss-of-function
MRE	Metal-responsive element
MT	Metallothionine

MTF	MRE-binding transcription factor
PCD	PAL-motif containing domain
pZIP4	*Pteropus Alecto* ZIP4
SCD-EDS	Spondylocheiro dysplastic Ehlers–Danlos syndrome
SLC	Solute Carrier
SNP	Single-nucleotide polymorphism
TGN	*trans*-Golgi network
TLR	Toll-like receptor
TM	Transmembrane helix
TMD	Transmembrane domain
TNZD	Transient neonatal zinc deficiency
WHO	World Health Organization
ZIP	Zrt- and Irt- like protein
ZnT	Zinc transporter
Zrt	Zinc-regulated transport

CHAPTER 1

INTRODUCTION

1.1. ZINC BIOCHEMISTRY

Some transition metal elements are essential micronutrients for all domains of life those demonstrate diverse and variety of biological functions. For humans, transition metal ions manifest their importance from the very origin of life, during early embryosis and carry on their vital roles in human respiratory, immune, growth and digestive systems throughout lifetime of humankind. According to World Health Organization (WHO) iron, zinc, copper, cobalt, manganese, and molybdenum have been classified as essential transition metal elements for human health (Nutrition and Organization, 1973). Deficiency of any of these transition metal elements manifest numerous diseases as apparent combination of biological multisystem malfunction, whereas excess uptake of these trace elements having toxic effects on human health. Prescribed adequate amounts of these transition metal ions must be supplied through nutrition during pregnancy, infancy, adolescence and adulthood on daily basis (Bhattacharya et al., 2016). Among these trace transition metal elements this work focuses on biofunction of zinc and briefly discussed in this chapter.

1.1.1. Discovery of zinc: an essential transition metal element

The presence of zinc in an organism as a trace nutrient was first discovered in *Aspergillus niger* in 1869, that established zinc as an essential factor for growth of the fungus by Jules Raulin who was mentored by Louis Pasteur (Raulin, 1869). In late 1920s, endogenous presence of zinc in human tissues was discovered at the Harvard and was postulated that zinc possibly serves biological functions (Drinker, 1926; Lutz, 1926). Historic consensus is that the biochemistry of zinc formally began in 1939 when the first zinc enzyme, erythrocyte carbonic anhydrase, was discovered containing stochiometric zinc content and zinc was shown to be essential component for enzymatic activity of carbonic anhydrase (Keilin and Mann, 1939). Fifteen years later, zinc

involvement in bovine pancreatic carboxypeptidase was identified by Bert L. Vallee and his colleagues in 1954, that counted for second discovered zinc enzyme (Vallee and Neurath, 1955). [B. L. Vallee, "Mr. Zinc", is distinguished pioneer of zinc biochemistry and zinc enzymology. His contributions to the field led to discovery of many other zinc metalloproteins. He passed away in 2010, in age of ninety]. Since then nearly 3000 zinc binding human proteins have been predicted which correlates to ~10% of human genome (Maret, 2013).

Zinc is indispensable trace nutrient and the second most abundant transition metal ion present in humans after iron. Opposed to iron (ferric and ferrous states) and copper (cupric and cuprous states) zinc ion is a redox inert, stable divalent cation (Zn^{2+}) under all biologically applicable pH conditions thanks to its filled *d* shell and is acting as Lewis acid in biological reactions (Lee, 2018). Zinc has both catalytic and structural roles, used as a cofactor for 2000 transcription factors in gene expression and required for catalytic activity of over 300 enzymes, covering all enzyme classes (Bafaro et al., 2017; Maret, 2013). Zinc is also found to be an important component for integrity and stability of many proteins. Equally important, zinc also serves as signaling molecule by taking part in cellular signaling transduction pathways (Tóth, 2011; Yamasaki et al., 2007).

Because zinc is involved in thousands of proteins such as in activation of numerous transcription factors, depletion of zinc brings huge consequences. Zinc deficiency in humans was first discovered by Dr. A. Prasad in 1961 when he traveled to Iran for medical expedition (Prasad, 2012). He diagnosed "Iran Dwarf" patients with growth retardation whom many thought because of iron deficiency at the time, however, clinical features of the disease such as testicular atrophy and hypogonadism could not be explained by merely iron deficiency according to Dr. Prasad's observations. Shortly after, he observed similar syndromes in Egyptian patients with common symptoms. After further laboratory investigations he concluded that these patients' symptoms are

due to zinc deficiency as a result of low dietary zinc intake for very prolonged time. After his findings, zinc metabolism gained noticeable interest and his intellectual observations were one of the first steps to save many human lives. Nowadays, its well characterized that zinc deficiency leads to serious diseases with symptoms of growth retardation, impaired immunity, diarrhea, skin abnormalities, alopecia, hypogonadism, neurological disorders and cognitive impairment (Kambe et al., 2014). Astonishingly, even today 2 billion people are at risk for inadequate zinc supplementation in current developing world as it still remains global health problem (Prasad, 2012). Globally, it has been estimated zinc deficiency is accountable for 4% of child diseases and mortality (Penny, 2013). Meanwhile, zinc has low toxicity rate and cases subjected to excessive zinc are very rare. The incidence of schizophrenic patient ingested plenty of zinc coins led to zinc toxicity and subsequently inadequate copper absorption (Rink, 2011). Based on discoveries have been made in past few decades, it has become more demanding to understand zinc regulation and hemostasis which is critical factor for human health and must be studied thoroughly.

1.1.2. Zinc metabolism

In an average adult human 2-3 grams of zinc is distributed throughout their body where majority of zinc ions (90%) are incorporated in skeletal muscles and bones, 5% in the skin and liver, and the remaining in other tissues (**Figure 1.1**) (Kambe et al., 2015). Dietary food is primary zinc supply to the body where zinc is freed from ingested food during digestion. Zinc administrated within liquid food is taken in more effectively compared to zinc from solid diet. [General accepted effectiveness of zinc absorption is 33% in humans]. Once liberated, zinc ions may bind to endogenously secreted ligands before they absorbed by enterocytes located in apical surface of gastrointestinal tract and then followed by release of zinc ions to the blood circulation, from which expediated zinc delivery to necessary organ tissues (Roohani et al., 2013). Only 0.1% of total zinc,

about 70 – 120 μg/dL (10-18 μM) of zinc ions circulate in human blood plasma. About 80% of zinc ions in blood plasma loosely bound to albumin creating exchangeable pool, whilst 20% tightly bound to α2-macroglobulin (Kambe et al., 2014). Since there are no zinc stocking systems in large amounts in the body, zinc has to be ingested on regular basis in order to maintain zinc homeostasis. Beginning of infancy up to 6 months, 2.0 mg/day of zinc is considered to be adequate amount which is provided by mother's milk. After 6 months of postpartum zinc concentration in mother's milk decline considerably compared to first few months, whereas recommended dietary zinc allowance of 7 months baby to 3 years increase to 3.0 mg/day. Therefore, mother's milk alone is not an adequate zinc source, thus, cow's milk preferred to be more sustainable after that stage. Zinc allowance in kids from 4 to 8 years is 5 mg/day; 9 to 13 years, 8 mg/day; older than 13 years in women and men are 9 mg/day and 11 mg/day, respectively. 12 mg/day zinc allowance recommended for pregnant women (Maverakis et al., 2007).

Majority of zinc excretion occurs through feces by approximate zinc loss of 34 μg/kg/day, whereas urinal excretion 7.5 μg/kg/d is much less due to effective reabsorption of zinc from the tubules in the kidney. Other possible routes of zinc loss include sweat, bleeding, hair, semen and integument (Roohani et al., 2013).

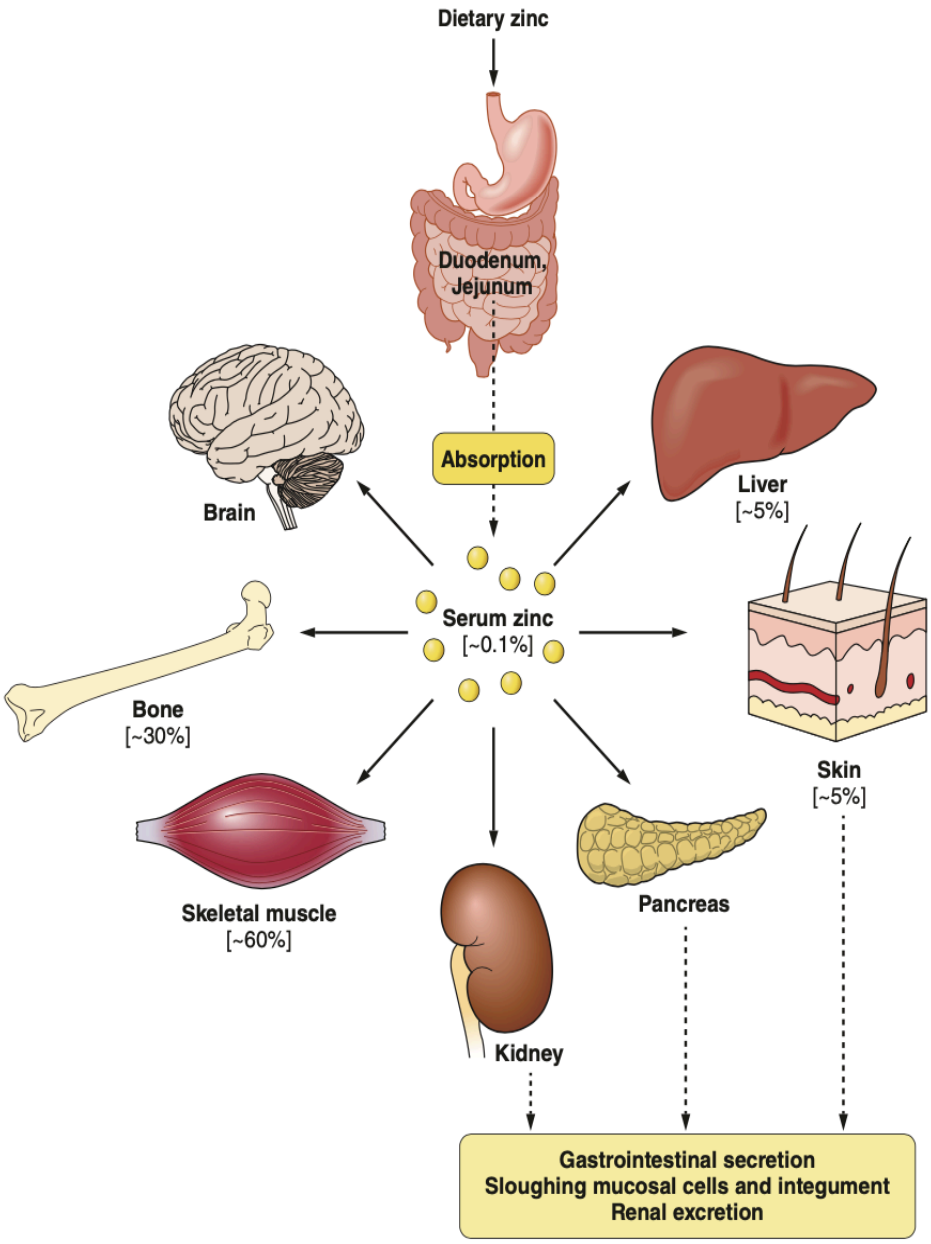

Figure 1.1. Schematic representation of zinc distribution in the body.
Dietary zinc is absorbed through small intestine (duodenum and jejunum) and then distributed to different organ tissues via blood circulation. Approximate zinc amount found in the peripheral tissues given in percentages reference to total zinc in the body. 60% of zinc reside in skeletal muscle, 30% in bones, 5% in the liver and skin. Only ~0.1% of total zinc found in human serum. Routes of zinc excretion are highlighted in yellow. This illustration is taken from Kambe et al., (2015).

1.1.3. Cellular zinc homeostasis

Cellular zinc homeostasis is achieved by coordinated actions of zinc transporters, zinc buffer proteins/molecules, zinc storage proteins and zinc utilizing proteins (**Figure 1.3**). In cellular level, zinc plays an essential role in a vast array of functions including gene transcription, protein translation, cell differentiation and proliferation, immune system activation and programmed cell death. However, determining compartmental zinc concentrations in the cell has been highly challenging due to diverse forms of zinc within cells. Total zinc concentration in pancreatic β-cells, mast and neuronal cells thought to be as high as in sub-millimolar range. However, zinc is bound to multitude of proteins in the cytosol and also isolated into intracellular granules, therefore, labile zinc concentration is considered to be very low and estimated between sub-nanomolar and picomolar range (Haase and Rink, 2014). Subcellular zinc distribution in cytoplasm (50%), nucleus (~40%) and membrane (10%) reflects to its diverse roles in the cellular system (Haase and Rink, 2014). In cytoplasm, portion of zinc is tightly bound to metallothionines (MTs) and also incorporated into intracellular vesicles such as endosomes, lysosomes, synaptic and insulin granules. Thoroughly demonstrated, zinc is required for insulin crystallization in pancreatic β-cells which is important for insulin storage in the granules (Zalewski et al., 1994). Similarly, high concentration of zinc is detected in sperm cells, pancreatic exocrine cells, Paneth cells in the intestine and pigment cells in the retina (Kambe et al., 2015). Although labile zinc determination in intracellular compartments such as endoplasmic reticulum (ER), Golgi apparatus and mitochondria have been studied, current existing data are inconclusive and inconsistency between results have not been well explained. Further elucidation in this matter is needed.

1.1.4. MTs and their regulation in zinc homeostasis

MTs are small, ubiquitous, cysteine rich protein molecules (~7 kDa) known for detoxification and sequestration of many transition metal ions including zinc which plays central role in buffering cytoplasmic zinc concertation. There are a dozen of MTs known in humans serving multipurpose biological functions. Mammalian MTs are composed of 61-68 amino acids, 20-21 of which are highly conserved cysteine residues (Coyle et al., 2002; Miles et al., 2000). A total of seven zinc ions bind per molecule, forming strong interaction with thiol groups (SH) found in cysteine residues with flexible tetrahedral coordination. MTs consist of two subdomains, α and β, where four and three zinc ions, respectively, bind with stability constant of $10^{11} – 10^{14}$ (Juárez-Rebollar et al., 2017). Experimentally calculated binding constant of MTs ($10^{11} – 10^{14}$) explain nanomolar and picomolar range of labile zinc concentration in principal, however, zinc distribution, regulation and transfer of zinc from tight binding sites of MTs to other proteins still remain as unanswered questions (Thirumoorthy et al., 2011). β-domain is considered to be more dynamic in exchange of zinc compared to stable α-domain; thereby early zinc release occurs from β-domain (Kägi and Kojima, 1987). MTs possess their secondary structure in metal-bound form, whereas apo-MTs are largely unstructured which makes them vulnerable to proteolytic digestion. If there is insufficient amount of zinc in the surroundings to stabilize a MT molecule, it is rapidly proteolyzed and zinc ions released during degradation to maintain cytoplasmic zinc balance (Kimura and Kambe, 2016). Contrarily, excessive rise of cytoplasmic zinc interferes with other metal-dependent processes, especially with calcium and copper, and therefore, zinc homeostasis must delicately regulated and MTs play fundamental role in achieving this purpose (Maret, 2000).

MT genes harbor metal-responsive element (MRE) regions such as the TATA box and cis-acting response elements which are regulatory regions for gene expression (Lichtlen and

Schaffner, 2001). The MREs are short sequences of DNA found in promoter region of the of zinc-regulated genes, cluster of nucleotides those accommodating binding site for MRE-binding transcription factor-1 (MTF-1) and other zinc-dependent transcription factors (Giedroc et al., 2001). The consensus is that MRE fragment constitutes 12-base pair sequence that contains two distinct segments, in which a core segment of highly conserved 7-base pair 5'-TGCRCNC-3' motif is followed by a less conserved 5-base pair 5'-GGCCC-3', GC rich motif (R = A/G; N=Any base) (Stuart et al., 1985).

MTF-1 is a metalloregulator zinc finger transcription factor and the only known zinc ion sensor in eukaryotic system (Maret, 2013). On basal zinc levels MTF-1 is inhibited by zinc-sensitive inhibitors that dissociates from MTF-1 in elevated zinc conditions, followed by MTF-1 translocation from the cytoplasm to nucleus for DNA binding through modulation of zinc fingers in response to increased zinc levels in the cytoplasm (Langmade et al., 2000). MTF-1 contains six Cys_2His_2 zinc fingers, where zinc binding to MTF-1 allows the protein to bind to the proximal MRE promoters for activation of *MT* genes and some zinc transporter genes whose translational products are involved in reducing cytoplasmic zinc concentration (Kimura et al., 2009). MTF-1 zinc fingers are believed to have lower zinc binding affinity compared to other zinc finger motifs, thus allowing it to regulate when zinc levels exceed basal norm. Intriguingly, silencing *MTF-1* changed zinc-responsiveness of almost 200 zinc related genes in human transcriptome (Hardyman et al., 2016), suggesting MTF-1 regulates several levels of zinc as a master zinc sensor and mediates intracellular zinc concentrations by direct participation in gene expression of MTs and zinc transporters. Mice *MTF-1* gene knockout study has shown that lacking MTF-1 protein fails to transcribe *MT-I* and *MT-II* genes and its lethal in approximately day 14 in the uterus due to liver failure (Günes et al., 1998).

1.1.5. Zinc in gene expression

One of huge breakthroughs in zinc biochemistry was discovery of zinc finger proteins by biochemical approach in transcription factor IIIA (TFIIIA) of *Xenopus laevis* by a graduate student, J. Miller, in 1985 (Miller et al., 1985). Few years later, crystallographic approaches revealed that zinc finger motif consists of two β-sheets and one α-helix where zinc is bound to Cys_2His_2 in tetrahedral coordination (Pavletich and Pabo, 1991) with femtomolar affinity (Chan et al., 2014). Apo state of a zinc finger is typically unfolded and upon incorporation of zinc ions, spontaneous folding leads to its functional ββα state (Chan et al., 2014). Conserved cysteines and histidines together with a zinc ion are fundamental components to form framework of zinc finger motif, whereas variable outward extending side-chain residues from α-helix make direct contact with DNA determining the specificity of each domain (Klug, 2010). Variability in side-chain residues while main framework remaining the same offers large number of combinatorial possibilities for the specific DNA or RNA recognition. Zinc fingers are the most abundant motifs found within transcription factor domains in eukaryotic system. In fact, zinc is required for the function over 2000 transcription factors (Jeong and Eide, 2013a). These transcription factors play huge role in DNA recognition, DNA-repair and transcriptional regulation during cell differentiation, division, survival and proliferation; especially in skeletal development (Ganss and Jheon, 2004). 90% of total zinc in the human body residing within skeletal bone and muscle tissues comes with no surprise as zinc is essential for tertiary structure formation of thousands of transcription factors.

1.1.6. Zinc in metalloenzymes

Standout chemical properties of zinc among first row transition metal elements can be attributed to its filled *d* orbital (d^{10}) and therefore does not participate in redox reactions but rather

functions as a Lewis-acid by accepting lone pairs from electron-donor ligands. Consequently, zinc ion has room for flexibility in its coordination geometry hence it has zero ligand-field stabilization energy in all liganding geometries due to filled *d*-shell (Huheey et al., 1993). Nevertheless, distorted tetrahedral geometry is the most encountered coordination in zinc enzymes. Also, Zn^{2+} is classified somewhat in between, and does not belong to either "hard" (not very polarizable) or "soft" (highly polarizable) metal ion groups and does not have a fixed preference for coordinating with either nitrogen, oxygen or sulfur atoms. In proteins zinc is found coordinating more frequently to sulfur of cysteine, nitrogen of histidine, carboxylate oxygen of glutamate and aspartate, whereas in rare occasions it has also been observed coordinating with hydroxyl of tyrosine, carbonyl oxygen of glutamine and asparagine (Gregory et al., 1993; McCall et al., 2000). Moreover, Zn^{2+} has a rapid ligand exchange characteristic, which makes it important component in enzymes for rapid product dissociation that required for fast turnover (Cotton and Wilkinson, 1988). Thus, the zinc ion is an ideal metal cofactor for enzymes that require a redox-stable ion to function as a Lewis acid–type catalyst. Zinc is required for activity of ~300 enzymes in humans and necessary for sustaining structural integrity and stability of many others, spanning all six classes of enzymes *i.e.*, hydrolases, ligases, transferases, oxidoreductases, lyases and isomerases (Maret and Li, 2009). In enzymes major role of zinc can be either catalytic, co-catalytic (regulatory) or structural.

In **catalytic** zinc sites, zinc is located at active site and directly involved in bond-breaking or -making mechanism. A unique feature of these sites is that zinc is not fully saturated, usually bound to three ligands, leaving open coordination for at least one water molecule or a substrate to bind. In catalytic zinc sites, histidine is far more frequently observed side chain residue, followed by glutamic acid, aspartic acid and then cysteine (Vallee and Auld, 1992a, 1992b). The N_ε atom of histidine is the most encountered zinc liganding site in zinc enzymes by the head-on and in-

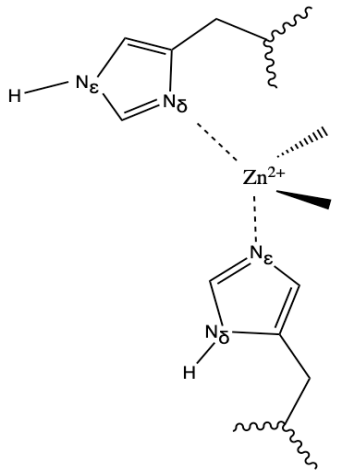

Figure 1.2. Tetrahedral coordination of zinc. Example of histidine coordinations from two different N_ε and N_δ sites.

plane interaction of the *sp*² lone pair of the N_ε atom with the metal ion (Chakrabarti, 1990; Vedani and Huhta, 1990), although N_δ coordination also has been observed (**Figure 1.2**). At active site of such enzymes zinc serves as an electrophilic catalyst in three ways; 1) Majority of zinc enzymes catalyze hydrolysis or closely related reactions. In an active site of hydrolases, the zinc ion serves as strong electrophile providing suitable environment for activation of water molecule as a nucleophile (Coleman, 1998). 2) Stabilization of the negatively charged intermediates by zinc in the transition state such in aldolases (Galkin et al., 2009). 3) Another role of zinc is to polarize carbonyl of the scissile bond as observed in matrix metalloproteinase-3 (MMP-3) cleavage mechanism (Pelmenschikov and Siegbahn, 2002). A common feature to all zinc active sites is that the metal ion is confined by hydrophilic interior which is embedded within a larger hydrophobic shell (Yamashita et al., 1990). Customarily, the amino acid side chains serving as zinc ligands often make hydrogen bond interactions with other residues, perhaps to perform the metal binding

site and attenuate entropic cost of the zinc binding. Such (re)orientation sequels enhance the zinc-ligand electrostatic interactions and modulate the zinc-water pK_a (Christianson, 1991).

In **co-catalytic** zinc sites, two or more zinc ions present in close proximity where one of zinc ions participates in catalytic reaction while other(s) imposes supportive role to enhance catalysis. Typically, either glutamate or aspartate forms a bridge between two zinc ions by simultaneously binding both zincs through carboxylate group (McCall et al., 2000). Such multi-metal pockets are found in nuclease P1 (three zinc ions), phospholipase C (three zinc ions), alkaline phosphatase (with two zinc ions and one magnesium ion), and leucine aminopeptidase (two zinc ions), which all catalyze the hydrolysis of phosphate esters (Vallee and Auld, 1993).

In **structural** zinc sites, zinc coordination sphere is fully saturated with four side chain residues unlike in catalytic sites, leaving no space for additional ligand in tetrahedron geometry, thus excluding the solvent from inner sphere. Cysteine is by far the most frequently observed chelating residue found in these sites, perhaps because Zn-S provides tighter interaction (Lovejoy et al., 1994), followed by histidine which is also being observed in many cases. In structural sites the main purpose of zinc is to deliver stability to both local and global tertiary structure of a protein in a way analogous to disulfide bond (Vallee et al., 1991). Another distinction from catalytic zinc sites is that the ligands participate in structural sites can be located in flexible loop rather than a perfect sitting spot for a zinc ion in a defined secondary structure pocket.

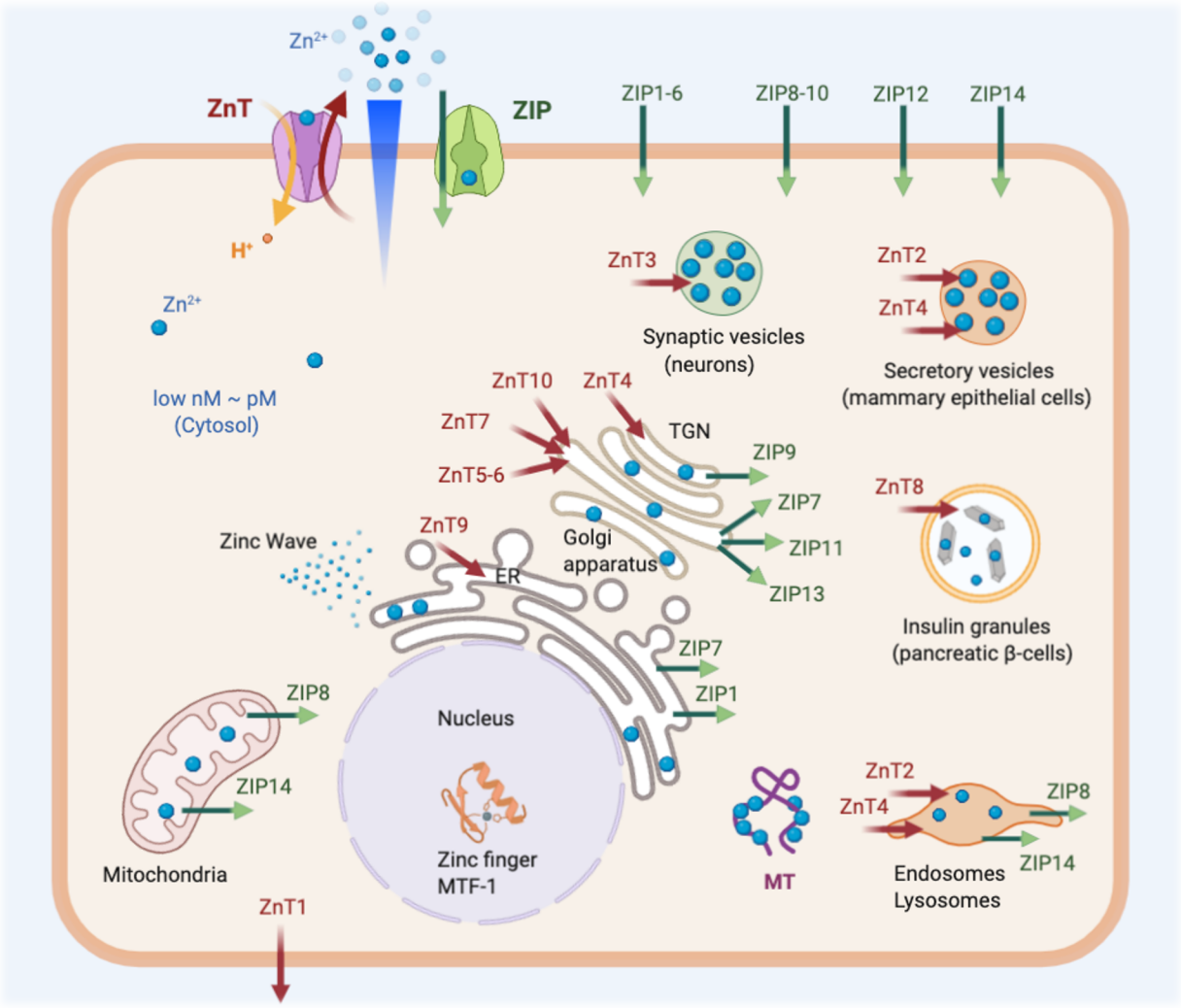

Figure 1.3. Schematic illustration of zinc homoeostasis in cells.
ZIP (in green) and antiporter ZnT (in red) are carrier proteins transporting zinc. The direction of zinc mobilization is shown with arrows. Fading colors of arrows indicate zinc gradient with bolded side and faded side representing higher and lower zinc concentrations, respectively. Labile zinc gradient is shown with blue indicator between extracellular space and the cytoplasm. Almost all zinc ions are either bound to MTs or sequestrated into intracellular organelles and cytosolic labile zinc is in between sub-nanomolar and picomolar range. Zinc wave that is involved in zinc signaling is shown near to ER. ββα motif, zinc finger transcription factor MTF-1 is shown in the nucleus. Subcellular localization of ZnT and ZIP members are shown according to literature. Commonly known, high zinc containing cell-specific intracellular vesicles include synaptic vesicles in neurons, secretory vesicles in mammary gland and insulin granules in pancreatic β-cells. The figure is made by using BioRender ©.

1.1.7. Zinc signaling

One of key roles of zinc in human physiology, besides its structural and functional roles, is acting as a signaling molecule. As a signaling molecule zinc has been identified to play roles in neurotransmission (Tóth, 2011) and as an intracellular second messenger (Yamasaki et al., 2007). In glutamatergic neurons, zinc can be found co-sequestrated together with glutamate which takes part in broad functions in nervous system (Pérez-Clausell and Danscher, 1985). Zinc is sequestrated into synaptic vesicles from the cytosolic zinc pool by a neuron-specific ZnT3 transporter (Palmiter et al., 1996) (see below). Zinc ions released through exocytosis into surrounding milieu interact with various postsynaptic receptors and channels which triggers variety of biological cascades in response (Hirano et al., 2008). Elimination of zinc from synaptic vesicles by knocking out *Znt3* gene led mice to be more susceptible to seizures and neuronal damage (Tb et al., 2000). In humans, ZnT3 associated with learning deficits and memory loss; and it has been proposed that zinc in a way mimics signaling molecules likes of hormones, cytokines and growth factors by mediating cell-to-cell signaling. Thus, zinc has a neurotransmitter characteristics (Hirano et al., 2008)

New phenomenon of "zinc as an intracellular second messenger" was brought up for the first time in 2007 by Yamasaki et al. when they showed zinc is released within minutes to the cytosol from perinuclear and ER region by induction of Fc epsilon receptor I (FcεRI) via extracellular stimulus in mast cells (Yamasaki et al., 2007). In contrast to zinc signaling in neurons which increases cytosolic zinc concentration by intaking zinc from extracellular milieu, the study of Yamasaki et al. demonstrated extracellular zinc is not involved in their case, zinc is rather being released from intracellular compartments to the cytosol which plays role in mast cell activation process via FcεRI stimulation by immunoglobin E antigen. Thus, zinc has been characterized as

novel intracellular second messenger, transducing extracellular stimuli into intracellular signaling cascade of events. This phenomenon was called as “zinc wave” and also characterized as “early zinc signaling” due to fast stimulation within few minutes after induction in mast cells (Hirano et al., 2008; Yamasaki et al., 2007).

Zinc also acts as a conventional second messenger by directly transducing extracellular stimuli into intracellular signaling. For instance, well-characterized study has shown Toll-like receptor (TLR)-mediated signaling induces a decrease in the intracellular zinc concentration by downregulating ZIPs and upregulating ZnTs which is important for dendritic cell activation (Kitamura et al., 2006) (see below). This signaling process is completely dependent on transcriptional regulation and requires biosynthesis of zinc transporters to respond the cytosolic zinc concentration which takes several hours after stimulation, thereby, is called “late zinc signaling” to distinguish from “early zinc signaling and zinc waves” (Hirano et al., 2008).

1.2. ZINC TRANSPORTERS

Zinc is an indispensable metal element for multitude of human proteins that displays unique and various functions. Zinc is absorbed from small intestine through zinc specific transporters, and then transferred to blood vessels where zinc is transported again by tissue specific zinc transporters into the target tissues. On the other hand, excessive zinc uptake has cytotoxic effects causing copper deficiency which leads to adverse health issues; therefore, zinc excretion is equally important. Essentially, zinc transporters play central roles in systemic and cellular zinc homeostasis and regulation. In humans, zinc excretion and absorption are regulated by two major integral membrane protein families, Zinc Transporter (ZnT) family and Zrt- and Irt-like protein (ZIP) family, respectively. These two families play fundamental roles in precise zinc level

maintenance by dominating zinc fluxes across bio-membranes and participating in zinc distribution and storage, which are briefly reviewed as follows (**Figure 1.3**).

1.2.1. Discovery and current understanding of ZnT transporters

ZnT family, also known as the Solute Carrier 30 (SLC30) family, belongs to superfamily of Cation Diffusion Facilitator (CDF) transporters and also classified as a member of Electro Chemical Potential-driven Transporters' superfamily (Haney et al., 2005). The first zinc transporter, Zrc1, was identified in the yeast, *Saccharomyces cerevisiae* (Kamizono et al., 1989), and few years later discovery of mammalian homolog, ZnT1, from mouse led to quick discovery of other ZnT members (Palmiter and Findley, 1995). The mammalian ZnT family consists of ten members (ZnT1-10) that are involved in moving cytoplasmic zinc into intracellular compartments, such as ER, Golgi and mitochondria to supply zinc for zinc requiring proteins and intracellular vesicles for zinc sequestration. Just as important, ZnT family is responsible for effluxing zinc out to the extracellular space to preclude excessive cytoplasmic zinc (Huang and Tepaamorndech, 2013, p. 30; Palmiter and Huang, 2004).

Bacterial CDF homologs ZitB and Yiip from *Escherichia coli (E. Coli)* have been characterized functionally and structurally, respectively, which shares 25 to 30% sequence similarity with their mammalian ZnT counterparts. Kinetic study of ZitB has demonstrated an antiporter mechanism, catalyzing the obligatory exchange of Zn^{2+} for H^{+} in 1:1 stoichiometric ratio (Chao and Fu, 2004; Lu and Fu, 2007). In 2007, the first structure of CDF family member was obtained by crystallization of Yiip, revealing homodimerization at the cytoplasmic interface in parallel orientation, whereas the two transmembrane domains arranged in a Y-shaped structure **(Figure 1.4C)**. Interestingly, four zinc ions found to be bound to each monomer at three different

sites where Y-shaped transmembrane domains facing outwards (Lu et al., 2009; Lu and Fu, 2007). Later on, inward-facing conformation has been captured by cryo-EM establishing alternating access mechanism for Zn^{2+}/H^{+} transport **(Figures 1.4A)** (Coudray et al., 2013; Lopez-Redondo et al., 2018). Based on homology modelling, mammalian ZnTs predicted to be sharing common features with Yiip, composed of six transmembrane helices (TMs) and a hydrophilic C-terminal domain (CTD) located in the cytoplasm and likely to use the similar mechanism to move zinc ions within the cell (Gupta et al., 2014; Huang and Tepaamorndech, 2013; Shusterman et al., 2014). Among six TMs, TM 1, 2, 4 and 5 form helical bundle where zinc ion tetrahedrally coordinated with three highly conserved aspartic acid residues and one histidine residue extending side chains from TM2 and TM5 (Lu and Fu, 2007). Sequential experiments demonstrated that conserved DD–HD at metal binding site I (**Figure 1.4C**) in the bacteria important for selectivity and transport of both zinc and cadmium, whereas tuned HD–HD motif in mammalian ZnTs is specific for zinc selection (Hoch et al., 2012; Ohana et al., 2009).

1.2.2. Physiological and cellular functions of ZnT transporters

ZnT1 (SLC30A1) is the only member of ZnT family that ubiquitously expressed on the plasma membrane of all types of mammalian cells and tissues, and the major exporter of cytoplasmic zinc to the extracellular space (Kelleher and Lönnerdal, 2003; Ohana et al., 2006). Specifically, ZnT1 expression is localized at the basolateral surface of intestinal epithelial cells that responsible for zinc export into the blood portal, facilitating systemic zinc transport (McMahon and Cousins, 1998). High cytosolic zinc concentration upregulates *Znt1* expression via MTF-1/MRE mediated pathway, similar to *MT* gene activation (Langmade et al., 2000, p. 1). Upregulation of ZnT1 on the cell surface protects cells from excessive zinc accumulation. Mice experiments demonstrated that homozygous knock-out of *Znt1* is embryonic lethal at day nine of

pregnancy, thus ZnT1 is essential during embryonic development. (Andrews et al., 2004). Upregulated ZnT1 in response to lipopolysaccharide (LPS) stimulation mediated by TLR signaling decreases intracellular zinc levels in dendritic cells, that is important for triggering the immune cell activation (Kitamura et al., 2006). Thus, ZnT1 is essential for systemic zinc movement, vital in early embryonic survival and important for normal immune function.

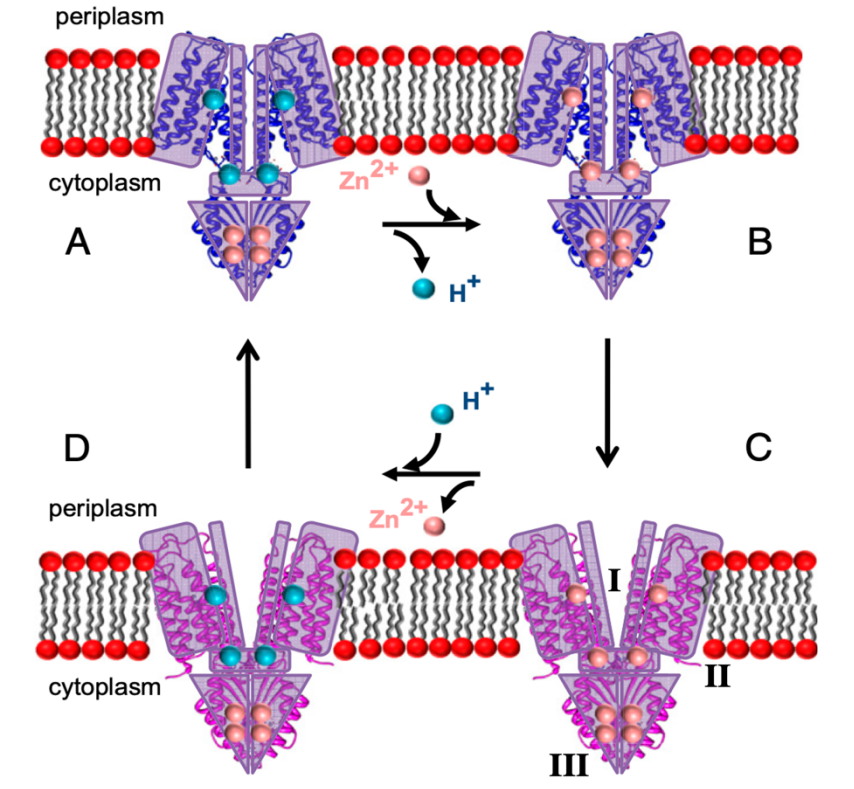

Figure 1.4. Alternating access mechanism for Yiip Zn^{2+}/H^+ antiporter.
Inward-facing conformation **(A)** was obtained from cryo-EM and outward-facing conformation **(C)** corresponds to the X-ray structure solved in the presence of Zn^{2+}. (**B**) and (**D**) are predicted transitions showing Zn^{2+} and H^+ replacement and vice versa. The proton motive force provides a driving force for exporting Zn^{2+} from the cytoplasm. Three zinc binding sites are shown in roman numerals that were seen in the crystal structure. The figure is adapted from Coudray et al., 2013.

Majority of ZnT members reside in sub-cellular localization, on the membrane of various intracellular organelles (**Figure 1.3 and Table 1.1**). For example, ZnT2 moves remnant cytosolic zinc into lumen of endosomes and lysosomes (Falcón-Pérez and Dell'Angelica, 2007), supplies zinc into the zymogen granules in pancreatic acinar cells (Guo et al., 2010, p. 5), and also has been linked with zinc import to the mitochondria of mammalian cells (Seo et al., 2011). ZnT2 is critical for zinc sequestration into secretory vesicles in human mammary gland where zinc is mobilized to breast milk by exocytosis. Several cases were reported breast-fed infants developing transient neonatal zinc deficiency (TNZD) which were associated with low milk zinc concentration in mother's breast milk due to mutations in ZnT2 (Chowanadisai et al., 2006).

Mammalian ZnT3 is required for the transport of zinc into synaptic vesicles in neurons which is stated to regulate normal cognitive function (see above). Cognitive loss by age is reflected to lessening ZnT3 expression in elderly humans (Adlard et al., 2010) and in patients with Alzheimer's disease or Parkinson's disease (Whitfield et al., 2014). Defects in ZnT3 can result in enhanced sensitivity to kainate-induced seizures (Cole et al., 1999).

ZnT4-7 and ZnT10 are found in Golgi apparatus and *trans*-Golgi network (TGN) (**Figure 1.3**) (Bosomworth et al., 2012; Cp and L, 2002; Huang et al., 2002; Liuzzi et al., 2003; McCormick and Kelleher, 2012; Suzuki et al., 2005). Contributive role of ZnT4 for zinc export to mammalian breast milk also has been suggested (McCormick and Kelleher, 2012), however, there has been no indication of *Znt4* gene deficits causing TNZD (Ackland and Michalczyk, 2006). ZnT5 and ZnT6 orthologues are heterodimers, whereas all other ZnT members form homodimer (Fukunaka et al., 2009). ZnT5 and ZnT6 are poorly understood because they differ the most from the other ZnT transporters. Nullifying *Znt7* gene in mice leads to growth retardation, poor body weight gain and reduced zinc absorption from diet suggesting ZnT7 is involved in zinc intake from diet and in the

regulation of body adiposity (Huang et al., 2007). However, typical symptoms of dermatitis that occurs in zinc-deficient animals and humans was not observed, thus ZnT7 is dispensable for epidermal cell growth (Huang et al., 2012).

ZnT8 is known as a pancreatic β-cell-specific zinc transporter and primarily expressed in insulin-containing granules that is preeminent for zinc accumulation in the granules for insulin-zinc crystallization and storage before secretion (**Figure 1.3**) (Chimienti et al., 2004). Knock-out of *Znt8* mice displayed drastically low circulating insulin concentrations in both globally and locally (in β-cell) and consequently impaired glucose tolerance due to diminished insulin secretion (Lemaire et al., 2009; Pound et al., 2009). ZnT8 has been widely characterized to be associated with type 2 diabetes by genome-wide studies in numerous occasions (Saxena et al., 2007; Scott et al., 2007; Sladek et al., 2007; Wijesekara et al., 2010) and has been one of the hot points of discussions in the recent decade.

Table 1.1. Summary of Human ZnTs

Human ZnTs			
Members	*Subcellular localization*	*Tissue/Cell distribution*	*Pathological implications*
ZnT1	Plasma membrane	Ubiquitous	Embryonic lethal*
ZnT2	Endosome, lysosome, secretory vesicle	Mammary gland, pancreas, prostate, retina, intestine, kidney	Transient neonatal zinc deficiency (TNZD) †
ZnT3	Synaptic vesicles	Brain, pancreas, testis	Seizures*, memory loss*†
ZnT4	*trans* -Golgi, endosome, lysosome, secretory vesicle	Mammary gland, placenta, prostate, kidney, brain	Lethal milk*
ZnT5	Golgi, vesicles	Heart, placenta, prostate, ovary, testis, intestine, thymus, bone	Bone abnormalities*, heart failure*
ZnT6	Golgi, vesicles	Brain, lung, intestine	Alzheimer's disease†
ZnT7	Golgi, vesicles	Intestine, pancreas, prostate, placenta, testis, retina, muscle	Reduced adiposity*
ZnT8	Secretory granule	Pancreas, thyroid, testis	Type 2 Diabetes†
ZnT9	ER	Brain, muscle, kidney	Unknown
ZnT10	Golgi	Brain, retina, liver	Syndrome of hepatic cirrhosis, hypermanganesemia†

†Human
*Mice

1.2.3. ZIP family of metal transporters

ZIP family, also known as SLC39 family, is the opposite counter partner of ZnT family. ZIPs are responsible for zinc influx either from extracellular space or intracellular vesicles into the cytoplasm, increasing cytoplasmic zinc concentration (**Figure 1.3**). ZIP is an ancient family, encompassing thousands of transporters that are found in all domains of life and have been identified at all phylogenic levels (Jeong and Eide, 2013b). Currently standing, ZIP family is lesser characterized, and their identification is more complicated compared to ZnT family. The first member of the family to be identified was iron-regulated transporter-1 (Irt-1) from *Arabidopsis*

thaliana which turned out to have preference to iron import (Eide et al., 1996; Grotz et al., 1998). Shortly afterwards, two other members of the family, zinc-regulated transporter-1 and -2 (Zrt-1, Zrt-2) were identified from the yeast, *Saccharomyces cerevisiae*, by utilizing the Irt-1 sequence (Zhao and Eide, 1996a, p. 1, 1996b, p. 2). Hence, acronym for the family (*i.e*. ZIP) reflects "Zrt- and Irt-like protein". ZIP2 and ZIP1 were the first two mammalian members identified (Gaither and Eide, 2001, 2000, p. 2), followed by subsequent identification of entire ZIP members after the human genome sequencing completion (Kambe et al., 2006; Lichten and Cousins, 2009).

There are fourteen members of ZIP transporters being encoded by human genome. These fourteen ZIPs have been further grouped into four subfamilies based on sequence similarities, *i.e*. I (ZIP9), II (ZIP1-3), guf-A (ZIP11) and LIV-1 (ZIP4-8, ZIP10 and ZIP12-14) (**Table 1.2**) (Schmitt-Ulms et al., 2009). All the ZIPs predicted to have evolutionarily conserved transmembrane topology with eight spanning TMs (TM1– TM8) with both N- and C-termini exposed to either extracellular space or lumen of organelles (Zhang et al., 2017). Evidently through later in evolution, some of ZIPs are incorporated with a soluble extracellular domain (ECD) at the N-terminus (**Figure 1.5A**). LIV-1 is the largest among four subfamilies, containing nine out of fourteen ZIPs which possess ECD in common and the structure of a mammalian representative ECD of ZIP4 has been solved from *Pteropus Alecto* (black fruit bat, pZIP4-ECD) (Zhang et al., 2016).

Table 1.2. Summary of Human ZIPs

Human ZIPs					
Members	*Subfamily*	*Specificity*	*Subcellular localization*	*Tissue/Cell distribution*	*Pathological implications*
ZIP1	ZIPII	Zn	Plasma membrane, ER	Prostate, small intestine, kidney, liver, pancreatic α cells	Prostate cancer, neurodegeneration*
ZIP2	ZIPII	Zn	Plasma membrane	Prostate, uterine, epithelial cells, liver, skin	
ZIP3	ZIPII	Zn, not strictly	Plasma membrane	Testis, pancreatic cells, mammary cells	Neurodegeneration*
ZIP4	LIV-1	Zn	Plasma membrane	Small intestine, stomach, colon, cecum, kidney, pancreatic β-cells	Acrodermatitis Enteropathica (AE), pancreatic and liver cancer, embryonic lethal*
ZIP5	LIV-1	Zn	Plasma membrane	Liver, kidney, colon, pancreas	
ZIP6	LIV-1	Zn	Plasma membrane	Testis, pancreatic β-cells	Breast, pancreaticd, cervicale, prostate cancer, neuroblastoma
ZIP7	LIV-1	Zn, Mn	Golgi, ER	Brain, liver, pancreatic β-cells	Breast cancer
ZIP8	LIV-1	Zn, Mn, Cd, Fe	Plasma membrane, mitochondria, lysosome, endosomes	Pancreas, placenta, lung, liver, testis, thymus, red blood cells	Inflammation, breast cancer
ZIP9	ZIPI		Plasma membrane, *trans* -Golgi	Prostate	
ZIP10	LIV-1	Zn	Plasma membrane	Testis, kidney, breast, pancreatic α cells, red blood cells	Breast cancer
ZIP11	gufA		Golgi	Mammary gland, testis, ileum and cecum	
ZIP12	LIV-1	Zn		Neurons, endothelial, smooth muscle, interstitial cells	
ZIP13	LIV-1	Zn	Golgi, ER	Retinal pigment epithelial cell line, osteoblasts	Spondylocheiro dysplastic Ehlers–Danlos syndrome (SCD-EDS)
ZIP14	LIV-1	Zn, Mn, Cd, Fe	Plasma membrane, mitochondria, lysosome, endosomes	Liver, heart, placenta, lung, brain, pancreatic α cells	Asthma, inflammation, colorectal cancer

*Observed from mice knock-out experiments. The rest belongs to human pathogenesis, collected data from patients.

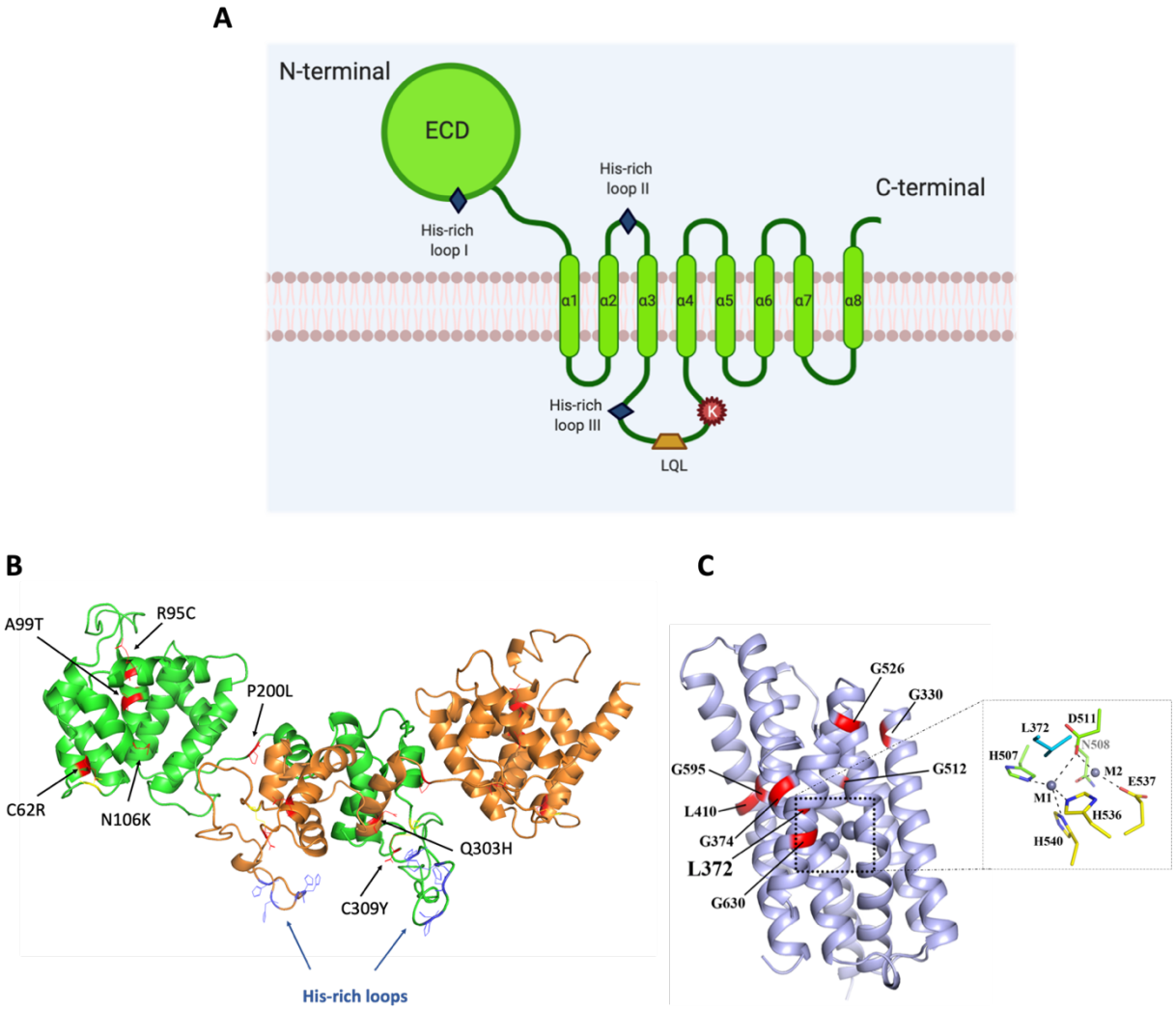

Figure 1.5. Mammalian ZIP4 topology and human ZIP4 model structures.
(A) Topology of mammalian ZIP4 with large N-terminal ECD and eight α-helical TMD in which C-terminal is exposed to the extracellular space. Putative locations of three His-rich loops are indicated. Newly identified LQL motif and universally conserved lysine-ubiquitination site are also shown. **(B)** and **(C)** are model structures of hZIP4-ECD and -TMD, respectively. Homology modeling was performed using the SWISS-MODEL server. The proteins are shown in cartoon mode. **(B)** Model structure of human ECD dimer in which monomers are shown in green and orange. AE-disease causing mutations are highlighted in red. Dynamic His-rich loops indicated in blue. **(C)** Structural model of the TMD with BMC. The AE-mutations are labeled and highlighted in red. Zoomed-in view of the BMC is shown in which metal-chelating residues coordinating modeled Zn^{2+} ions those depicted as gray spheres. The Figure C was adapted from (Zhang et al., 2017).

1.2.4. Structural insights of ZIPs

TMD. As of today, the first and only structural framework of ZIP transmembrane domain (TMD) has been obtained from *Bordetella bronchiseptica* (BbZIP) as it was crystallized in metal-bound inward-facing form, revealing a novel 3+2+3TM architecture with a binuclear metal center (BMC) (Zhang et al., 2017). The first three TMs (TM1-3) and the last three TMs (TM6-8) are sandwiching TM4 and TM5 in symmetrically related arrangement revealing unusual folding for metal transporters. Atypically, two proximal metal ions, M1 and M2, found in midway of TM4 and TM5 chelated by bridging carboxylate (Asp/Glu) and other metal binding ligands (**Figure 1.5C**). BMCs usually found in enzymes with co-catalytical purpose but are rare in transporters. Shortly after in functional study, the BMC site has been elucidated where M2 is more of an auxiliary and most likely contributing to the metal binding properties of the M1 site (T. Zhang et al., 2020). Consistent with many fungal and plant ZIPs lacking M2 site, M2 is not absolutely required for metal ion transport (Eide, 2020; T. Zhang et al., 2020). Further, mutagenesis and functional assays pointed out M1 site is rapidly exchangeable and HH-HD tetrahedral coordination is likely tuned for the zinc selection in the human protein (**Figure 1.5C**) (Zhang et al., 2017; T. Zhang et al., 2020). Human ZIPs (hZIPs) and BbZIP share highly conserved residues at the metal binding sites and in the vicinity of metal transport pathway, therefore, fundamental structural features and utilized transport mechanism by the transporters believed to be very similar. Outward-facing conformation is still not available, and thereby more detailed structural and metal binding studies are needed to establish ultimate zinc transport mechanism and driving force of the transporter.

ECD. The structure of mammalian representative ZIP4-ECD from *Pteropus Alecto* has been solved, making ZIP4 the most characterized member of the ZIP family. pZIP4-ECD has been

crystallized in apo form at the resolution of 2.85 Å and shares 68% identical residues with hZIP4-ECD (Zhang et al., 2016). Globular structure of pZIP4-ECD is stabilized by total of four disulfide bonds, where two cysteine mutations C62R and C309Y in human (**Figure 1.5B**) (C64 and C305 in pZIP4) are associated with Acrodermatitis enteropathica disease (see below), therefore, disulfide bonds must be critical for correct folding (Kambe and Andrews, 2009; Zhang et al., 2016). As highlighted, the structure of pZIP4-ECD revealed a homodimer, where an individual monomer has two structurally independent subdomains (**Figure 1.5B**). The N-terminal subdomain composed of nine α-helical (α1-9) cluster and was named as helix rich domain (HRD). The C-terminal subdomain accommodates the signature PAL motif (Pro-Ala-Leu) and was named as PAL motif containing domain (PCD) as for self-explanatory identification. PAL, the three-residue segment is highly conserved in ZIP4-ECD across species and within LIV-1 subfamily of ZIPs. Based on pZIP4-ECD structure, PCD consists total of five α-helices (α10-14) where they fold in helix-turn-helix pattern and the PAL motif reside in the middle of the long α14. Dimerization of ZIP4-ECD occurs via hydrophobic interaction of perfectly aligned with a 2-fold symmetric axis. All the helices in PCD contributes to dimerization, whereas PAL harboring α14 directly interacts with α14* of the other protomer, playing central role in dimerization. HRD and PCD are connected through short unstructured loop where it was referred as H-P linker. Functional assays implemented on the human cells have shown that deletion of HRD and whole ECD resulted in ~60% and ~75% decrease in zinc uptake activity, respectively, suggesting ZIP4-ECD is crucial for optimal zinc transport, although, is not absolutely essential (Zhang et al., 2016). Within PCD, a segment of ~25 residues between α11 and α12 that containing cluster of histidines was unable to be captured in the crystal structure due severely disordered nature of the loop, but it has been

modeled using SWISS-modelling (**Figure 1.5B**). One of the main focus of this thesis work is to characterize the histidine-rich loop and address to its role in ZIP4-mediated zinc transport.

Histidine-rich loops. One of distinctive features of ZIPs is possessing His-rich loops. Such His-rich loops are known for their metal chelating tendency and subsequently orchestrating various functions as a metal ion sensor, selectivity filter, involvement in transport activity and post-translational regulations (Chun et al., 2019; Mao et al., 2007; Milon et al., 2006; Nishida et al., 2008). Since this thesis work is focused on ZIP4 characterization, exemplary emphasis is put on ZIP4 among the ZIP family. ZIP4 possesses a total of three His-rich loops in the full-length protein, where two of them reside in TMD and one is in ECD (**Figure 1.5A&B**). In TMD, an exposed His-rich loop located between TM2 and TM3 facing to the extracellular space, whereas the second one is exposed to the cytosol between TM3 and TM4 (**Figure 1.5A**). The TM2-3 loop is much shorter compared to the TM3-4 loop. In the BbZIP structure a metal ion found to be bound TM2-3 loop region and speculated to be initial transfer site (Zhang et al., 2017); and the recent study has identified the loop as an extracellular zinc sensor and playing role in high-affinity zinc-stimulated endocytosis in mammalian cells (Chun et al., 2019). The long cytosolic His-rich loop accommodates a couple of distinctive regions thought to take part in different stages of post-translational regulation. Regarding the TM3-4 His-rich loop, several studies have unequivocally demonstrated its role as cytosolic zinc sensor (Mao et al., 2007) with nanomolar binding affinity (Bafaro et al., 2015) and involvement in zinc-induced endocytic degradation of ZIP4 (Gitan et al., 1998, p. 1; Gitan and Eide, 2000, p. 1; Kim et al., 2004). Intriguingly, recently identified LQL (Leu-Gln-Leu) motif has been proposed to be structurally coupled with the transport site and postulated changing into recognizable structure once stimulated, by yet to be identified adaptor protein in clathrin-dependent endocytosis of ZIP4 (C. Zhang et al., 2020). Third region of the

loop, besides the histidine cluster and LQL motif, is the lysine (K463) harbored region which is engaged in ubiquitination-mediated degradation post-endocytosis (**Figure 1.5A**) (Kerkeb et al., 2008). Such cytosolic His-rich loop was also shown as a requirement for zinc transport across the membrane in human ZIP1 (Milon et al., 2006, p. 1).

The His-rich loop of ZIP-ECDs is the least characterized and little known about its function (**Figure 1.5B**). Reportedly, highly conserved N-terminal His-rich loop of ZIP7 exerts critical function(s) by sequestrating zinc ions in the ER for against stress protection and speculated about its potential contribution in ER zinc homeostasis (Adulcikas et al., 2018). In spite of the report, information about the His-rich loop of ZIP-ECDs is very limited. This thesis work takes this matter in hand and scopes deeper on biochemical, biophysical and functional characterization aspects of the His-rich loop.

1.2.5. Current opinion on metal ion transport mechanism of ZIPs

Straightforwardly, the zinc transport mechanism of ZIP transporters has not been well established. Agreeably, most of ZIP transport studies have demonstrated ATP-independence and saturable kinetics suggesting a carrier-like transport mechanism.

Studies on human ZIP2, mouse ZIP8 and ZIP14 have proposed HCO_3^-/Zn^{2+} symport mechanism because of zinc uptake were stimulated by increased HCO_3^- and inhibited by acidic pH < 7.0 (Gaither and Eide, 2000; Girijashanker et al., 2008, p. 14; Nebert et al., 2012). ZIP8 was shown co-transporting two HCO_3^- anions per divalent cation to preserve electroneutrality (Liu et al., 2008). However, the proposal of HCO_3^-/Zn^{2+} ZIP symporter has been strongly challenged by another research group stating heavy contradiction to what has been previously reported in the reassessment study of human ZIP2 zinc transport mechanism (Franz et al., 2018, 2014). In their

case of study, human ZIP2 was stimulated in lower pH rather being inhibited in presence of H^+ and the metal ion transport driven force was independent of HCO_3^- and H^+. They have concluded, since the cytoplasmic zinc levels are kept in picomolar range, inwardly directed electro-chemical gradient of Zn^{2+} is sufficient to facilitate Zn^{2+} transport downhill (Franz et al., 2018). Thus, they have suggested human ZIP2 possibly mediates Zn^{2+} transport simply by passive transport and have raised pressing questions whether each member of the ZIP family should be studied separately.

Although current information are speculative and contradictory, these are promising steps towards establishing well-accepted and proven metal ion transport mechanism of ZIP transporters. For example, solving the outward-facing conformation of a ZIP transporter will shed big light to clarify remaining puzzle of the transport mechanism.

1.2.6. Physiological and cellular functions of ZIP transporters

ZIP transporters play predominant roles in physiology and regulation of zinc in humans. They are being expressed in various tissues and cell types; and differ from each other based on distinct subcellular localizations, biochemical properties and regulation mechanisms (**Figure 1.3**). Mammalian ZIP transporters mainly transport zinc, but few members can also transport iron, manganese, and cadmium (**Table 1.2**) (Fujishiro et al., 2012; Gao et al., 2008; Jenkitkasemwong et al., 2012). Deficits due to mutational perturbation and/or mis-regulation of almost any ZIPs are known for their association with disease pathogenesis.

ZIP1 has widespread expression in nearly all organ tissues such as prostate gland, small intestine, kidney, liver and pancreatic α-cells. ZIP1 is mainly found on the plasma membrane of the cells but translocation of ZIP1 to intracellular organelles also has been observed when cells cultured in zinc-replete media (Franklin et al., 2003, p. 1; Gaither and Eide, 2001; Gyulkhandanyan

et al., 2008; Milon et al., 2001). ZIP1 is the major protein responsible for zinc accumulation to epithelial prostate cells, importing zinc from the circulating blood plasma through basolateral surface of prostate cells (Franklin et al., 2003, p. 1; Huang et al., 2006). Decrease in zinc levels because of ZIP1 downregulation in malignant prostate cells alters intracellular zinc-signaling pathways leading to prostate tumor progression (Costello and Franklin, 2006). Therefore, ZIP1 thought to be highly critical for normal prostate metabolism and as a cancer suppressor gene in the prostate gland.

ZIP2 is known to be present on the plasma membrane of prostate, uterine, epithelial, ovary liver and leukemia cells, importing zinc from the extracellular space (Cao et al., 2001; Gaither and Eide, 2000). In addition to ZIP1 expression in the prostate, ZIP2 has been identified on the apical surface of prostate cells with probable function of reabsorption of zinc from the prostatic fluid. Similar to ZIP1, ZIP2 also displays declined expression in prostate carcinogenic cells (Desouki et al., 2007, p. 2).

ZIP3 has been identified as a tissue specific transporter, plays a major role in zinc uptake into mammary epithelial cells and is regulated in response to prolactin (Kelleher and Lönnerdal, 2005). Although ZIP3-mediated zinc import was requisite for survival of mammary epithelial cells in cell culture, homozygous *Zip3* knock-out mice were viable, albeit having sensitivity to zinc deficiency (Dufner-Beattie et al., 2005). Similarly, homozygous single knock-out of *Zip1* or *Zip2*, double knock-out of *Zip1* and *Zip2*, and triple knock-out of *Zip1*, *Zip2* and *Zip3* mice were viable when fed adequate zinc diets, however, embryos developed abnormally compared to wild-type when zinc is limited, indicating ZIP1, ZIP2, and ZIP3 play redundant roles during embryonic development. (Dufner-Beattie et al., 2006; Kambe et al., 2008). Further, strong expression of ZIP1

and ZIP3 in hippocampal pyramidal neurons have been identified to contribute to zinc homeostasis in neuronal cells (Qian et al., 2011).

Human ZIP4 (hZIP4) is highly expressed in the gastrointestinal tract (*i.e*. entire small intestine and colon) and localized on apical surface of enterocytes (Dufner-Beattie et al., 2003; Wang et al., 2002). ZIP4 is exclusive for zinc transport and plays an indispensable role in zinc uptake from dietary food in mammals (Geiser et al., 2012). In addition, ZIP4 is a key factor for zinc loss prevention through urine by reabsorbing zinc from the proximal tubules in the kidney. ZIP4 is associated with a rare, genetically inherited lethal disorder, Acrodermatitis enteropathica (AE) disease, occurs due to severe zinc deficiency (**Table 1.2**). (Küry et al., 2002; Wang et al., 2002). Homozygous knock-out *Zip4* mice shown to be embryonic lethal and heterozygosity causes hypersensitivity to zinc deficiency, displaying developmental defects in offspring, such as anophthalmia, exencephalia and growth retardation (Dufner-Beattie et al., 2007). ZIP4 is strictly regulated transcriptionally and post-translationally, depending on zinc status of the cell. In response to zinc depletion ZIP4 accumulates on the plasma membrane due to increased *Zip4* mRNA levels by two suggested ways; *i.e*. zinc-finger transcription factor, Krüppel-like factor 4 (KLF4), binds to promoter of *Zip4* gene upon zinc limitation to induce ZIP4 expression (Liuzzi et al., 2009). An alternative regulation is simply due to *Zip4* mRNA stabilization during zinc depletion rather than increased transcription of the gene (Weaver et al., 2007). Upon zinc repletion, *Zip4* mRNA is degraded and ZIP4 is rapidly internalized from the plasma membrane by endocytosis (Kim et al., 2004; Weaver et al., 2007). Recently identified the LQL segment of ZIP4 that is exposed to the cytoplasm is essential for endocytosis process (C. Zhang et al., 2020). Exposure of the cells to excessive zinc, further triggers ubiquitination, internalization and degradation of ZIP4 (Mao et al., 2007). Noteworthy to mention, it has been suggested the N-

terminal of ZIP4 proteolytically cleaved during prolonged zinc starvation, as one of post-translational regulation mechanisms (Kambe and Andrews, 2009). ZIP4 is also expressed on the plasma membrane of pancreatic β-cells, however, aberrant over-expression of ZIP4 is associated with tumor progression and migration in pancreases (Li et al., 2007; Lin et al., 2013).

Zinc plays a significant role in mammary gland during lactation and ZIP5 is expressed on the plasma membrane of mammary epithelial cells which is participating in zinc supplementation to breast milk (McCormick et al., 2014). Interestingly, ZIP5 is being regulated reciprocally compared to ZIP4, that is ZIP5 presence on the cell surface is reduced during zinc-deplete conditions (Dufner-Beattie et al., 2004). ZIP5 was detected at the basolateral surface of pancreatic acinar cells which was indicated to take part in zinc removal from the blood through pancreas and protect cells from zinc-induced pancreatitis (Geiser et al., 2013). ZIP5 is also expressed in sclera and retina and involved in the development of eyeballs (Guo et al., 2014).

ZIP6 is also localized on the plasma membrane and functions as zinc importer. Maternally-derived ZIP6 together with ZIP10 controls zinc uptake to the human oocyte, driving oocyte-to-egg transition (Kong et al., 2014). Disruption of these ZIPs result in cell cycle arrest at a telophase I-like state due to insufficiency of the intracellular zinc quota, thus indicates ZIP6 and ZIP10 are essential for female gamete development (Kong et al., 2014). Also, ZIP6 has been shown as zinc uptake regulator in the resting neuroblastoma cells (Chowanadisai et al., 2008). Elevated expressions of ZIP6 and ZIP10 have been strongly linked with breast cancer where they promote cell motility by high glucose stimulation (Hogstrand et al., 2013, p. 6; Takatani-Nakase et al., 2014).

ZIP7 is localized in subcellular compartments including the ER and Golgi apparatus (Huang et al., 2005). In mammary gland, ZIP7 is highly expressed in the Golgi apparatus during

lactation in particular and exports zinc ions to the cytosol, suggesting those zinc ions accumulated to the Golgi by ZnT2 are being remobilized by ZIP7 during lactation (Kelleher et al., 2012). Disturbance of zinc homeostasis caused by abnormal ZIP7 expression enhances aggressiveness of breast carcinogenic phenotypes (Hogstrand et al., 2009; Taylor et al., 2008).

ZIP8 is localized in the plasma membrane, mitochondria, endosomes and lysosomes (Aydemir et al., 2009; He et al., 2006; Liu et al., 2013). In addition to zinc, ZIP8 can also transport iron, cadmium and manganese (Fujishiro et al., 2012). ZIP8 has been identified as the transporter responsible for cadmium-induced testicular toxicity in mice model experiments (Dalton et al., 2005).

Recombinant human ZIP9 characterization in DT40 chicken cells demonstrated TGN residence of the protein (Matsuura et al., 2009; Taniguchi et al., 2013). Dissimilar study has shown ZIP9 of Atlantic croaker to be an androgen receptor in the plasma membrane (Berg et al., 2014). In human pathogenesis, upregulation of ZIP9 is reported in malignant prostate and breast biopsies (Thomas et al., 2014).

ZIP11 is thought to be presented at the nucleus or Golgi but very little known about ZIP11 regulation (Martin et al., 2013).

ZIP12 is found on the plasma membrane of neuronal cells with a higher affinity to zinc compared to other ZIPs (K_m < 10 nM) and exhibits critical functions in neuronal differentiation by taking part in tubulin polymerization and neurite extension by facilitating influx of extracellular zinc into the cytosol (Chowanadisai et al., 2013).

ZIP13 is localized at the ER, Golgi apparatus and intracellular vesicles. ZIP13 moves zinc from the lumen of those compartments and plays decisive roles in cellular zinc-signaling close to

the ER region such as in BMP/TGF-β signaling pathways (Fukada et al., 2008). The *Zip13* gene is associated with spondylocheiro dysplastic Ehlers–Danlos syndrome (SCD-EDS), a heritable connective tissue disorder, due to ZIP13 loss of function (Bin et al., 2011; Giunta et al., 2008). Because of dysfunctional ZIP13, zinc ions are believed to be entrapped in the ER or in the zinc carrying vesicles between the ER and Golgi compartments by making it unavailable for use in the cell signaling (Jeong et al., 2012).

ZIP14 is a plasma membrane zinc importer and appeared to be involved in G-protein-coupled receptor (GPCR)-mediated cAMP signaling pathway (Hojyo et al., 2011). *Zip14* knock-out mice exhibited impaired skeletons and dwarf body sizes which were obvious growth defects. Similar to ZIP8, ZIP14 also has broader range of divalent metal ion specificity and is able to transport manganese, cadmium and iron apart from zinc (Fujishiro et al., 2012). The ability of ZIP14 to transport a nontransferrin-bound iron (NTBI) during iron-overload conditions is postulated to be physiological contribution of ZIP14 to iron homeostasis (Pinilla-Tenas et al., 2011).

1.2.7. Deficits in ZIP4 originate Acrodermatitis enteropathica

AE was first reported in 1936 when it was identified as familial pattern unique disease entity, often fatal with unknown cause ("Dermatitis in children with disturbances of the general condition and the absorption of food elements," 1936). It had taken more than 40 years to understand that the true cause of the disease is severe zinc deficiency due to zinc malabsorption in the small intestine, which enables zinc therapy to treat the patients (Barnes and Moynahan, 1973; Moynahan, 1974; Moynahan and Barnes, 1973). First genetic homozygous mapping was obtained from AE carrying Middle Eastern kindreds which placed defects on chromosome 8 (8q24.3)

(Wang et al., 2001). Shortly thereafter, the defective gene was determined as *SLC39A4*, which encodes the ZIP4 transporter (Küry et al., 2002, p. 4; Wang et al., 2002).

Currently, it is well known that AE is a genetically inherited autosomal recessive disorder, with estimated occurrence of 1 per 500,000 in newborn infants, with no discernible predilection to sex or race, and if not treated promptly by zinc therapy it can be eminently fatal (Van Wouwe, 1995). AE symptoms manifest within days in infancy, due to baby's inability to absorb enough zinc through gut because of defects in ZIP4. Although AE is mainly known as an inherited disease, it can be also acquired. For instance, TNZD manifests same symptoms as AE due to low zinc supplementation to the body from breast milk. Unfortunately, TNZD can be easily misdiagnosed as AE which could yield severe health implications with mistreatment due to zinc over-supplementation such as inducing copper deficiency linked to Wilson's disease (Yuzbasiyan-Gurkan et al., 1992). Because of that, the cause of zinc deficiency must be diagnosed accurately and carefully (Aggett et al., 1980; Lee et al., 1990). Another acquired form of AE is due to diets lacking appropriate amount of zinc that causes disorder in zinc metabolism. Reportedly by WHO, geographically marking, AE symptoms are more frequently encountered in children of poorer countries such as in Southeast Asia and sub-Saharan Africa where inadequate zinc consumption is one of major health problems (Shrimpton et al., 2005). The acquired form of AE generates similar symptoms as inherited one.

Genetic and Rare Disease (GARD) Information Center lists characteristics of AE as of (1) skin inflammation with blisters (pustular dermatitis), occurring around body openings such as the eyes, nose, mouth, ears, genitalia and anus. Usually followed by inflammation of skin on hands, elbows, knees, and feet (**Figure 1.6**). Skin lesions (vesicobullous) slowly evolve into erosions and patients can develop total alopecia (hair loss) without zinc therapy. (2) Mild or severe chronic

diarrhea with presence of excessive fat in the feces (steatorrhea), (3) cerebral cortical atrophy of the brain due to loss of brain cells which may lead to irritability and emotional disturbances in drastic phases. (4) Nail dystrophy due to malnourished tissue around the nails ("Acrodermatitis enteropathica | Genetic and Rare Diseases Information Center (GARD) – an NCATS Program," n.d.). Noteworthy to mention, not every AE-carrying patient may have all the symptoms, occurrence of symptoms may vary person to person.

Application of zinc therapy and supplementation of appropriate amount of zinc on daily basis alleviate symptoms of inherited AE, and patients usually have normal lives. Acquired form of AE can be treated much easily by simply replacement of multi-nutrient diet and then by gradually returning to regular diet where nutritionists recommend 10-15 mg of zinc per day is appropriate amount to sustain healthy adult life (Kambe et al., 2014). Given the fact that majority of population have good diet standards in the United States (US), zinc deficiency in the US is not that common (Maverakis et al., 2007). However, certain groups such as alcoholics, vegetarians, premature infants and the malnourished are subject to risk. Zinc bioavailability in meat products is much higher compared to plant food products, on top of that, presence of phytate in some of plant foods induces inhibitory effects in zinc absorption to the body. Therefore, daily zinc requirement for vegetarians may be 50% more than nonvegetarians. Studies suggest alcoholics may have low zinc status due to irregular diet and increased urinary excretion (Maverakis et al., 2007).

Inherited form of AE requires diligence treatment by zinc therapy. Theoretically believed, mutations in *SLC39A4* gene preclude function of ZIP4 transporter in zinc uptake, which is primarily expressed in small intestine and colon, and responsible for zinc uptake from diet. Normally once zinc is absorbed into enterocytes by ZIP4, ZnT family (mainly ZnT1 member)

facilitates efflux of zinc into the blood circulation. Therefore, blood zinc concentration status is a good indicator in diagnosis of AE. In average healthy person's serum zinc concentration is somewhere between 66 to 110 μg/dL (Roohani et al., 2013). Patients with AE may have zinc status as low as 40 μg/dL which is one of revealing indicators of the AE diagnosis (Hambidge et al., 1972; Walravens et al., 1983). Current zinc therapy includes 3 mg/kg/day of elemental zinc (50 mg of zinc in 220 mg of zinc sulfate) in AE treatment, that is ~20-fold higher compared to regular zinc dose for average sized adult person's requirement. Once zinc is ingested in excessive amount, presumably it goes through other low binding affinity transporters and/or paracellular routes.

Long term zinc over-supplementation has a theoretic risk of interfering copper absorption, thus has risk to emerge Wilson's disease due to copper deficiency (Yuzbasiyan-Gurkan et al., 1992). Side effects of extra zinc is known to lead to gastric irritation with nausea and vomiting. Accidental zinc overdoses may generate multisystem organ failure which may cause unfortunate fatality (Brocks et al., 1977). AE is formally documented in the website of Online Mendelian Inheritance in Man (OMIM®) with # 201100 tag and historic dates are highlighted relevant to AE development (https://www.omim.org/entry/201100).

Figure 1.6. AE symptoms and affected patients.
(A) to **(D)**, Sharply demarcated erythematous scaly plaques and pustules involving acral, periorificial, and anogenital areas in 13-years-old child. **(E)** and **(F)**, Erythematous eroded and symmetrical plaques involving periorificial, acral, and anogenital areas in infant. The images and caption are taken from (Maverakis et al., 2007) as is.

1.2.8. Mapping of AE-causing mutations

Earliest, the AE gene (*SLC39A4*; GeneID: 55630) was cloned in 2002 by two independent research groups (Küry et al., 2002; Wang et al., 2001), covering 4.5 kb of chromosomal region 8q24.3. The human *SLC39A4* gene is composed of 12 exons and 11 introns, encoding 647–amino acid protein, ZIP4, with 68 kDa size (GenBank RefSeq: NP_570901). In two separate studies more than fifty individuals, including a total of eighteen affected were tested from ten families which were known for AE-carriers because of family history. In one of the studies, pedigrees of eight Tunisian families had been assessed, placing deleterious mutations in both alleles in affected individuals, including nonsense mutations with premature stop codons encoding truncated proteins. In the same study, three homozygous missense mutations P200L, G374R and G526R were identified from AE-carrying members, concluding these are not merely common single-nucleotide polymorphisms (SNPs). Unaffected family members were tested either heterozygous or non-carriers (Küry et al., 2002). In the parallel study, voluntary members of AE-carrying Jordanian and Egyptian families were tested, adding another three distinct homozygous missense mutations of highly conserved residues, G330D, L372P and G630R to the AE-disease causing mutations list. In the same study, a French affected patient found to be carrying compound heterozygous missense mutation, N106K, while the other allele was identified harboring ~2-kb upstream deletion, thus verified the allele not being expressed (Wang et al., 2002). Since then, dozens of disease-causing missense variant case reports have been published, numerous SNPs have been identified and few review articles have been written updating the list of AE-disease causing mutations in the *SLC39A4* gene. Notably, fifteen of these missense mutations captured more interest throughout last two decades, in which seven of mutations (C62R, R95C, A99T, N106K, P200L, Q303H and C309Y) located in the ECD, whereas eight mutations (G330D, L372P, L410P,

G374R, G512W, G526R, G595V, and G630R) reside in the TMD (**Figure 1.5 B, C**) (Abu-Duhier et al., 2018; Kasana et al., 2015; Schmitt et al., 2009; Wang et al., 2002, 2008; Zhong et al., 2020). This thesis project solely focuses on the mutations at the ECD which discussed in later chapters. Although there are few scientific discrepancies among researchers involved in investigation of ZIP4 regulation and effect of mutant variants, overview of current opinion has been briefly concluded in this work. In short, functional studies and animal models of AE variants have been characterized fairly well, separating mutations into groups of unexpressed gene due to fragment deletions within promoter region; frameshifts; truncated immature proteins; missense mutations those hindering ZIP4 protein trafficking to the apical cell surface; and those not preventing surface presence.

Some of *SLC30* and *SLC39* genes characterized for harboring MREs in proximity of promoter region of the genes (Zheng et al., 2008). Bioinformatically, nine distinct MREs have been identified close to enhancer region of the *SLC39A4* gene (Schmitt et al., 2009). Seven out of nine putative MREs are located within frequently encountered ~2-kb upstream deletion, presumably accidental during recombination (Wang et al., 2002). Homozygous deletion state of the genes has been encountered in AE patients while heterozygosity appears to be not affecting significantly. Based on these observations, it has been hypothesized biallelic loss of the seven MREs could substantially reduce *SLC39A4* gene expression due to absence of MTF-1 activity and thereby alter zinc absorption. However, further experimental analysis is required to elucidate this deduction. (Schmitt et al., 2009).

The functional study of six AE-disease causing variants, one is within ECD (P200L) and the other five (G330D, L372P, G374R, G526R, and G630R) are located within TMD, had been carried with corresponding mutations (P200L, G340D, L382P, G384R, G539R and G643R) in

mouse ZIP4 (mZIP4) transiently expressed in HEK293 cells (Wang et al., 2004a). Among these six variants, four of them had diminished surface expression level associated with loss of N-glycosylation (G340D, L382P, G384R, G643R). Interestingly, total protein accumulation of L382P, G384R and G643R variants were substantially weaker and/or undetectable, due to presumable accelerated degradation by ER quality control mechanism. Despite high levels of total protein expression of the G340D variant, it considerably failed to localize at cell the surface. Other two alleles, P200L and G539R, were shown to have similar N-glycosylation compared to wild type and were able to localize in the plasma membrane. However, these mutations reduced uptake activity by ~70% whilst apparent K_ms were unaffected compared to wild type. Also, based on the authors' results, they have shown P200L and G539R variants are no longer responsive to post-translational endocytosis in zinc repleted condition (Wang et al., 2004a). First glimpse of AE-causing mutational investigations suggested that missense mutations are associated with loss of N-glycosylation, led to a misfolding and/or a mistrafficking. Those presented on the cell surface had diminished zinc uptake effectiveness and/or cause impairment in protein regulation. Recently, hZIP4 has been shown to mediate H^+/Zn^{2+} co-transport in pH dependent manner (Hoch et al., 2020). Also, in the same study, P200L variant in hZIP4 was shown to localize on the plasma membrane and mediate zinc transport just as wild type. Irreconcilably, another study in the hZIP4 has demonstrated pH independence of zinc transport activity, strongly questioning basis of H^+/Zn^{2+} co-transport mechanism (T. Zhang et al., 2020). Second part of this thesis work heavily focuses on implications of AE-disease causing mutations on the human protein. Collectively, functional, biochemical and biophysical data obtained in the second part of my thesis project evoke disparity between few of previously reported articles on this subject and deeming to shed light on the true cause of AE.

1.2.9. ZIP4 in Pancreatic Cancer

The pancreas is an organ locating in the abdomen behind the stomach of vertebrates, with two distinct physiological functions as an endocrine and a digestive exocrine gland. As an endocrine, pancreatic gland includes α, β and δ cells, in which α-cells help to control hypoglycemia by secreting the glucagon hormone. ZIP1, ZIP10 and ZIP14 are the most abundantly expressed ZIPs in the plasma membrane of α-cells and zinc acts as a signaling molecule to inhibit glucagon secretion (Gyulkhandanyan et al., 2008). Primary function of pancreatic β-cells is to regulate blood sugar level by insulin secretion, where previously stated zinc is important for insulin biosynthesis, storage and exocytosis (Dodson and Steiner, 1998; Emdin et al., 1980; Zalewski et al., 1994). Pancreatic β-cells shelter the highest cellular zinc concentration in the body and ZIP4 (Hardy et al., 2015) mediates zinc influx to the cytoplasm along with ZIP6 and ZIP7 (Liu et al., 2015) on the plasma membrane, whereas ZnT8 loads zinc into the zinc-rich granules to produce zinc-insulin complex (Chimienti et al., 2004). As an exocrine gland of digestive system, pancreatic acinar cells secrete enzymes to mixture of pancreatic juice to help food digestion. ZIP5 is primary zinc importer expressed on the plasma membrane of acinar cells (Geiser et al., 2013, p. 5) and ZnT2 uptakes zinc from the cytosolic pool to transport into the zymogen granules (Guo et al., 2010, p. 5).

The second leading cause of annual (2018) global death is cancer. Pancreatic cancer is the third leading cause of mortality due to cancer in the US according to the recent Cancer Statistics 2020 report with the lowest survival rate (9%) and no effective treatment due to absence of biomarkers to detect malignancy at early stages (Siegel et al., 2020). At metastatic stage pancreatic cancer considered to be untreatable and deadly. One of the first compelling implications came from Li et al. when they reported aberrant overexpression of *Zip4* mRNA in pancreatic cancer cells

suggesting ZIP4 transporter significantly contributes to human pancreatic carcinogenesis and tumor progression (Li et al., 2007). The discovery was followed by mouse model experiments which showed that when *Zip4* expressing mRNA was down-regulated in pancreatic cancer xenografts, survival of tumor implanted mice increased due to reduced cancer cell proliferation, migration and invasion (Li et al., 2009). They implied upregulation of *Zip4* mRNA in pancreatic tumor presumably increases zinc uptake and thereby zinc is important factor for cancer progression. ZIP4 suggested to be promising biomarker for pancreatic cancer and proposed as potential drug target for pancreatic cancer therapy. Short after, this presumption had been challenged by Costella et al., measuring actual zinc concertation by zinquin fluorescent staining and reporting it to be significantly lower in pancreatic adenocarcinoma compared with normal epithelium (Costello et al., 2011). In the same report downregulation of ZIP3 zinc importer was emphasized but ZIP4 was not quantified, although, they questioned *Zip4* mRNA upregulation does not necessarily mean overexpression of ZIP4 transporter (Costello et al., 2011). In similar study, mRNA of all ZnTs and ZIPs were downregulated except that of ZIP4 in the pancreatic cancer tissues (Yang et al., 2013).

Investigative field of ZIP4 involvement in carcinogenesis is still young, although one thing is certain that zinc homeostasis, ZIP4 and some other ZIPs (and ZnTs) are dysregulated in the pancreatic tumor cells. This pathogenesis should not be overlooked and pressing research demands should be applied by health-care organizations to unravel undisclosed questions.

1.3. SPECIFIC AIMS

Mechanism of ZIP transporters still remain unclear. Specifically, physiological and functional importance of the N-terminal ECD of LIV-1 subfamily is still to be established. Previous structural, biochemical and cell biological studies have indicated that ZIP4-ECD plays crucial role in optimal zinc uptake to the human cell, however, how ZIP4-ECD exerts such a role is still unclear. The first goal of this thesis project is to understand the molecular mechanism of ZIP4-ECD in zinc transport.

Notably, about half of the AE-causing mutations of ZIP4 occur within the ECD. However, how and why AE-causing mutations on ZIP4-ECD cause ZIP4 dysfunction is still not well elucidated. Especially, systematic analysis of AE-disease causing mutations on the human protein has not been done. The second goal of this thesis project is to clarify the molecular mechanism of ZIP4 dysfunction caused by the AE-causing mutations on ZIP4-ECD.

1.3.1. Specific aim 1: Characterize zinc binding on ZIP4-ECD.

The first crystal structure of ZIP4-ECD solved in Hu group has revealed several potential zinc binding sites and our preliminary data have demonstrated that isolated ZIP4-ECD has tendency towards zinc binding. We therefore hypothesized that zinc binding on ZIP4-ECD is crucial for ZIP4 function. In light of this, sub-specific aims of this thesis project are to:

1. Determine zinc binding affinity of ZIP4-ECD using fluorescence competitive titration.
2. Identify zinc binding site(s) using combined biochemical and structural approaches.
3. Clarify biological significance of zinc binding on ZIP4 function using a cell-based activity assay.
4. Investigate the effects of zinc binding on ZIP4-ECD structure using biophysical approaches.

1.3.2. Specific aim 2: Clarify the molecular mechanism of ZIP4 dysfunction due to AE-causing mutations on ZIP4-ECD.

Nearly half of the AE-causing missense mutations occur in ZIP4-ECD, and we hypothesized that these mutations may affect protein folding, reduce protein stability, impair zinc binding and alter the structure, all of which account for dysfunction of ZIP4 mutants. Considering these, sub-specific aims of this thesis project are to:

1. Examine the effects of AE-mutations on hZIP4 function in a cell-based activity assay.
2. Investigate post-translational modifications using Western-blot and proteases.
3. Locate AE-disease causing variants in the HEK293T cells using fluorescent tag and confocal laser scanning microscope.
4. Apply biophysical approaches to study folding and thermal stability of isolated ZIP4-ECD AE-disease causing variants *in vitro*.

CHAPTER 2

The histidine-rich loop in the extracellular domain of ZIP4 binds zinc and plays a role in zinc transport

Tuo Zhang[1,*], Eziz Kuliyev[2,*], Dexin Sui[1] and Jian Hu[1,2]

[1]Departments of Biochemistry and Molecular Biology & [2]Chemistry,

Michigan State University, East Lansing, MI, USA

[*]**These authors equally contributive to this work.**

Published in Biochemical Journal, June 2019, Volume 76, Issue 12, pg. 1791-1803.

This work was accomplished by an equal contribution between Dr. Tuo Zhang and I, which is indicated by our listing as co-first authors. Dr. Sui performed PCR and prepared necessary constructs. Dr. Hu helped designing experiments and writing the manuscript. I was able to obtain isolated pZIP4-ECD and crystallize in apo form (Figure 2.2) Dr. Zhang and I performed fluorescence competition titration through mutagenesis of potential zinc binding residues in the His-rich loop (Figure 2.4) and Dr. Zhang has generated data in Figure 2.3. I performed proteolysis assay of pZIP4-ECD (Figure 2.6) and CD spectra (Figure 2.7). I was responsible for implementing intrinsic fluorescence titration (Figure 2.8). Dr. Zhang was responsible for carrying out zinc uptake activity assay and generating (Figure 2.10) and I contributed to ensuring data reproducibility (Figure 2.10 A, B and D).

2.1. SUMMARY

The ZIP family mediates zinc influx from extracellular space or intracellular vesicles/organelles, playing a central role in systemic and cellular zinc homeostasis. Out of the 14 family members encoded in human genome, ZIP4 is exclusively responsible for zinc uptake from dietary food and dysfunctional mutations of ZIP4 cause a life-threatening genetic disorder, AE, and almost half of them found within the ECD. Previously we have shown that ZIP4–ECD is crucial for optimal zinc uptake but the underlying mechanism has not been clarified. In this work, we examined zinc binding to the isolated ZIP4–ECD from *Pteropus Alecto* and located zinc-binding sites with a low micromolar affinity within a histidine-rich loop ubiquitously present in ZIP4 proteins. Zinc binding to this protease-susceptible loop induces a small and highly localized structural perturbation. Mutagenesis and functional study on human ZIP4 by using an improved cell-based zinc uptake assay indicated that the histidine residues within this loop are not involved in preselection of metal substrate but play a role in promoting zinc transport. The possible function of the histidine-rich loop as a metal chaperone facilitating zinc binding to the transport site and/or a zinc sensor allosterically regulating the transport machinery was discussed. This work helps to establish the structure/function relationship of ZIP4 and also sheds light on other metal transporters and metalloproteins with clustered histidine residues.

2.2. INTRODUCTION

Out of the 14 ZIPs encoded in the human genome, ZIP4 is specifically expressed in gastrointestinal system where it plays an essential role in zinc uptake from dietary food (Jeong and Eide, 2013b). Our previous study has shown that deletion of the ECD reduces zinc transport activity of ZIP4 by 75% (Zhang et al., 2016), indicating that although ZIP4–ECD is not absolutely

required for ZIP4 function, it is crucial for optimal zinc transport. Besides its role in promoting zinc transport, ZIP4–ECD was also suggested to be involved in zinc sensing. For instance, it has been reported that an AE-causing mutation in the ECD largely abolished zinc-elicited endocytosis (Wang et al., 2004a). Another report showed that several AE-causing mutations in the ECD affected ZIP4 proteolysis triggered by zinc deficiency and since there are many conserved metal-chelating residues (cysteine, histidine, glutamate and aspartate) in ZIP4–ECD, it was suggested that these residues are potentially involved in zinc binding (Kambe and Andrews, 2009). In the structure of pZIP4–ECD (from *Pteropus Alecto*), it was found that all the eight invariant cysteine residues formed four disulfide bonds (Zhang et al., 2016). Based on the crystal structure of a prokaryotic ZIP (Zhang et al., 2017) and a coevolution-based computational model (Antala et al., 2015), we generate a human ZIP4 structure model (**Figure 2.1A**) where the histidine-rich loop in the ECD is in close proximity to the transport entrance and forms a potential zinc-binding site. Although sequence alignment across several closely related species indicates that this segment is highly variable (**Figure 2.1B**), the clustered histidine residues is a common feature of ZIP4, suggestive of a certain function.

In this work, we demonstrated that the histidine residues in the His-rich loop form the primary zinc-binding sites of pZIP4–ECD, and zinc binding to this highly dynamic and protease-susceptible loop induces a small and localized conformational change. Mutagenesis and functional assays on human ZIP4 showed that this loop is not involved in substrate selection, but plays a role in promoting zinc transport, partially accounting for the function of ZIP4–ECD.

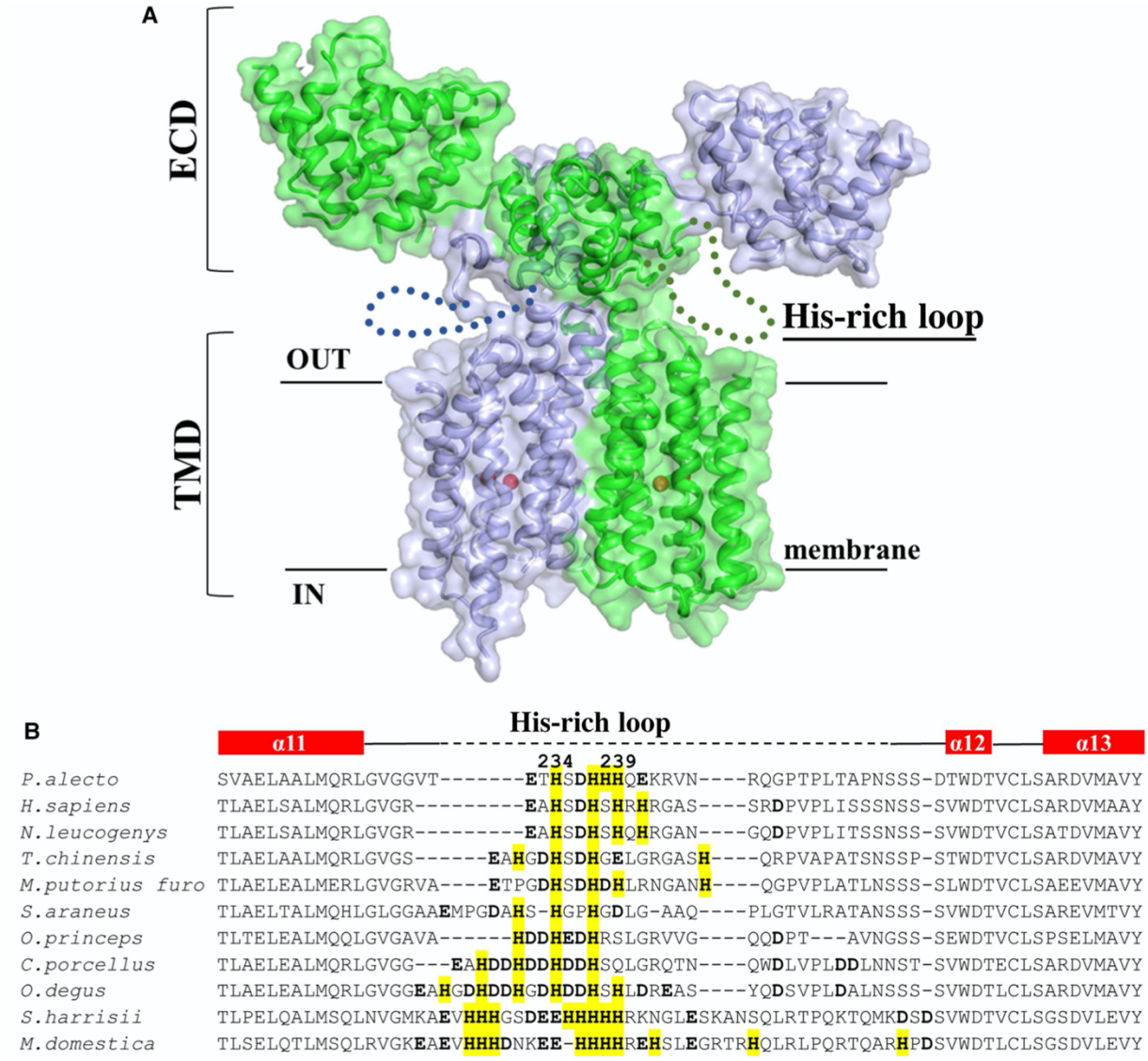

Figure 2.1. The His-rich loop in ZIP4–ECD.
(A) Structural model of the full-length human ZIP4 homodimer. The model was built based on structures of the pZIP4–ECD and a prokaryotic ZIP (Zhang et al., 2016, 2017). The dimerization interface of the TMD was adapted from a computational model of human ZIP4 with minor manual adjustment (Antala et a., 2015). The protein is shown in both cartoon mode and surface mode. The metal ions bound at the transport site are depicted as red balls. The unstructured His-rich loops are drawn as dotted lines. The length of the His-rich loop is roughly proportional to the number of amino acid residues. **(B)** Sequence alignment of the His-rich loops from closely related mammalian ZIP4s. The potential metal chelating residues within the loop are in bold and the histidine residues are highlighted. The secondary structure of pZIP4–ECD is shown on the top of the alignment. The first and the last histidine residues in the His-rich loop of pZIP4 are numbered.

2.3. MATERIALS AND METHODS

2.3.1. Transformation, protein expression and purification

The DNA encoding pZIP4–ECD (gene ID: ELK11751) was subcloned into a pLW01 vector (gift from Dr. Lucy Waskell at University of Michigan). The DNA plasmid was gently mixed with the *E. coli* strain of Origami™ B(DE3) pLysS (Novagen) and kept on ice for 30 min, and then heat shocked at 42°C for 60 seconds, followed by on ice for 2 mins. Then incubated at 37°C for 1hr by gently shaking in 2YT medium. Finally, culture was plated onto LB plate (with 100 μg/mL Ampicillin) and followed by overnight incubation at 37°C.

Scratched colonies were transferred to a flask with 1 L lysogeny broth (LB) medium with 100 μg/mL Ampicillin and were grown in a 37°C shaker until OD_{600} reaches to ~0.6. Afterwards, flasks were kept on ice for 30 mins and induced by 0.2 mM IPTG before transferring to 220 rpm overnight shaking at 16°C. Bacterial pellets were harvested by centrifuging at 6500 rpm in bottles. Cells were resuspended with purification buffer (Tris-HCl 20 mM pH 8.0, 300 mM NaCl, 10% Glycerol), and added 0.1% TX-100 and 1 mM PMSF as final concentrations to prepare for cell lysis. After cell lysis by sonication, the bacterial juice was centrifuged at 10,000 rpm for 50 mins at 4°C. Pellet was discarded and supernatant was kept for further purification.

pZIP4–ECD was purified using nickel-nitrilotriacetic acid column and eluted with 300 mM imidazole in purification buffer after washing three times. Collected protein sample were dialyzed in dialysis tubing (molecular weight cut-off: 6-8 kDa) into 2 L buffer (50 mM Tris-HCl pH 8.0 with 20 mM NaCl). with overnight magnetic stirring at 4°C. Then, protein sample was concentrated to 1-2mg/ml for N-terminal His_6-tag was removal by thrombin cleavage which was incubated with Thrombin enzyme for 5 hr at room temperature. Then, the protein treated by 10

mM EDTA as final concentration before purified by ion exchange chromatography on a Mono-Q column (GE Healthcare), followed by size-exclusion chromatography (GE Healthcare) in the buffer containing 10 mM HEPES, pH 7.3 and 100 mM NaCl or 10 mM Tris–H_2SO_4, pH 7.0 (**Figures 2.2A&B**). Final purity of protein was checked with reducing 10% SDS-PAGE gel (**Figure 2.2C**). The mutants were purified in the same way. Inductively coupled plasma mass spectrometry experiment confirmed the purified protein is in apo form (**Table 2.1**).

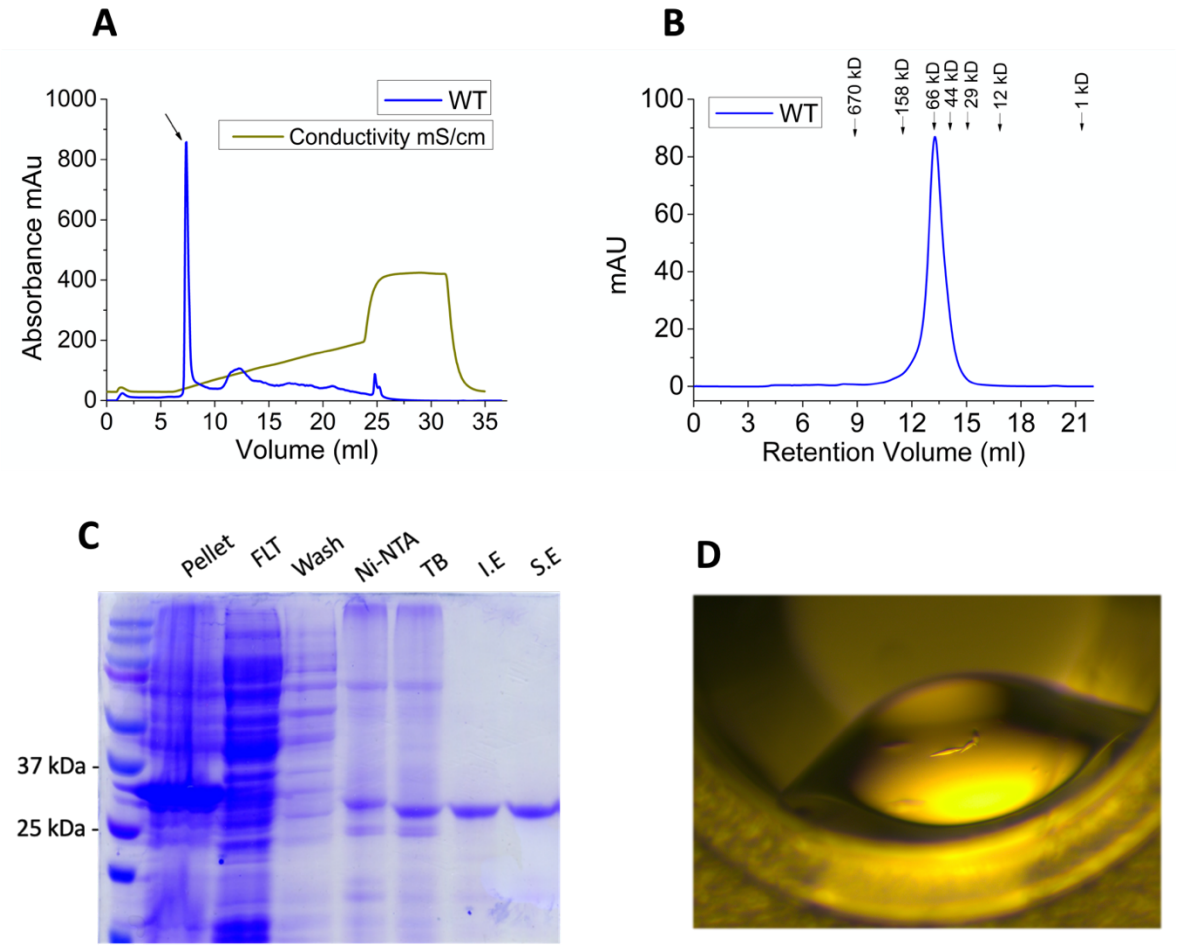

Figure 2.2. pZIP4-ECD purification and crystallization in apo form.
(A) Ion exchange chromatography profile of pZIP4-ECD purification. Collected dimer sample shown with arrow. **(B)** Profile of size-exclusion chromatography. Corresponding particle sizes to retention volume are shown on top of graph. **(C)** 10% SDS-PAGE with sample order: pellet, flow-through (FLT), wash, Ni-NTA, thrombin cleavage (TB), ion exchange (I.E), size-exclusion (S.E). **(D)** Apo pZIP4-ECD crystals in 100 mM MES, 100 mM NH_4Cl, 17% PEG 3350, pH 6.5 condition.

2.3.2. Fluorescence Titration

To determine the dissociation constant towards zinc ions, FluoZin-1 (Thermo Fisher Scientific) was dissolved in a buffer containing 50 mM HEPES pH 7.3, 100 mM NaCl at the concentration of 5 μM, and titrated with the indicated concentration of $ZnCl_2$. The fluorescence spectra were recorded at 25°C in a 0.5 cm × 1 cm quartz cuvette in the same buffer. The fluorescence was excited at the wavelength of 490 nm and the spectra were recorded in the range of 500–650 nm (Cary Eclipse Fluorescence Spectrophotometer, Agilent). The excitation and emission slits were set to 2.5 and 5 nm, respectively. For the competition titration, 10 μM apo form pZIP4–ECD was mixed with 5 μM FluoZin-1 in the same buffer and titration was performed in the same way. Free zinc concentrations were calculated using the recorded fluorescence intensity and the determined apparent K_d of FluoZin-1, and zinc occupancies (the number of bound zinc ions per protein molecule) were calculated using the followed equations:

$$T_{Zn} = [Zn] + [Zn \cdot Dye] + [Zn \cdot P] \quad (1)$$

$$T_{Dye} = [Dye] + [Zn \cdot Dye] \quad (2)$$

$$T_P = [P] + [Zn \cdot P] \quad (3)$$

$$K_{d,Dye} = [Zn] \times [Dye]/[Zn \cdot Dye] \quad (4)$$

$$F/F_{max} = [Zn \cdot Dye]/T_{Dye} \quad (5)$$

$$Occupancy = [Zn \cdot P]/T_P \quad (6)$$

Where T_{Zn}: total Zn concentration, T_{Dye}: total FluoZin-1 concentration, T_p: total protein concentration, [Zn]: free Zn^{2+} concentration, [Dye]: free FluoZin-1 concentration, [P]: apo form protein concentration, [Zn·Dye]: Zn-FluoZin-1 complex concentration, and [Zn·P]: Zn–protein

complex concentration, K_d: dissociation constant, F/F_{max}: normalized fluorescence change. F_{max} was measured by adding zinc up to 1 mM at the end of the titration. The fluorescence intensities have been calibrated to compensate volume change during titration. To obtain apparent dissociation constant, occupancy (y) was plotted against free zinc concentration (x) and then curve fitting was conducted using the Hill model (OriginPro 8.5):

$$y = B_{max} \times x^n/(K_d^n + x^n) \qquad (7)$$

where B_{max} is the number of binding sites and the Hill coefficient (n) indicates the cooperation among the binding sites. To estimate the averaged apparent dissociation constants of the first two zinc-binding sites, B_{max} was set at 2 and only the data with free zinc concentration below 3 μM were used to minimize the effects of additional low-affinity zinc-binding sites on curve fitting.

Table 2.1. Detection of residual zinc in pZIP4-ECD using ICP-MS

Sample	Zn (ppb)	Zn (nM)	Signal stability (%)
nitric blank	0.165	2.52	8.0
10 mM Tris buffer	6.707	102.5	0.9
650 nM pZIP4-ECD in Tris buffer	5.017	76.7	1.2

2.3.3. Trypsin proteolysis

To optimize the partial proteolysis condition, 2 μl of trypsin dissolved in water with variable stock concentrations was added into 18 μl pZIP4–ECD (0.15 mg/ml in 10 mM Tris–H_2SO_4, pH 7.0). After incubation at room temperature for 20 min, the reaction was stopped by adding 6 μl l of SDS–PAGE loading buffer containing 1 mM PMSF. To test the effects of zinc ions on partial proteolysis, the reaction was performed in the presence of different concentrations

of $ZnSO_4$ at the optimized protein:trypsin ratio (300:1, m/m). Partial proteolysis was analyzed by SDS–PAGE.

2.3.4. Mass spectrometry of pZIP4-ECD and its proteolytic fragments

The unprocessed and fully processed pZIP4–ECD by trypsin in 10 mM Tris–H_2SO_4, pH 7.0 were analyzed using a Waters G2-XS quadrupole-time-of-flight mass spectrometer using electrospray ionization (ESI–TOF– MS) operating in positive ion mode and scanning a mass range of m/z 200–2000 with 1 scan per second. Protein mass spectra were deconvoluted using the MaxEnt algorithm in the Waters Masslynx software package.

2.3.5. Circular Dichroism

The circular dichroism (CD) spectra of 6 μM pZIP4–ECD or the mutant in 10 mM Tris–H_2SO_4 (pH 7.0) were recorded in a 1 mm quartz cuvette by using a Chirascan™ CD Spectrometer. Concentrations of the proteins were measured by using a NanoDrop ND-1000 Spectrophotometer. In zinc titration, aliquots of 3.75 μl $ZnSO_4$ were sequentially added into 300 μl protein samples. The $ZnSO_4$ stock solutions were made in water without buffer or any other salt. After adding $ZnSO_4$, the samples were allowed to balance at room temperature for 5 min before the spectra were scanned. Three scans were recorded and averaged at each step. The CD spectra were analyzed using the K2D3 server at http://cbdm-01.zdv.uni-mainz.de/~andrade/k2d3/.

2.3.6. Intrinsic tryptophan fluorescence titration

Intrinsic tryptophan fluorescence spectra of 5 μM pZIP4–ECD or the mutant in 10 mM Tris–H_2SO_4 (pH 7.0) were recorded in a 10 mm quartz cuvette by using a Varian Cary Eclipse Fluorescence Spectrophotometer. Aliquots of 2.8 μl of $ZnSO_4$ were sequentially added into the

cuvette containing 700 µl protein sample. Excitation wavelength was 295 nm and ex/em slits were set to 5 nm/5 nm. After adding $ZnSO_4$, the samples were allowed to balance at room temperature for 5 min before the spectra were recorded in the range of 310– 410 nm. Three scans were averaged at each step. Zinc titration to the wild-type pZIP4–ECD in the presence of 10 mM EDTA was conducted in the same way.

2.3.7. Cell Culture and Transfection

The complementary DNA of human ZIP4 from Mammalian Gene Collection was purchased from GE Healthcare (Gene ID: BC062625). hZIP4 was subcloned into a modified pEGFP-N1 vector (Clonetech) in which the downstream EGFP gene was deleted and an HA tag was inserted before the stop codon. All the mutations were made using QuikChange mutagenesis kit (Agilent) and Wizard® Genomic Kit was used for DNA purification.

Human embryonic kidney cells (HEK293T, ATCC) were cultured in Dulbecco's modified Eagle medium (DMEM, Invitrogen) supplemented with 10% (v/v) fetal bovine serum (Invitrogen) and Gibco Antibiotic–Antimycotic (Invitrogen). Zinc depletion medium was prepared using Chelex 100 (Bio-Rad). A suspension of 1.3% (w/v) Chelex 100 beads in DMEM medium supplemented with 10% fetal bovine serum was incubated at 4°C for 2 h with a constant gentle shake, followed by filtration of the supernatant through a 0.22 mm filter. Cells were seeded on 24-wells trays for 16 h in basal medium, followed by transiently transfection with an expression vector containing human ZIP4 gene (gene ID: BC062625) by the Lipofectamine 2000 reagent (Invitrogen). Cells were allowed to grow for another 36 h before $^{65}Zn^{2+}$ uptake and ZIP4 surface expression assays.

2.3.8. ^{65}Zinc uptake assay

HEK293T cells were washed by zinc uptake buffer (10 mM HEPES pH 7.3, 142 mM NaCl, 10 mM Glucose, 5 mM KCl) and then incubated with the indicated concentration of $ZnCl_2$ (containing 40% $^{65}ZnCl_2$) in the Chelex-treated media at 37°C for 20 min with occasional gentle shaking. Uptake was stopped by adding the same volume of stop buffer (ice-cold zinc uptake buffer with 1 mM EDTA) and cells were collected into Eppendorf tubes on ice. Cells were gently washed two times by zinc uptake buffer and lysed in 0.5% Triton X-100. Cell-associated radioactivity was measured with a Packard Cobra Auto-Gamma γ-counter and the amount of zinc was calculated using a standard $^{65}Zn^{2+}$ radioactivity curve. The cells transfected with the vector without inserted ZIP4 gene (empty vector) were treated in the same way and used as control in the assay. The amount of zinc transported into the cells through hZIP4 was calculated by subtracting the zinc uptake in control cells from the zinc uptake in the cells transfected with hZIP4–HA. The zinc uptake rate is expressed as pmol min^{-1} mg^{-1} protein and the total protein concentrations in the samples were measured using Bradford method (Bio-Rad). The zinc uptake data were firstly calibrated with the surface expression level and then fitted using the Michaelis–Menten equation. Metal selectivity of hZIP4 was carried out with 10 μM $ZnCl_2$ (containing 40% $^{65}ZnCl_2$) plus non-radioactive $ZnCl_2$, $CaCl_2$, $MgCl_2$, $CoCl_2$, $NiCl_2$, $CuSO_4$ and $MnCl_2$ at 200 μM, 2 mM, 20 mM, 200 μM, 200 μM, 200 μM and 200 μM, respectively. The same experiment was also conducted in the presence of 200 μM $FeSO_4$ and 1 mM ascorbic acid. Each individual experiment included three repeats, and statistical significance was tested with the Student's *t*-test.

2.3.9. hZIP4-HA surface expression assay

hZIP4–HA expressed at the plasma membrane was indicated by the surface-bound anti-HA antibodies recognizing the C-terminal HA tag of hZIP4. After washing twice with Dulbecco's

phosphate-buffered saline (DPBS), cells were fixed for 5 min in 4% formaldehyde at room temperature. Cells were then washed three times in DPBS and incubated with 3 μg/ml anti-HA antibody (Invitrogen) diluted with 5% BSA in DPBS for 2 hr at room temperature. Cells were washed five times with DPBS to remove unbound antibodies and then lysed in SDS–PAGE loading buffer. The anti-HA antibody bound to the surface hZIP4–HA in cell lysates was detected in Western blot with HRP-conjugated goat anti-mouse immunoglobulin-G (1:2500). As a loading control, β-actin levels were detected using an anti-β-actin antibody (1:2500) followed by a goat anti-rabbit immunoglobulin-G (1:3000) by chemiluminescence. All antibodies were purchased from Cell Signaling Technology unless indicated otherwise.

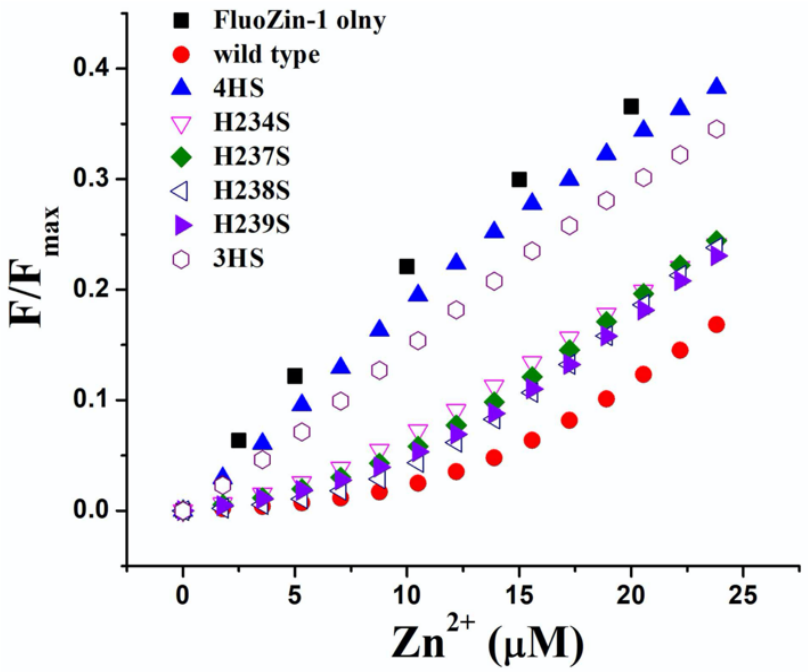

Figure 2.3. Zinc binding to pZIP4–ECD.
FluoZin-1 (5 μM) was titrated by $ZnCl_2$ in the absence and presence of pZIP4–ECD or the His-rich loop mutants (10 μM). The apparent zinc binding affinities were estimated and shown in Figure 2.4.

2.4. RESULTS

2.4.1. The his-rich loop contains multiple primary zinc binding sites in pZIP4-ECD

To test zinc binding to ZIP4–ECD, we conducted zinc titration in the presence of a zinc-specific fluorescence probe, FluoZin-1, of which fluorescence intensity increases upon zinc binding (Lin et al., 2010). Zinc-specific fluorescence probes have been used in estimating zinc-binding affinity of a variety of proteins through competition titration (Bauer et al., 2008; Krężel and Maret, 2007). As shown in **Figure 2.4A**, we firstly measured the zinc-binding affinity of FluoZin-1 under our experimental condition. After curve fitting using the one-site model, we obtained an apparent dis- sociation constant (K_d) of 29 μM, which is larger than the reported value (8 μM). We reason that salt included in the buffer reduced zinc binding to FluoZin-1. We then included the purified pZIP4–ECD in apo form as a zinc competitor in titration (**Figure 2.3**). The zinc-binding curve of FluoZin-1 was significantly right-shifted and there was only very small fluorescence increase at the beginning of the titration, indicating that pZIP4–ECD binds zinc ions with an affinity much higher than FluoZin-1. By using the experimentally determined apparent K_d of FluoZin-1 and the fluorescence intensities measured during titration, we calculated and plotted the number of bound zinc ion per protein (zinc occupancy) against free zinc concentration. Curve fitting using the Hill model allowed us to estimate the averaged dissociation constant (0.62 μM) for the first two zinc-binding sites (**Figure 2.4B**, see details in Materials and methods).

To locate the metal binding sites in pZIP4–ECD, we tried to obtain the co-structure by either co-crystallization or soaking the apo protein crystals with zinc ions (**Figure 2.2D**), but these trials failed due to lack of crystal in the presence of zinc or destroyed crystal lattice upon zinc soaking. Potential metal binding sites can be identified by manually checking the apo form structure (**Figure 2.5**), but none of them, except for the His-rich loop (**Figure 2.1**), contains more

than one histidine residue which is highly preferred for zinc ion binding. We then focused on the His-rich loop of pZIP4–ECD, which contains four clustered histidine residues (H234, H237, H238 and H239). To examine their roles in zinc binding, we mutated all the histidine residues into serine residues (the 4HS mutant). Compared with alanine, serine was chosen to preserve hydrophilicity, which would produce less structural disturbances caused by mutations. Indeed, the CD spectrum of the purified 4HS mutant is essentially the same as that of the wild-type pZIP4–ECD (**Figure 2.7A**). As shown in **Figure 2.3**, the 4HS mutant protein barely shifted the zinc-binding curve of FluoZin-1, indicating that the primary high-affinity zinc-binding sites have been eliminated by the mutations. This result unambiguously demonstrated that the primary zinc-binding sites of pZIP4–ECD are only present in the His-rich loop. Similar to the 4HS mutant, the H237S/H238S/H239S triple mutant (the 3HS mutant) only slightly shifted the zinc-binding curve, indicating that a single histidine residue (H234) is not adequate to support zinc binding with low micromolar affinity. To further dissect the role of each histidine residue, we made four His-to-Ser single mutations (H234S, H237S, H238S and H239S) and tested zinc binding under the same condition (**Figure 2.3**). The results showed that, when compared with the wild-type protein, the mutants caused a smaller right-shift of the zinc-binding curve, suggestive of reduced zinc-binding affinity (**Figure 2.4B**). Therefore, the four histidine residues are all contributive to zinc binding and their effects appear to be additive. It is plausible that there is no defined zinc-binding mode in the His-rich loop. Instead, as suggested in a recent NMR study of the intracellular His-rich loop of hZIP4 (Bafaro et al., 2019), the zinc-bound state can be best described as a conformational ensemble where zinc ion is co-ordinated with several combinations of histidine residues. As shown in **Figure 2.1**, close to the histidine residues, there are two carboxylate residues (E232 and D236) which may be potentially involved in zinc binding. We then made two mutants (E232S and D236S) and found

that these mutations did not affect zinc-binding capacity of pZIP4–ECD (**Figure 2.4C**), reinforcing the notion that zinc binding at the His-rich loop is primarily mediated by the four histidine residues.

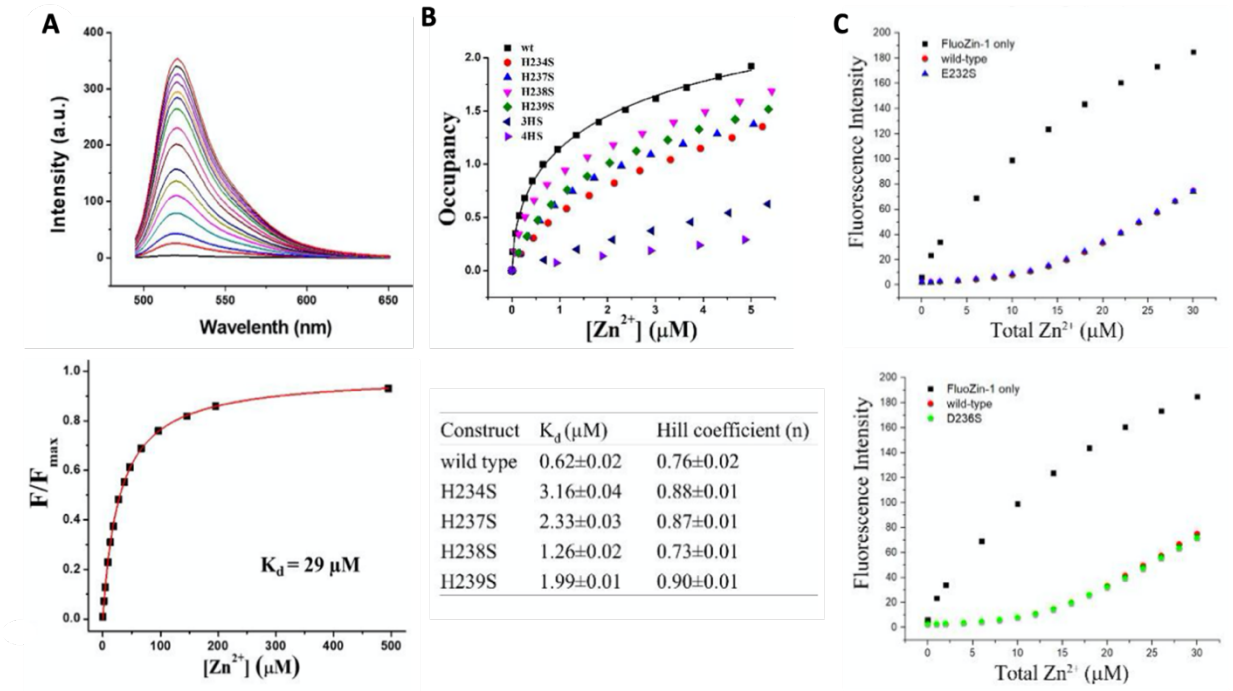

Construct	K_d (μM)	Hill coefficient (n)
wild type	0.62±0.02	0.76±0.02
H234S	3.16±0.04	0.88±0.01
H237S	2.33±0.03	0.87±0.01
H238S	1.26±0.02	0.73±0.01
H239S	1.99±0.01	0.90±0.01

Figure 2.4. Estimation of zinc binding affinity.
(A) Determination of apparent dissociation constant (K_d) of Zn^{2+}/FluoZin-1 complex under the experimental condition. The fluorescence spectra in zinc titration are shown on the left, and the curve fitting using one-site model is on the right. **(B)** Estimation of apparent K_ds of the wild type pZIP4-ECD and the mutants. The number of bound zinc ion per protein molecule (Zn/Protein) and free zinc concentration ($[Zn^{2+}]$) were calculated based on the determined FluoZin-1 affinity shown in **(A)** and the measured fluorescence intensities during titration. The Hill model was used for curve fitting. Note that when free zinc concentration is higher than 3 μM, the zinc binding curves became linear, suggestive of additional low-affinity zinc binding sites. To minimize their effects on curve fitting, only the data with free zinc concentration lower than 3 μM were used. In order to obtain the averaged K_d of the first two zinc binding sites, the number of binding site (B_{max}) was set at 2. **(C)** Zinc binding to FluoZin-1 in the presence of the wild type pZIP4-ECD or the his-rich loop mutants. *Left:* E232S. *Right:* D236S. FluoZin-1 (5 μM) was titrated by $ZnCl_2$ in the presence of pZIP4-ECD or the mutants (10 μM) in the buffer containing 10 mM Hepes, pH 7.3, 100 mM NaCl.

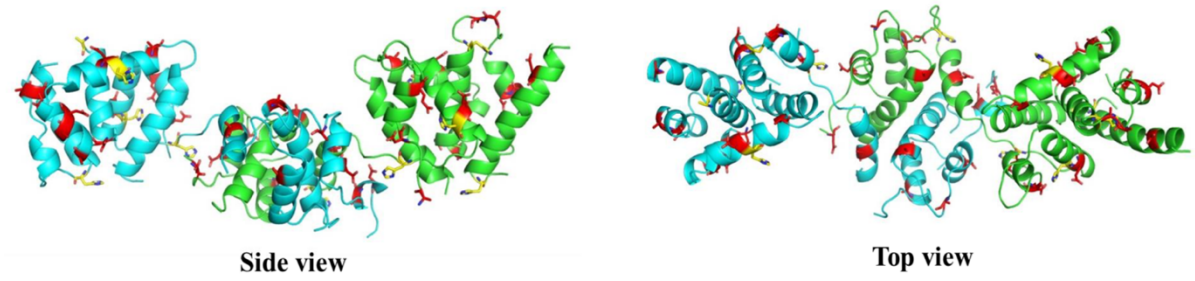

Figure 2.5. Mapping of potential metal sites in the apo form structure of pZIP4-ECD. The putative metal chelating residues are shown in stick mode. The aspartate and glutamate residues are in red and the histidine residues are in yellow.

2.4.2. The his-rich loop is a solvent-exposed, highly flexible and unstructured region.

During pZIP4–ECD purification, we noticed that the protein is highly vulnerable to proteolysis. We then used partial proteolysis and mass spectrometry to locate the most vulnerable region. As shown in **Figure 2.6A**, incubation of pZIP4–ECD with trypsin at a mass ratio of 300:1 (protein:protease) at room temperature for 20 min led to ~50% digestion of the full-length protein and incubation with more trypsin led to a fully processed and protease-resistant species with an apparent molecular mass of 24 kDa. ESI–TOF–MS analysis showed that the primary cleavage sites are all within the His-rich loop (**Figure 2.6B**). This result suggested that the His-rich loop must be most solvent exposed and largely unfolded so that the protease can reach and process it at a rate much higher than proteolysis at other potential cleavage sites. This deduction is consistent with the observation in the crystal structure of pZIP4–ECD where the His-rich loop is severely disordered, as well as the prediction by PSIPRED that the His-rich loop has no secondary structure. The highly superimposable CD spectra of the wild-type pZIP4–ECD and the 4HS mutant also supported that the histidine residues are not involved in secondary structure formation (**Figure 2.7A**).

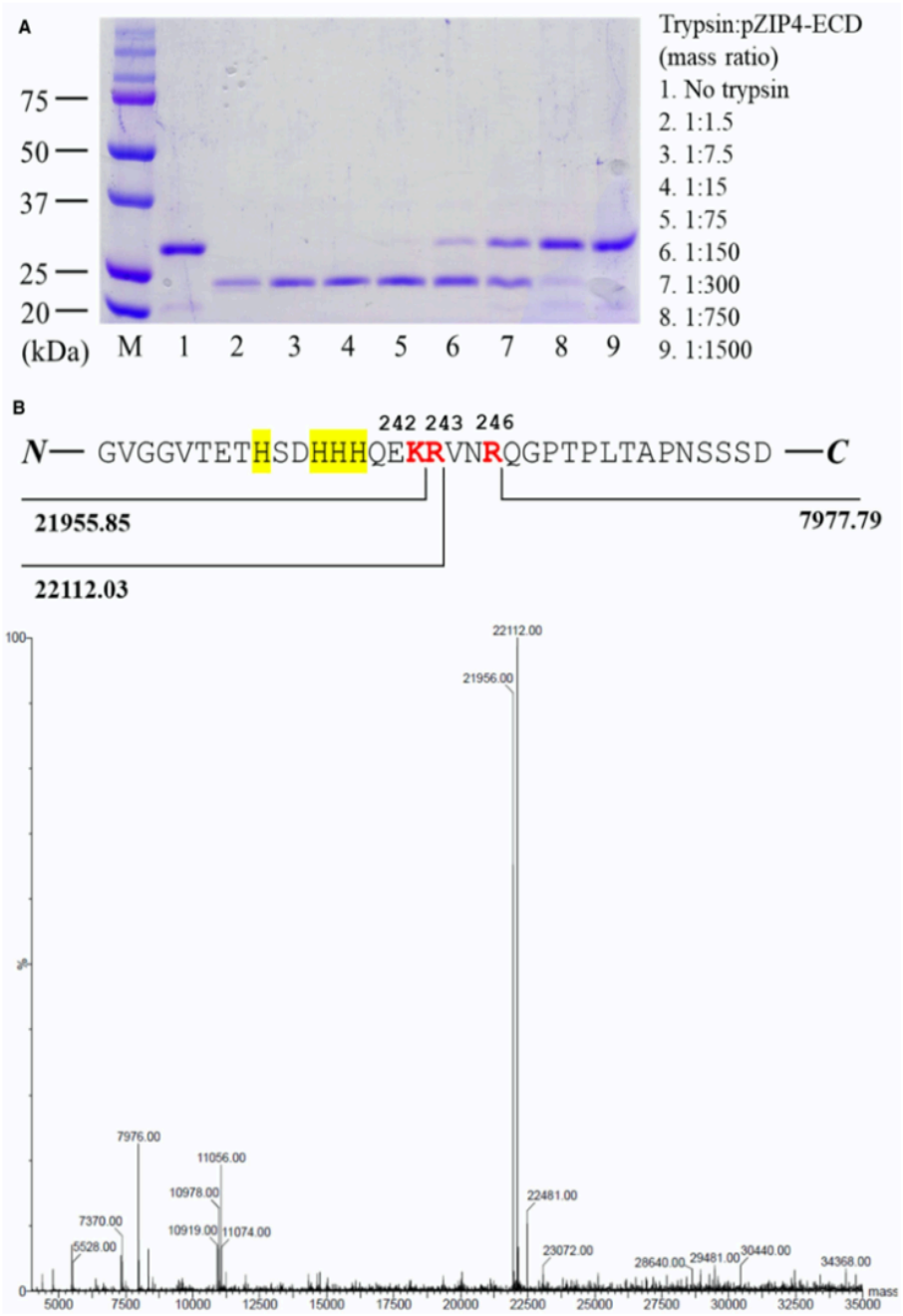

Figure 2.6. Proteolysis of pZIP4–ECD by trypsin.
(A) pZIP4–ECD proteolysis by indicated amount of trypsin. The concentration of pZIP4–ECD is 0.15 mg/ml (5 μM). The trypsin band (~24 kDa) could be overlapped with the proteolytic products in SDS–PAGE. **(B)** ESI–TOF–MS spectrum of the fully processed pZIP4–ECD by trypsin (sample 5 in **(A)**). The assigned fragments are underlined in the spectrum. The determined cleavage sites in the His-rich loop are colored in red. Note that the disulfide bonds within each fragment have been considered in the calculation of the theoretical average molecular mass.

2.4.3. Zinc binding to the his-rich loop induces only minor and localized structural changes

Since the His-rich loop binds zinc ions, we are interested in examining the effects of zinc binding on the structure of pZIP4–ECD. We firstly compared the CD spectra of pZIP4–ECD in a zinc titration experiment. As shown in **Figure 2.7B**, addition of $ZnSO_4$ up to 24 μM to the apo form pZIP4–ECD (6 μM) did not lead to a significant change in spectrum. Adding zinc higher than 30 μM caused protein precipitation. Given the estimated binding affinities of pZIP4–ECD towards zinc ions (**Figure 2.4**), the zinc-binding sites in the His-rich loop must have been saturated before protein precipitation. Therefore, the lack of CD spectrum change indicated that zinc binding to the His-rich loop did not affect the secondary structure of pZIP4–ECD.

We then tested whether zinc binding has any effect on the intrinsic fluorescence of pZIP4–ECD, which is a sensitive indicator of conformational changes. We found that although the peak wavelength of the fluorescence spectra (332 nm) was not shifted upon zinc binding, a small but significant decrease in fluorescence intensity was observed (**Figure 2.8A**), suggestive of structural changes around the fluorophores. When excited at 295 nm, the fluorescence changes generally reflected the local environment changes of the tryptophan residues (W111, W262 and W289, **Figure 2.9**). As W111 and W289 are buried in the N-terminal subdomain and the C-terminal subdomain, respectively, W262, which is immediately downstream of the His-rich loop, is most likely responsible for the decreased fluorescence intensity. To test whether zinc binding at the His-rich loop causes fluorescence decrease, we conducted the same zinc titration experiment on the 4HS mutant. As shown in **Figure 2.8A&B**, adding zinc only resulted in a small decrease in fluorescence intensity at 332 nm, confirming that zinc binding to the histidine residues is responsible for the decreased fluorescence intensity of the wild- type protein during titration.

If zinc binding greatly affects the structural and dynamic properties of the His-rich loop, a changed protease susceptibility would be expected. As shown in **Figure 2.8C**, zinc appears to partially protect pZIP4–ECD from proteolysis by trypsin, particularly when zinc concentration is at or higher than 20 μM, suggesting that zinc binding may slightly affect the structure of the His-rich loop and its surrounding residues. Collectively, the small intrinsic fluorescence change and the partial protective effect against proteolysis reflect a highly localized structural change induced by zinc binding to the His-rich loop.

2.4.4. The his-rich loop plays a minor role in zinc transport of human ZIP4

Next, we examined the role of the clustered histidine residues in the His-rich loop for hZIP4 function. Because the amino acid sequence of the His-rich loop of pZIP4 has considerable similarity to its counterpart in hZIP4 (**Figure 2.1B**), we think the overall structural features and zinc-binding properties of pZIP4–ECD should be largely preserved in hZIP4. To test hZIP4 function, we conducted zinc uptake assay on hZIP4–HA (C-terminal HA tag) transiently expressed in HEK293T cells in the Chelex-treated cell culture media, rather than the zinc uptake buffer we used before (Zhang et al., 2017, 2016). Markedly, we found that the cells transfected with the empty vector absorbed much less radioactive ^{65}Zn than the cells expressing hZIP4 (**Figure 2.10D**), resulting in a considerably reduced background level allowing for detection of a small change in zinc transport activity. We reasoned that the serum proteins in the Chelex-treated culture media sequestered zinc ions from solution (Cp and L, 2002; Wang et al., 2004b), which suppressed zinc transport through HEK293T cells' endogenous zinc uptake systems much more than the overexpressed hZIP4. By using this approach, we compared the zinc uptake activities of the wild type hZIP4 and the 4HS mutant (H238S/H241S/H243S/H245S). After calibration of zinc uptake activity using hZIP4–HA surface expression level, we found that the V_{max} of the 4HS mutant

decreased by ~20%, whereas the K_m was not affected (**Figure 2.10A**). The cell surface expression level and the extent of glycosylation did not indicate any issue of misfolding and/or mistrafficking of the 4HS mutant.

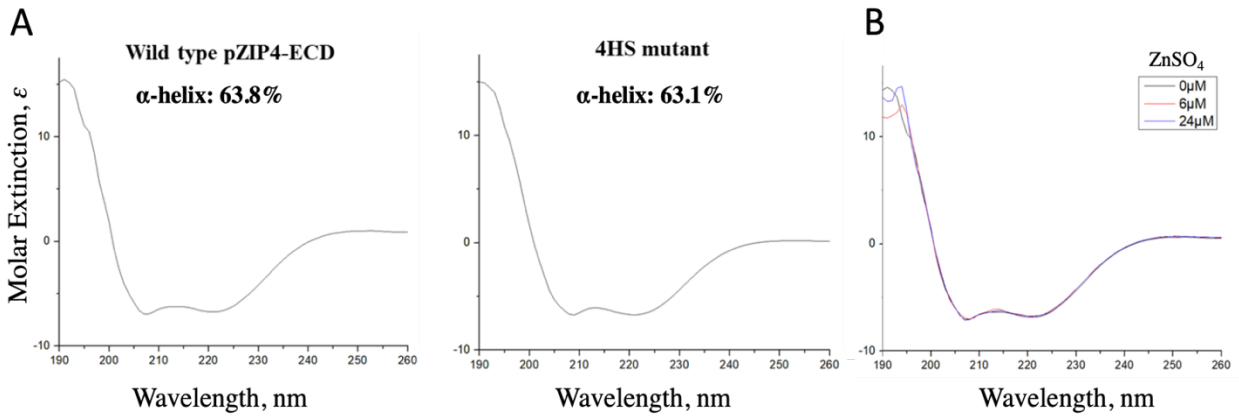

Figure 2.7. CD spectra of wild type pZIP4-ECD and 4HS mutant.
(A) CD spectra of the wild type pZIP4-ECD and the 4HS mutant. The curve fitting and the secondary structure contents estimated at the K2D3 server. **(B)** CD spectra of 6 μM wild type protein in the absence and presence of $ZnSO_4$ at the indicated concentrations.

Considering that the His-rich loop is right on the top of the transport entrance, it is plausible that it may function as an extracellular filter conducing a preselection of metal substrate. To test this, we firstly conducted zinc uptake assay in the presence of the excessive amount of several other divalent metal ions (Ca^{2+}, Mg^{2+}, Co^{2+}, Ni^{2+}, Cu^{2+} and Mn^{2+}) (**Figure 2.10B**). The results indicated that only non-radioactive Zn^{2+} greatly and significantly reduced ^{65}Zn uptake, which is consistent with the notion that hZIP4 is a zinc-specific transporter. If the His-rich loop is contributive to zinc specificity by preselecting zinc ions over other metal ions, the 4HS mutant devoid of all the histidine residues would exhibit lower zinc transport activity in the presence of other metal ions. However, the result did not support this hypothesis as none of the tested metal ions, except for the non-radioactive Zn^{2+}, substantially reduced zinc transport activity. Taken

together, the functional characterization of the 4HS mutant suggested that the His-rich loop is involved in zinc transport but does not play a role in preselecting metal substrate.

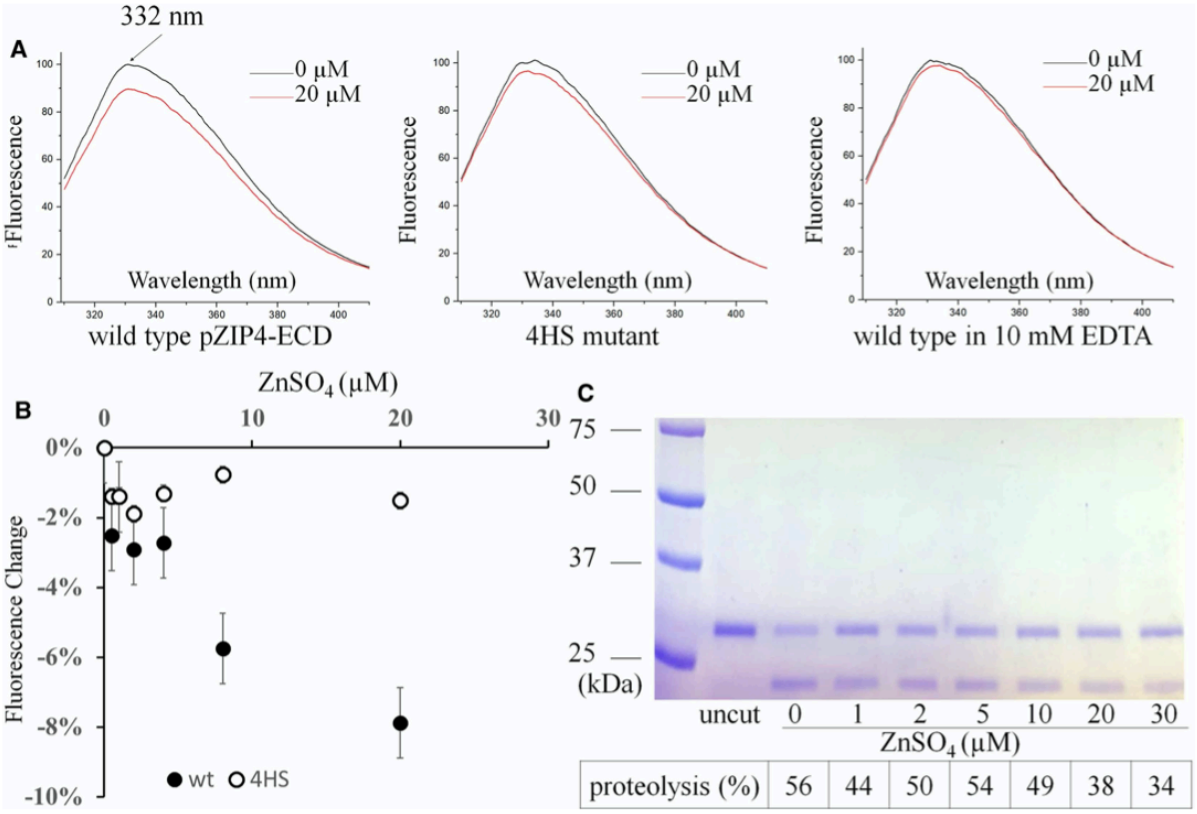

Figure 2.8. Detection of zinc-induced conformational change of pZIP4–ECD.
(A) Fluorescence spectra of pZIP4–ECD and the 4HS mutant in the absence and presence of zinc. **(B)** Fluorescence intensity changes at 332 nm of the wild-type protein and the 4HS mutant during zinc titration. Non-specific effect of zinc ion on fluorescence (the third panel in **(A)**) was subtracted. **(C)** Partial proteolysis of pZIP4–ECD (6 μM) in the presence of zinc sulfate at the indicated concentrations. Trypsin was added at the mass ratio of 300:1 (pZIP4–ECD:protease). Proteolysis was quantified and shown as a percentage below each lane.

2.5. DISCUSSION

The His-rich loop in the N-terminal ECD is a common feature of ZIP4, but so far there is no characterization of this loop except that it was shown to be severely disordered in the crystal lattice (Zhang et al., 2016). In this work, we found that the His-rich loop of pZIP4–ECD harbors at least two zinc-binding sites with low micromolar affinity (**Figure 2.3 and Figure 2.4**). Biochemical and biophysical characterization showed that zinc binding at this protease-susceptible and highly dynamic loop only induces small and localized conformational changes (**Figures 2.6 and 2.8**). Mutagenesis and functional characterization indicated that the histidine residues in this loop play a role in zinc transport (**Figure 2.10**). These data allowed us to make a discussion in terms of the putative function of this loop.

The structural model of the full-length hZIP4 suggests the His-rich loop is right on the top of the TMD and appears to be in close proximity of the transport entrance (**Figure 2.1A**). Although the sequences of the His-rich loop are quite variable among ZIP4s (**Figure 2.1B**), the clustered histidine residues, probably together with the other neighboring metal chelating residues, likely confer a zinc-binding capability for all the ZIP4s, even though the number of zinc-binding site and/or binding affinities may vary depending on the exact sequence of the loop. Therefore, one putative function of the His-rich loop is to enrich zinc ions and increase effective zinc concentration at the pore entrance. However, the lack of change in the apparent K_m of the 4HS mutation suggests that zinc enrichment by the His-rich loop does not contribute much to the overall affinity of hZIP4 towards zinc (**Figure 2.10**). As a matter of fact, deletion of the whole ECD (ΔECD) had no effect on the K_m but drastically reduced the V_{max} by 75%. A careful kinetic analysis of the 4HS mutant showed ~20% decrease in the V_{max}, partially accounting for the reduced V_{max} of ΔECD. This result also excluded the possibility that the His-rich loop may play a role in inhibiting

zinc transport. Such an inhibitory effect was reported in the study of a ZnT family member, MTP1 from *Arabidopsis thaliana* (Kawachi et al., 2008, p. 1; Tanaka et al., 2013), where deletion of the cytosolic His-rich loop increased transport rate by more than 10 folds. Instead, the decreased transport rate of the 4HS mutant suggests that the His-rich loop may participate in zinc transport, presumably through the following two non-mutually exclusive mechanisms. For one, the loop may act as a chaperone facilitating zinc binding to the transport site in the TMD. Instead of acquiring free zinc ions from the extracellular space, the transport site may prefer accepting zinc ions already bound at the His-rich loop through rapid ligand exchange. The flexibility of the loop not only confers the transporter a more efficient way to capture zinc from the environment but also ensures a pool of liable zinc, rather than immobilized zinc, available for the transporter. The similar chaperone mechanism has been proposed in the studies of zinc transporters ZnuA (Banerjee et al., 2003) and ZntA (Banci et al., 2002; Mitra and Sharma, 2001). For the other mechanism, the His-rich loop may act as a zinc sensor allosterically regulating transporter's function. Although zinc binding only induces a small and highly localized conformational change, as indicated by the small change of tryptophan fluorescence intensity and partial protective effect against trypsin digestion (**Figure 2.8**), the His-rich loop is located at the 'bridging region' which was shown to be particularly important for ZIP4 trafficking and transport activity. It is conceivable that even a small structural perturbation, such as that induced by zinc binding in the His-rich loop, may sufficiently affect transporter's activity. In contrast, the cytosolic His-rich loop of the ZIPs between the third and the fourth transmembrane helices appears to have distinct functions. It has been shown that the cytosolic His-rich loop of hZIP4 binds zinc with nanomolar affinity (Bafaro et al., 2015) and acts as an intracellular zinc sensor responsible for zinc-induced endocytic degradation of ZIP4 (Mao et al., 2007). A recent study on a plant ZIP, IRT1 from *Arabidopsis thaliana*, suggested a

metal sensing function of the corresponding His-rich loop essential for transition metal-induced IRT1 ubiquitination and degradation (Dubeaux et al., 2018). This cytosolic His-rich loop was also reported to be associated with substrate specificity and transport activity for different ZIPs (Nishida et al., 2008).

Sequence comparison of human ZIPs has revealed that besides ZIP4, three other ZIPs also have a His-rich loop in their N-terminal ECDs. ZIP6 and ZIP10 were predicted to have a ZIP4-like extracellular dimerization subdomain (Zhang et al., 2016), where the two proteins have a His-rich loop containing 27 and 40 residues, respectively. The dimerization subdomain of ZIP7 appears to have degenerated, leaving 33 residues in an unstructured loop exposed to the lumen of the ER. It was speculated that the N-terminal His-rich loop of ZIP7 may play a role in ER zinc homeostasis (Adulcikas et al., 2018). Nevertheless, the exact functions of these very long His-rich loops in ZIP6/ZIP7/ZIP10 have not been experimentally established. This work on ZIP4 will shed light on the research of these ZIPs, as well as many other metal transporters and metalloproteins with a similar His-rich segment.

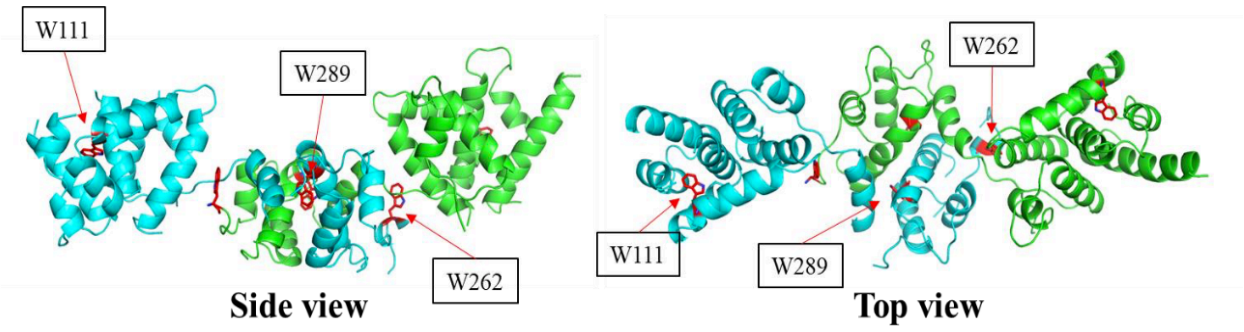

Figure 2.9. Intrinsic tryptophan residues of pZIP4-ECD.
Tryptophan residues (stick mode in red) shown in the structure of pZIP4-ECD.

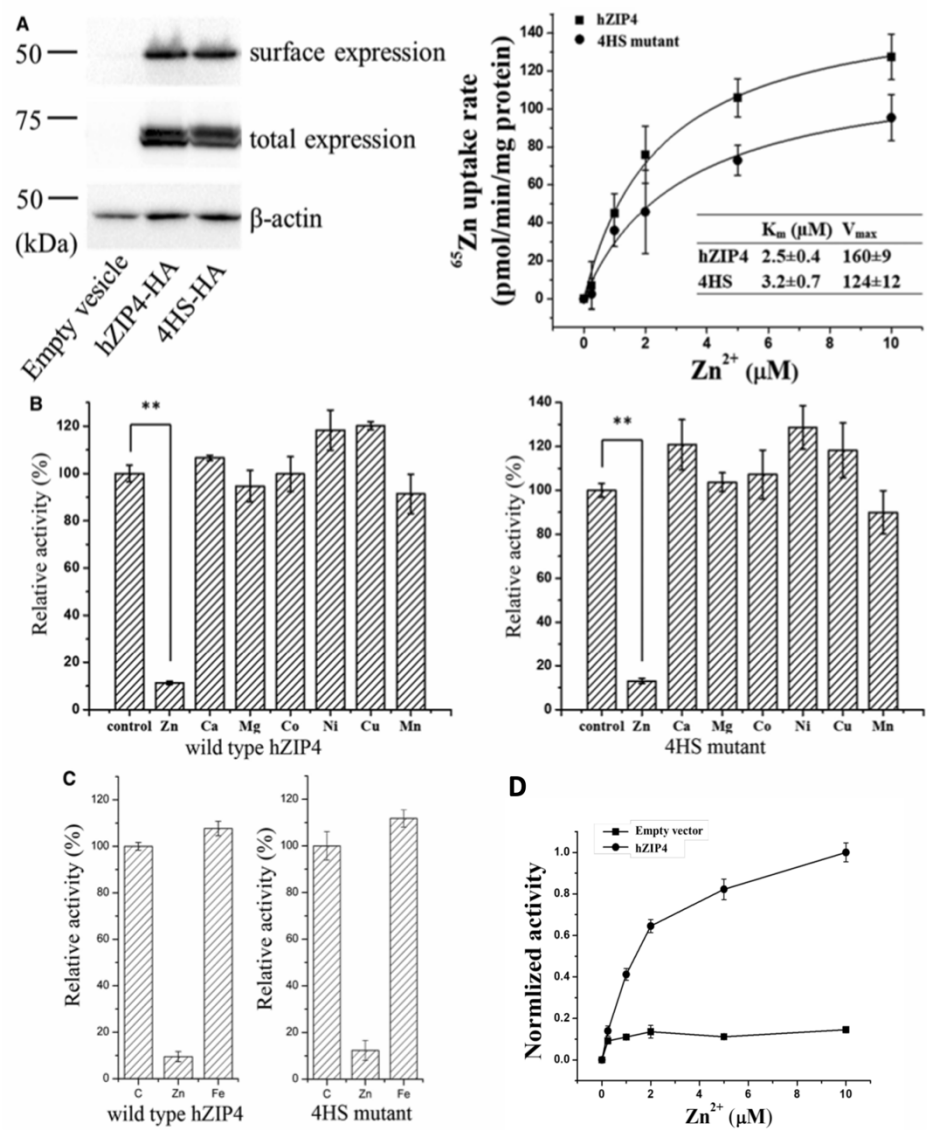

Figure 2.10. Functional characterization of the His-rich loop in hZIP4.
(A) Zinc uptake assays of the wild-type hZIP4–HA and the 4HS mutant transiently expressed in HEK293T cells. *Left:* Western blots showing the cell surface expression level (determined by surface-bound anti-HA antibody) and the total protein expression level of hZIP4 and the 4HS mutant. The upper band of total expression indicated the glycosylated form of hZIP4. *Right:* The processed zinc uptake data and curve fitting of one representative experiment. The kinetics parameters are shown in the inserted table. The V_{max} values have been calibrated using the surface expression levels shown in the left. ** $P < 0.01$. **(B)** Zinc uptake through hZIP4 and the 4HS mutant in the absence and presence of non-radioactive zinc and other divalent metal ions in excess. 10 μM ^{65}Zn was used in this assay and the concentrations of other metal ions are listed below. Non-radioactive Zn^{2+}: 200 μM; Ca^{2+}: 2 mM; Mg^{2+}: 20 mM; Co^{2+}: 200 μM; Ni^{2+}: 200 μM; Cu^{2+}: 200 μM; and Mn^{2+}: 200 μM. ** $P < 0.01$. **(C)** Zinc uptake through hZIP4 and the 4HS mutant in the presence of 200 μM ferrous (Fe^{2+}) and 1 mM ascorbic acid. **(D)** Zinc uptake assay conducted in the Chelex-treated culture media. Replacing the zinc uptake buffer with the Chelex-treated culture media in the assay greatly suppressed zinc absorption by the cells transfected with empty vector, resulting in a much lower background.

2.6. CONCLUSION

In this work, we focused our study on the extracellular His-rich loop by investigating its interactions with zinc ions and the importance of this unstructured, highly flexible loop for ZIP4 function. Our results indicated that zinc binding to the His-rich loop at the physiological zinc concentration only induces a small and localized structural perturbation. Mutagenesis and functional assays suggested that the histidine residues within this loop play a role in promoting zinc transport, but only to a small extent. In the study of ZnuA, when a functionally redundant ZinT protein was knocked out, the seemingly 'disposable' His-rich loop was demonstrated to be crucial for zinc acquisition in both *in vitro* and *in vivo* tests (Petrarca et al., 2010). Whether the extracellular His-rich loop of ZIP4 is a part of the 'Plan B' to enhance zinc absorption under a stressful condition would be interesting to explore in the future study.

2.7. ACKNOWLEDGMENTS

I thank Dr. Tuo Zhang at Department of Biochemistry and Molecular Biology for his big contributions to this project. I thank Dr. Dexin Sui at Department of Biochemistry and Molecular Biology for preparing constructs. I thank Dr. Jian Hu at Departments of Biochemistry and Molecular Biology & Chemistry for supervising the project experiments and manuscript writing. I thank Dr. Susanne Hoffmann-Benning for giving access to Cary Eclipse Fluorescence Spectrophotometer.

This work is supported by NIH R01GM115373 (to J.H.).

CHAPTER 3

Acrodermatitis enteropathica mutations in the extracellular domain cause mistrafficking and dysfunction of human ZIP4

Eziz Kuliyev[1,*], Chi Zhang[2,*], Dexin Sui[2], and Jian Hu[1,2]

[1]Departments of Chemistry & [2]Biochemistry and Molecular Biology,

Michigan State University, East Lansing, MI, USA

[*]**These authors equally contributive to this work.**

[This manuscript is currently under review]

This work was achieved by an equal collaboration between Dr. Chi Zhang and I, which is indicated by our listing as co-first authors. Dr. Sui helped making some constructs. Dr. Hu helped designing experiments and writing the manuscript. I was responsible for conducting zinc uptake assay (Figure 3.2 and 3.3). High quality Western-blot images were chosen from Dr. Zhang's data for the manuscript (Figures 3.2B&3.4A). Figure 3.4B was generated by collaborative input of Dr. Zhang and I. Figure 3.5 microscopy images were obtained by Dr. Zhang alone. Data for Figure 3.6 was obtained by me and courtesy of Mengxia Sun. I was responsible for carrying out biophysical experiments and generating Figures 3.7&3.8 and 3.9.

3.1. SUMMARY

ZIP4 is a representative member of the ZIP transporter family and responsible for zinc uptake from diet. Loss-of-function mutations of human ZIP4 drastically reduce zinc absorption, causing a life-threatening autosomal recessive disorder, AE. Although the zinc transport machinery is located in the TMD which is conserved in the entire ZIP family, half of the missense mutations occur in the ECD of hZIP4, which is only present in a fraction of mammalian ZIPs. How the AE-causing mutations in the ECD lead to ZIP4 malfunction has not be fully clarified. In this work, we characterized all the seven confirmed AE-causing missense mutations in hZIP4-ECD and found that the variants exhibited completely abolished zinc transport activity in a cell-based transport assay. Although the variants were able to be expressed in HEK293T cells, they failed to traffic to cell surface and were largely retained in the ER with immature glycosylation. When the corresponding mutations were introduced in the ECD of ZIP4 from *Pteropus Alecto*, a close homolog of hZIP4, the variants exhibited structural defects or reduced thermal stability, which likely accounts for intracellular mistrafficking of the AE-associated variants and as such a total loss of zinc uptake activity. This work provides a molecular pathogenic mechanism for AE, which lays out a basis for potential therapy using small molecular chaperones.

3.2. INTRODUCTION

Zinc deficiency is usually caused by inadequate zinc supply in foods or acquired diseases either reducing zinc uptake or increasing zinc loss (Prasad, 2003). In a rare case, inherited zinc deficiency, which is called acrodermatitis enteropathica, is caused by loss-of-function (LOF) mutations of ZIP4 (Küry et al., 2002, p. 39; Wang et al., 2002), the exclusive high-affinity zinc transporter in gastrointestinal system responsible for zinc uptake from regular diet (Dufner-Beattie

et al., 2007, 2003; Geiser et al., 2012; Wang et al., 2004a). AE is fatal without treatment, but lifelong high-dose zinc supplementation on daily basis can effectively alleviate the symptoms (Perafán-Riveros et al., 2002), implying the presence of secondary low-affinity zinc absorption mechanism(s).

ZIP4 is a representative member of the ZIP family (SLC39A) consisting of divalent transition metal transporters ubiquitous in all the kingdoms of life (Hara et al., 2017; Jeong and Eide, 2013b; Kambe et al., 2015, 2014, 2004; Lichten and Cousins, 2009; Liuzzi and Cousins, 2004). ZIP4 is specifically expressed on the apical side of enterocytes in small intestine and also in kidney where it is believed to be involved in zinc reabsorption from urine (Jeong and Eide, 2013b). The AE-causing mutations are evenly distributed along the 12 exons of *Zip4* gene without showing hotspot (Küry et al., 2016; Schmitt et al., 2009). As a result, half of the missense AE-causing mutations are mapped in the ECD and the other half in the TMD where the zinc transport machinery is located. A previous work has investigated several corresponding mutations in the TMD of mZIP4 but only one mutation in the ECD (equivalent to the P200L mutation hZIP4) was studied in the same report (Wang et al., 2004a). The P200L variant of hZIP4 was also characterized in a recent report (Hoch et al., 2020). So far, it is still unclear about how the other AE-causing mutations in the ECD affect hZIP4 function and the corresponding molecular mechanisms are also unknown.

The crystal structure of the ECD of ZIP4 from *Pteropus Alecto* (black fruit bat, pZIP4-ECD), which shares 68% sequence identity with hZIP4- ECD, provides a structural framework to deduce structural impacts of the AE-causing mutations on this accessory domain required for optimal zinc transport (Zhang et al., 2016). In this work, we functionally characterized all the seven confirmed AE- associated variants in a human cell line (HEK293T) and biophysically studied the

purified variants of pZIP4-ECD harboring the corresponding mutations. We found that all the variants showed little zinc transport activity in the cell-based transport assay. Although the variants were expressed, the cell surface expression was barely detectable. The variants were found to be immaturely glycosylated and aberrantly retained in the ER. For the purified pZIP4-ECD variants, biophysical studies revealed that the mutations caused structural defects or reduced thermal stability, providing a possible causative explanation for ZIP4 mistrafficking and dysfunction.

3.3. MATERIALS AND METHODS

3.3.1. Genes, plasmids and mutagenesis

The plasmids harboring hZIP4 (GenBank code: BC062625) or pZIP4-ECD (gene ID: ELK11751, residue 36-322) are the same as reported in Chapter 2. All the site-directed mutations were conducted using QuikChange mutagenesis kit (Agilent, Cat# 600250) and verified by DNA sequencing.

3.3.2. Cell culture, transfection and Western blot

Human embryonic kidney cells (HEK293T, ATCC, Cat #CRL-3216) were cultured in DMEM (Thermo Fisher Scientific, Invitrogen, Cat#11965092) supplemented with 10 % (v/v) fetal bovine serum (FBS, Thermo Fisher Scientific, Invitrogen, Cat#10082147) and Antibiotic-Antimycotic solution (Thermo Fisher Scientific, Invitrogen, Cat# 15240062) at 5% CO_2 and 37 °C. Cells were seeded on poly-D-lysine (Corning, Cat# 354210) coated 24-wells trays for 16 hours in the basal medium and transfected with 0.5-0.8 μg DNA/well by lipofectamine 2000 (Thermo Fisher Scientific, Invitrogen, Cat# 11668019) in OPTI-MEM medium.

For Western blot, all the samples were heated at 96 °C for 6 min before loading on SDS-PAGE gel. The protein bands were transferred to PVDF membranes (Millipore, Cat# PVH00010). After being blocked with 5% non-fat dry milk, the membranes were incubated with anti-HA antibody (Thermo Fisher Scientific, Cat#26183) at 4 °C overnight. Bound primary antibodies were detected with HRP-conjugated goat anti-mouse immunoglobulin-G at 1:5,000 (Cell Signaling Technoloy, Cat# 7076S) or goat anti-rabbit immunoglobulin-G at 1:2,500 (Cell Signaling Technology, Cat# 7074S) by chemiluminescence (VWR, Cat# RPN2232). The images of the blots were taken using a Bio-Rad ChemiDoc™ Imaging System.

3.3.3. PNGase F and Endo H glycosidase digestion

For PNGase F digestion, 500 units of enzyme was added to the cells lysed in the SDS-PAGE sample loading buffer and incubated for 1 hour at 37 °C before detection and analysis using Western blot.

For Endo H digestion, cell pellets were dissolved in diluted denaturation solution provided by the Endoglycosidase H kit (Promega). After vigorously mixing and heating at 95 °C for 5 mins, the samples were allowed to cool down to room temperature, followed by addition of 10x Endo H reaction buffer and 1250 units of Endo H enzyme and incubation for 15 hours at 37 °C. Control samples were treated in the exact same way except that the enzyme was not added. Samples were analyzed using 8% SDS-PAGE and Western blot.

3.3.4. Zinc transport assay

Twenty hours post-transfection, cells were washed with the wash buffer (10 mM HEPES, 142 mM NaCl, 5 mM KCl, 10 mM glucose, pH 7.3) followed by incubation with 10 μM $ZnCl_2$ (containing 30% $^{65}ZnCl_2$) in Chelex-treated 10% FBS/DMEM media for 20 mins at 37 °C. Then,

plates were transferred on ice and zinc uptake was stopped by addition of precooled 1 mM EDTA containing wash buffer. Cells were centrifuged at 3500 rpm and the supernatant was discarded. Cells were washed twice before lysis with 0.5% Triton X-100. Packard Cobra Auto-Gamma counter was used to detect radioactivity. The same procedure was used for activity assay of the P200L variant at designated zinc concentrations. The cells transfected with the empty vector were treated in the same way.

3.3.5. hZIP4-HA surface expression detection

hZIP4-HA expressed at cell surface was indicated by the surface bound anti-HA antibodies recognizing the C-terminal HA tag of hZIP4, as previously described (Mao et al., 2007; Wang et al., 2004a; C. Zhang et al., 2020; Zhang et al., 2016). In brief, after 24h transfection, cells were washed twice with DPBS on ice and then fixed for 10 min in 4% formaldehyde at room temperature. Cells were then washed three times in DPBS (5 minutes each wash) and incubated with 2.5 μg/ml anti-HA antibody diluted with 5% BSA in DPBS for 1.5 h at room temperature. Cells were washed seven times with DPBS to remove unbound antibodies and then lysed in SDS–PAGE loading buffer. The anti-HA antibody bound to the surface hZIP4-HA in cell lysates were detected in Western blot with HRP-conjugated goat anti-mouse immunoglobulin-G (1:5000). As loading control, β-actin levels were detected using an anti-β-actin antibody (1:2,500).

3.3.6. Immunofluorescence imaging and colocalization analysis

HEK293T cells were grown in 24-well trays for 16 h on sterile glass coverslips and transfected with plasmids harboring the genes of hZIP4 or its variants using lipofectamine 2000. To visualize cell surface expressed hZIP4 or its variants, cells were washed briefly by DPBS after 24h transfection and then fixed for 10 min at room temperature using 4% formaldehyde. The cells

were washed in DPBS (5 minutes each wash) and incubated with 2.5 μg/ml an FITC-labeled anti-HA antibody (Sigma, Product # H7411) diluted with 5% BSA in DPBS for 1.5 h at room temperature. After five washes with DPBS, coverslips were mounted on slides with fluoroshield mounting medium with DAPI (Abcam, Cat# ab104139). Images were taken with a 40X objective using a Spectral-based Olympus FluoView 1000 confocal laser scanning microscope (CLSM).

To detect intracellular localization of hZIP4 variants and calreticulin (an ER marker), after fixation by using formaldehyde, cells were permeabilized and blocked for 1h with DPBS containing 5% goat serum (Cell Signaling Technology, Cat# 5425S) and 0.1% Triton X-100 and then incubated with anti-HA antibodies at 1:500 (Thermo Fisher Scientific, Cat#26183) and/or anti-calreticulin antibodies at 1:300 (Thermo Fisher Scientific, Cat#PA3-900) at 4 °C for overnight. After three washes with DPBS (5-minute incubation for each wash), cells were incubated with Alexa-568 goat anti-mouse antibodies at 1:500 (Thermo Fisher Scientific, Cat# A-11004) and Alexa-488 anti-rabbit antibodies at 1:500 (Thermo Fisher Scientific, Cat# A-27034). After 3 washes with DPBS, coverslips were mounted on slides with fluoroshield mounting medium with DAPI (Abcam, Cat# ab104139).

For colocalization analysis, images were taken with a 100X oil objective. The analysis was performed under fixed thresholds using Image J with the JACoP plugins (Bolte and Cordelières, 2006). Pearson's correlation coefficient was used to quantify the degree of colocalization. For each construct, 7-10 images were taken and 4-7 images with the best quality were used in analysis. The images are shown as RGB representation.

3.3.7. Expression and purification of pZIP4-ECD and the variants

The wild type pZIP4–ECD and the variants were expressed as previously described in Chapter 2. In brief, the *E. Coli* cells of Origami™ B(DE3) pLysS (Novagen) transformed with the

pLW01 vector were grown at 37 °C in lysogeny broth medium until OD_{600} ~ 0.6, and expression was induced by 0.2 mM IPTG before the cells were transferred to 16 °C for overnight growth. After cell lysis by sonication, the His-tagged proteins were purified using a nickel-nitrilotriacetic acid column. After removal of N-terminal His_6-tag by thrombin, the proteins were dialyzed against a Tris-HCl buffer (pH 8.0) containing 10 mM EDTA, subjected to ion-exchange chromatography (Mono-Q, GE Healthcare), and then polished by size-exclusion chromatography (Superdex 200 10/300 GL, GE Healthcare) in a buffer containing 10 mM HEPES, pH 7.3 and 100 mM NaCl. The apparent molecular weight was estimated using the elution volumes of the protein standards.

3.3.8. Circular dichroism experiments

To prepare the samples for CD experiments, Thermo Scientific Slide-A-Lyzer MINI Dialysis Device was used for changing the sample buffer to 10 mM phosphate pH 7.3 over the course of a two-day dialysis at 4 °C with buffer change for three times. Sample concentrations were measured by using a NanoDrop ND-1000 Spectrophotometer and then adjusted to proper concentration using the dialysis buffer. The CD spectrum of 8 μM pZIP4–ECD (or the variants) in 300 μl of 10 mM phosphate buffer (pH 7.3) were recorded in Hellma® 1 mm QS cuvette sealed with PTFE stopper by using a JASCO-815 CD Spectrometer. Wavelength range was set between 190-260 nm, and data was collected at 1 nm wavelength increments with 1.5 s averaging time per wavelength point. Three scans were recorded and averaged. The K2D3 server (http://cbdm-01.zdv.uni-mainz.de/~andrade/k2d3/) was used to estimate secondary structure components of the proteins.

To monitor heat denaturation of the wild type protein, CD spectra were recorded in the range of 195-260 nm and starting temperature was set at 20 °C. Temperature was increased in 10 °C increments and waiting time was set to 5 minutes at each designated temperature before next

scanning. Three scans were recorded and averaged. After reaching 95 °C, temperature was cooled down to 20 °C and waited for 10 minutes before scanning. Three scans were recorded and averaged.

For thermal stability studies of WT and P193L, ellipticities at 222 nm were recorded while the temperature increased from 4 °C to 100 °C. Rate of temperature increase was optimized to 0.5 °C/min with a temperature tolerance of 0.15 °C. The average of three repeats was used in data processing and analysis.

Another set of thermal stability experiment was done (WT, C64R, R87C, A91T, P193L and Q299H with 3.0 °C/min temperature increase rate, ranging from 20 °C to 95 °C. These settings are recommended in a tutorial protocol (Greenfield, 2006). The average of three repeats was used in data processing and analysis. Unfolded fraction at temperature T ($F_{\text{unfolded,T}}$) was calculated as below:

$$F_{\text{unfolded,T}} = |\theta_{222,20} - \theta_{222,T}|/|\theta_{222,20} - \theta_{222,95}|$$

where $\theta_{222,20}$, $\theta_{222,95}$ and $\theta_{222,T}$ are the readings of θ_{222} at 20 °C, 95 °C and temperature T, respectively. Apparent $T_{m,a}$ was determined from the heat denaturation curve at which $F_{\text{unfolded}} = 0.5$.

3.3.9. Dynamic light scattering experiment

Stock solutions of protein samples (WT and the Q299H variant) were dialyzed using Thermo Scientific Slide-A-Lyzer MINI Dialysis Device for changing the buffer to 10 mM phosphate pH 7.3. Concentrations of both protein samples were adjusted to 15 μM and were filtered through 0.22 μm filter to remove large aggregates/dust. Dynamic light scattering (DLS) was performed using Zetasizer Nano (Malvern) and offset was kept the same for the buffer and

protein samples. Each measurement was an average of 20 acquisitions with 12 seconds per acquisition and performed at 25 °C using 633 nm wavelength.

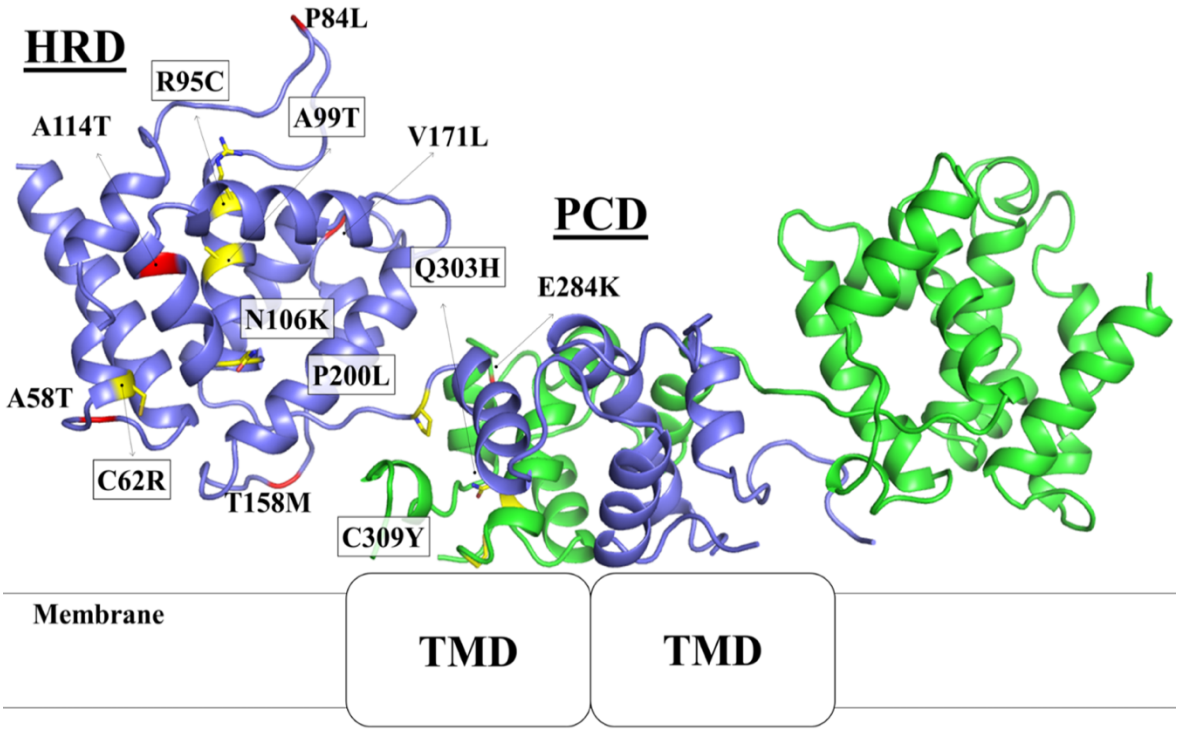

Figure 3.1. Mapping of the AE-causing mutations and the SNPs on the structural model of hZIP4-ECD dimer.
Seven residues subjected to AE-causing mutations (highlighted in boxes) are in yellow and stick mode with four in the HRD domain, two in the PCD domain, and one (P200L) in the linker connecting the two subdomains, whereas the residues at which SNPs occur are in red. Additional 3 SNPs not shown in the model are either in the highly disordered his-rich loop (R251W) or in the signal peptide (V2A and E10A).

3.4. RESULTS

3.4.1. The AE-causing mutations in the ECD of hZIP4 led to total loss of zinc transport activity

A total of 17 missense mutations in hZIP4-ECD have been documented, of which seven are confirmed AE-causing mutations and the others are benign single-nucleotide polymorphisms (SNPs), according to the MASTERMIND database (https://mastermind.genomenon.com/) and an early review (Schmitt et al., 2009). Mapping these residues on the hZIP4-ECD structural model (generated using SWISS-MODEL (Waterhouse et al., 2018)) shows that the residues subjected to AE-causing mutations (C62R, R95C, A99T, N106K, P200L, Q303H and C309Y) are all in the structured regions, whereas most of the residues where the SNPs occur are in loops or disordered regions (**Figure 3.1**). In this work, we characterized all the seven AE-causing mutations, including four homozygous mutations (C62R, P200L, Q303H and C309Y) (Küry et al., 2003, 2002; Nakano et al., 2003; Wang et al., 2002) and three heterozygous mutations (R95C, A99T and N106K) (Jung et al., 2011; Nakano et al., 2003; Wang et al., 2002), and studied their impacts on hZIP4 function. The hZIP4 variants with a C-terminal HA tag were transiently expressed in HEK293T cells and applied to the cell-based zinc transport assay (Wang et al., 2004a, 2002; T. Zhang et al., 2020; Zhang et al., 2019). As shown in **Figure 3.2A**, in sharp contrast to the wild type hZIP4, none of the cells expressing any variants uptook more zinc than the blank group in which the cells were transfected with an empty vector, which means that the variants have no detectable zinc transport activity with 10 μM of Zn^{2+} in culture media. For the wild type hZIP4, the previous studies have shown that zinc transport activity reaches plateau at 10 μM of Zn^{2+} under the same condition (T. Zhang et al., 2020; Zhang et al., 2019). To examine whether any activity can be detected at higher zinc concentration, the P200L variant was tested at various zinc concentrations up to 50 μM, but the results only confirmed no detectable activity (**Figure 3.3**).

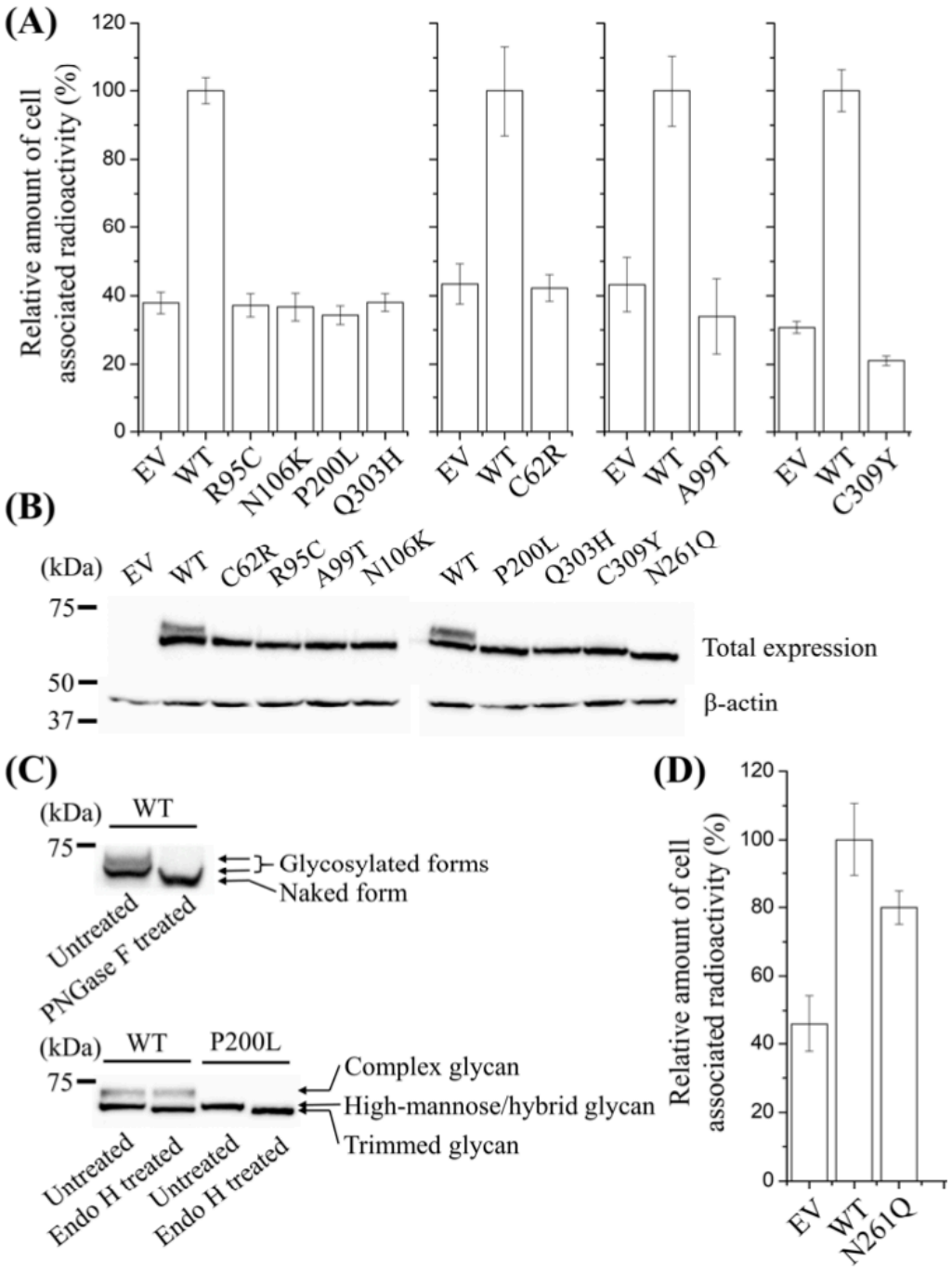

Figure 3.2. Expression and functional characterization of hZIP4 and the variants.
(**A**) Cell-based zinc transport assay of the AE-associated variants with 10 μM Zn^{2+} in the medium. The results of one out of 2-6 independent experiments are shown. (**B**) Total expression hZIP4 and the variants detected by Western blot using anti-HA antibody. β-actin was used as loading control. (**C**) Processing of hZIP4 by PNGase F and Endo H glycosidases. (**D**) Zinc transport assay of the N261Q variant. Data are expressed as average ± standard deviation (n=3).

3.4.2. The AE-associated variants were immaturely glycosylated

The previous study on mZIP4 has shown that the AE-causing mutations in the TMD led to significantly reduced expression levels, likely due to accelerated degradation (Wang et al., 2004a). To examine whether the AE-causing mutations in the ECD have similar effects, expression of the variants were detected in the whole cell samples using an anti-HA antibody in Western blot. As shown in **Figure 3.2B**, all the variants were expressed, but the wild type hZIP4 has two discrete bands at approximately 75 kDa, whereas the AE-associated variants have only one band corresponding to the lower band of the wild type protein. When treated with PNGase F, an enzyme cleaving the glycosidic bond directly linked with the asparagine residue, the two bands of the wild type protein merged into a single one with a smaller apparent molecular weight, indicating that the expressed hZIP4 harbors two distinct glycans (Wang et al., 2004a). When treated with Endo H, which is a glycosidase selectively hydrolyzing high-mannose or some hybrid glycans, the lower band was processed whereas the upper band was resistant (**Figure 3.2C**), indicating that the species in the upper band has a complex glycan whereas the lower band represents a species with immature glycosylation. In contrast, the P200L variant was completely processed by Endo H and the resulting species is of the same apparent molecular weight as the one corresponding to the lower band of the processed wild type protein. Thus, although the total expression levels of the variants were not drastically affected by the mutations in the ECD, defects in glycosylation was observed for all the AE-associated variants.

3.4.3. N-glycosylation is not required for hZIP4 activity

Proteins expressed at cell surface are often modified by N-glycosylation, which may play a key role in protein function (Spiro, 2002). As the AE-associated variants losing zinc transport activity is concomitant with defects in glycosylation, we asked whether the lack in glycosylation

is responsible for activity loss. Using the NetNGlyc server (http://www.cbs.dtu.dk/services/NetNGlyc/), we identified a potential glycosylation site at N261 in an "NxS/T" motif. We then generated the N261Q variant and expressed it in HEK293T cells. In Western blot, the N261Q variant showed a single band with an apparent molecular weight smaller than the lower band of the wild type protein (**Figure 3.2B**), confirming that N261 is indeed the only N-glycosylation site in hZIP4. Importantly, zinc transport assay of the N261Q variant only showed a modest reduction of transport activity (**Figure 3.2D**), indicating that glycosylation at N261 is not pivotal for zinc transport and therefore lack of glycosylation of the AE-associated variants does not account for loss of zinc transport activity.

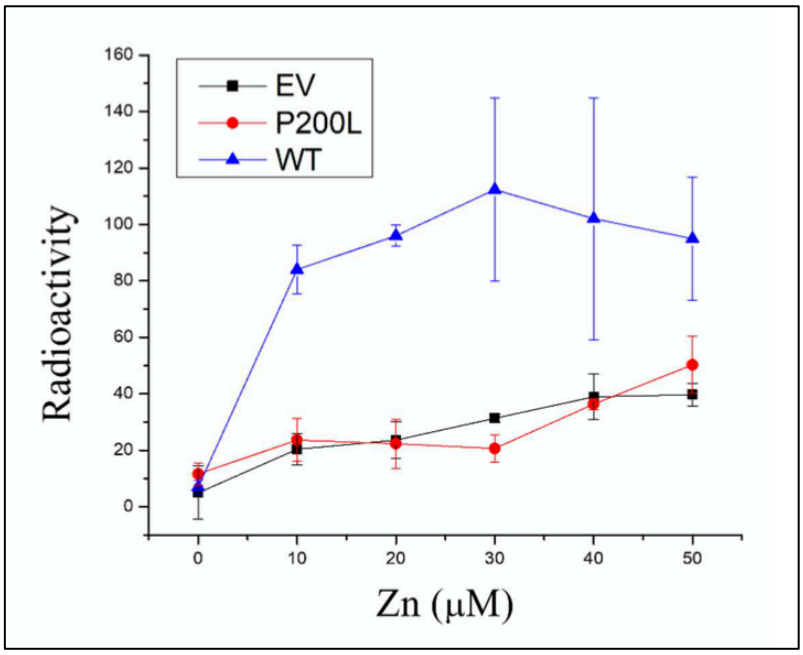

Figure 3.3. Zinc transport activity measurement at indicated zinc concentrations. Three technical repeats were averaged at each data point. The error bars indicate standard deviation (n=3).

3.4.4. The AE-associated variants had significantly diminished cell surface expression

As the glycans are added to the client membrane proteins in the ER, processed in the ER and then in the Golgi in a stepwise manner (Marinko et al., 2019), immature glycosylation is an indicator of defect in intracellular trafficking. To examine potential mislocalization, we tested cell surface expression levels of the AE-associated variants by applying the anti-HA antibody to the non-permeabilized cells fixed with formaldehyde. After extensive wash, non-specific bound antibody was removed, leaving those specifically bound with the C-terminal HA tag at cell surface. As shown in **Figure 3.4A**, all the AE-associated variants had substantially reduced cell surface levels when compared to the wild type hZIP4 in Western blot. Consistent with the zinc transport data, the N261Q variant missing the N-linked glycan had significantly higher level of cell surface expression than the variants linked with disease, indicating that the N-glycosylation at N261 is not a key factor for hZIP4 surface expression. We then applied immunofluorescence imaging to locate the AE-associated variants expressed in cells. To do that, the cells transiently expressing the wild type or the variants were fixed and permeabilized with formaldehyde and TX-100, followed by staining with an FITC-labeled anti-HA antibody. The samples were then checked under CLSM. Consistent with the Western blot shown in **Figure 3.2B**, the wild type and the variants were expressed in HEK293T cells at comparable levels (**Figure 3.4B**). To detect the transporters expressed at cell surface, the cells were fixed with formaldehyde and treated with the same anti-HA antibody, followed by extensive washing and checking under CLSM. In **Figure 3.4B**, fluorescence signals at cell surface can be convincingly detected for the wild type hZIP4 and the N261Q variant, whereas the signals of the AE-associated variants imaged under the same conditions were not detectable. Collectively, our data strongly indicate that the cell surface

expression levels of the AE-associated variants were largely suppressed, which is likely responsible for loss of zinc transport activity.

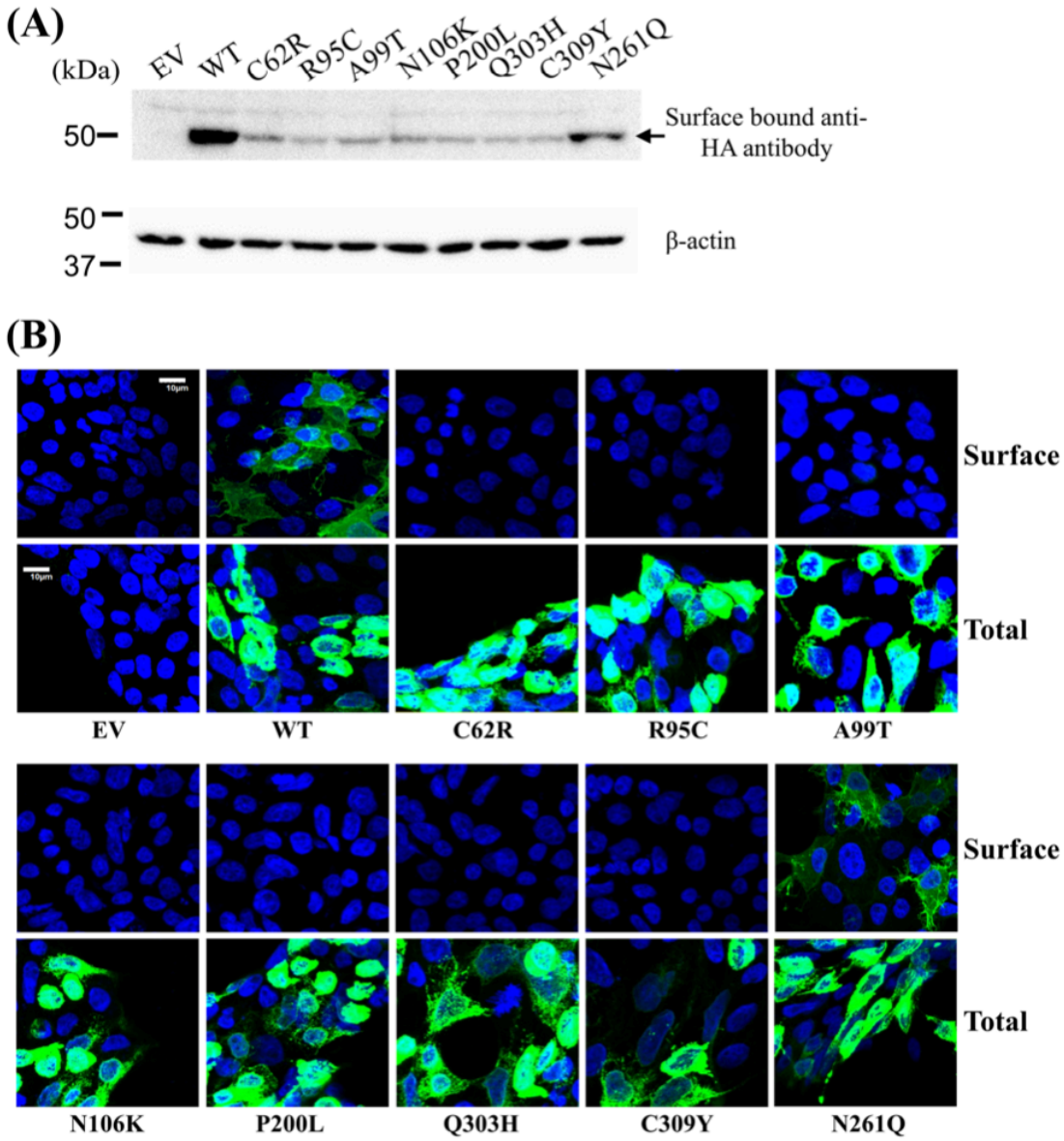

Figure 3.4. Cell surface expression of hZIP4 and the AE-associated variants.
(**A**) Surfaced bound anti-HA antibody for detection of surface expression of hZIP4-HA and the variants. β-actin was used as the loading control. (**B**) Detection of expression of hZIP4 and its variants. FITC-labeled anti-HA antibody was used to stain HA tagged hZIP4 in non-permeabilized cells (surface expression, upper row) or permeabilized cells (total expression, lower row). The scale bar = 10 μm.

3.4.5. The AE-associated variants were retained in the ER

Since all the AE-associated variants were expressed but not presented at cell surface, we then asked where the variants are located in cells. Endo H treatment experiment suggests that the variants are likely trapped in the ER (**Figure 3.2C**). To test this, we examined co-localization of hZIP4 and its variants with an ER-resident protein, calreticulin, and quantified the results using Pearson's correlation coefficient (PCC). As shown in **Figure 3.5**, the staining of the wild type hZIP4-HA (red) was partially superimposed with those of calreticulin (green), resulting in a yellow/orange color. The calculated PCC (0.37±0.06) indicates that a significant portion of hZIP4 expressed in HEK293T cells were retained in the ER, which is consistent with the results of the Endo H treatment which showed that more than half of the expressed hZIP4 were not maturely glycosylated. Overexpression driven by a strong CMV promoter in transient transfection could account for partial mistrafficking of the wild type protein. For all the AE-associated variants, more overlapped signals were detected and the PCCs (0.52-0.66) are significantly higher than that of the wild type protein (P<0.01) (**Figure 3.5**), indicating that these variants were retained in the ER to a greater extent than the wild type protein.

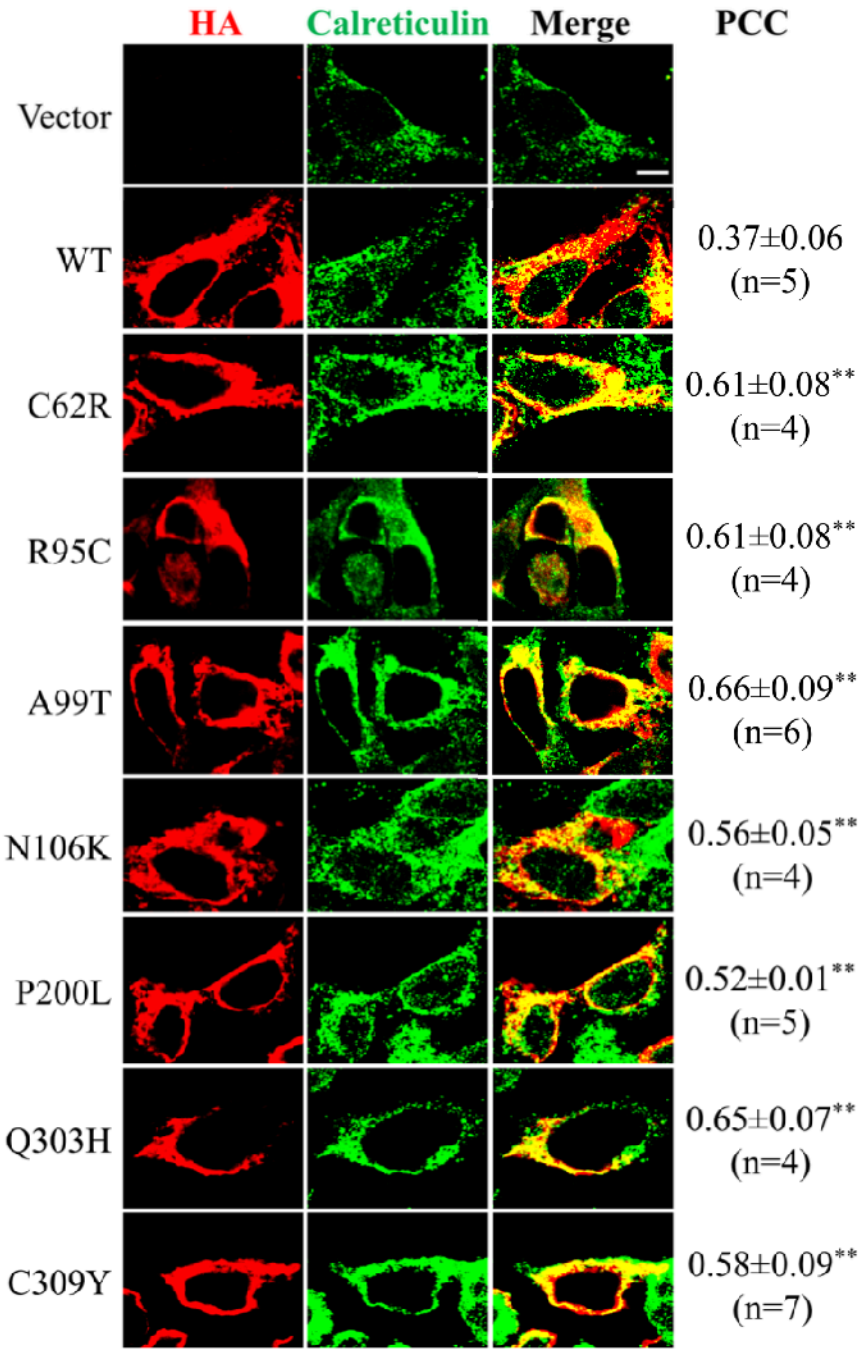

Figure 3.5. Colocalization of hZIP4 with the ER marker calreticulin.
Representative confocal images (100 X) of HEK293T cells transiently expressing hZIP4-HA or the variants are shown. hZIP4 and the variants were detected with an anti-HA tag antibody and an Alexa-568 goat anti-mouse antibody (red). Calreticulin was detected with an anti-calreticulin antibody and an Alexa-488 anti-rabbit antibody (green). Scale bar = 5 μm. Data are expressed as average ± standard deviation (n=4-7). ***: P*<0.01

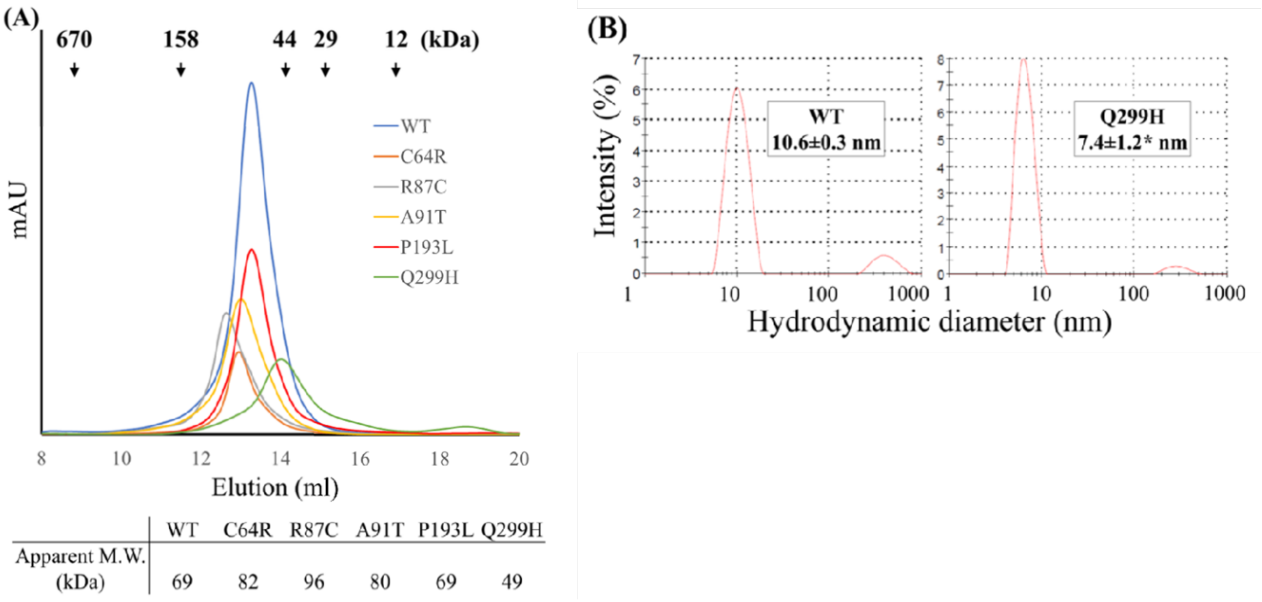

	WT	C64R	R87C	A91T	P193L	Q299H
Apparent M.W. (kDa)	69	82	96	80	69	49

Figure 3.6. Purification of pZIP4-ECD and the variants.
(**A**) Size-exclusion chromatography. The elution volumes of the protein standards are indicated by arrows, from which the apparent molecular weights of the purified proteins were estimated. (**B**) Dynamic light scattering of the wild type protein and the Q299H variant. Data are expressed as average ± standard deviation(n=2-3). *:$P<0.05$.

3.4.6. The AE-causing mutations led to structural defects or reduced thermal stability of pZIP4-ECD

Next, we attempted to clarify the molecular basis of the variants' mistrafficking. Given the difficulty of obtaining adequate amount of purified full length hZIP4 or hZIP4-ECD for biophysical characterization, we turned to the isolated pZIP4-ECD, which we have previously crystallized and biochemically characterized (Zhang et al., 2019, 2016). Given the high sequence identity, we believe that the results obtained from the study of purified pZIP4-ECD would help to understand how the disease-causing mutations affect the biophysical properties of the human counterpart. We introduced mutations in pZIP4-ECD on the residues topologically equivalent to those in hZIP4 (C64R, R87C, A91T, D98K, P193L, Q299H and C305Y). The variants were expressed and purified in the same way as the wild type protein, but the final yields were lower.

Particularly, the yields of two variants (D98K and C305Y) were too low to allow for further characterization. Therefore, we focused on the other five variants in later study.

In size-exclusion chromatography, all the variants were eluted as a single peak with apparent molecular weights at or greater than that of a homodimer (66 kDa), except that the Q299H variant has a smaller apparent molecular weight at approximately 50 kDa (**Figure 3.6A**). Consistently, the hydrodynamic diameter of the Q299H variant (7.4±1.2 nm), which was determined by DLS, is significantly smaller than that of the wild type protein (10.6±0.3 nm, $P<0.05$) (**Figure 3.6B**). There is no sign of a monomer-dimer equilibrium, but the current data cannot tell whether this variant preserve dimerization or becomes monomeric in solution.

The purified proteins were applied to CD spectrometer and the data were analyzed on the K2D3 server to estimate secondary structure contents (Louis-Jeune et al., 2012). As shown in **Figure 3.7**, the CD spectrum of the wild type pZIP4-ECD has a high α-helical content (66±2%) with the characteristic minima at 208 nm and 222 nm and maximum at 195 nm, which is consistent with the reported crystal structure (Zhang et al., 2016). When compared to the wild type protein, three variants exhibited lower levels of α-helical content – R87C (56±3%), A91T (59±3%), and Q299H (56±2%) ($P<0.05$). In addition, the ratios of ellipticities (θ) at 222 nm and 208 nm were significantly reduced. The $\theta_{222}/\theta_{208}$ ratio is an indicator of whether α-helices are packed to form coiled-coil like tertiary structures (Legardinier et al., 2009; Zhou et al., 1992). A value smaller than 1 may indicate poorly packed helices and lack of coiled-coils. For the wild type protein, the $\theta_{222}/\theta_{208}$ ratio (1.020) is slightly greater than one, which is consistent with the crystal structure where two helix bundles form two separate subdomains: in the N-terminal helix-rich domain (HRD), α4 is surrounded and packed with the other eight helices, whereas four helices (α10-α12) in the C-terminal domain (PAL motif-containing domain, PCD) are packed against the

counterparts from the other monomer to form a homodimer (Zhang et al., 2016). For four variants, the $\theta_{222}/\theta_{208}$ ratios are significantly smaller than one – C64R (0.934), R87C (0.829), A91T (0.937), and Q299H (0.844) ($P<0.05$). In contrast, the $\theta_{222}/\theta_{208}$ ratio of the P193L variant (0.998) is only slightly reduced. Together with the unchanged α-helical content, this result shows that this variant, unlike the other variants, has no detectable defects in secondary structure.

Next, we examined the thermal stability of the P193L variant and compared it with the wild type protein. For the latter, increasing temperature from 4 °C to 100 °C at the rate of 0.5 °C/min was accompanied with a decrease of θ_{222} and the plateau was reached at the end when the protein was mostly denatured with α-helical content dropping from 66% to 20% (**Figure 3.8A**). Although the ECD has two structurally distinct subdomains (the HRD and the PCD) with the PCD dimerizing through a large hydrophobic interface, the presence of only one transition in the heat denaturation curve suggests that the physical interactions between the two subdomains may synchronize their unfolding processes. We also noticed that, when the heat-denatured protein was allowed to refold at room temperature, the majority of the refolded protein was still a homodimer in solution as indicated in size-exclusion chromatography (**Figure 3.8B**), although the α-helical content was decreased by 10% and the $\theta_{222}/\theta_{208}$ ratio was reduced to 0.82. As pZIP4-ECD forms a stable homodimer, heat denaturation may go through two distinct pathways. In the first scenario, dimerization is preserved throughout the process of heat denaturation even when the protein is largely denatured at 100 °C. In the second scenario, while the protein is denatured by heat, the dimer breaks into monomers, most of which return to the dimeric state upon refolding. Although the current data cannot distinguish the two pathways, the result already indicates that pZIP4-ECD has a strong propensity to keep or form a dimer, which is consistent with the proposed ECD function of facilitating ZIP4 dimerization (Zhang et al., 2016). When the heat denaturation curve

of the P193L variant was compared with that of the wild type protein, a substantial left-shift was observed (**Figure 3.8C**), particularly at the first half of the curve, indicating that the thermal stability of this variant has been significantly reduced. In the crystal structure of pZIP4-ECD, P193 stacks with W262 from the other monomer through a proline-aromatic interaction (**Figure 3.8D**). Alanine substitution of W266 in hZIP4, which is topologically equivalent to W262 of pZIP4-ECD, cause the same immature glycosylation and loss of zinc transport activity as the P200L mutation (Zhang et al., 2016), indicating that this proline-tryptophan interaction is essential for proper trafficking of hZIP4. Reduced thermal stability caused by the proline mutation, as shown in **Figure 3.8C**, likely accounts for these defects. Although P193 does not participate in folding of the HRD or the PCD, the P193L mutation may affect stability of pZIP4-ECD by disrupting domain interactions. As the P193-W262 interaction is located at the bridging region which mediates communication of the HRD and the PCD, the P193L mutation may negatively affect the cooperativity of the two subdomains during heat denaturation and as such reduce the overall thermal stability. Another possibility, which is compatible with the first theory, is that the P193L mutation may destabilize dimerization since the P193-W262 interaction occurs between the two monomers (**Figure 3.8D**). In either scenario (or a combination), disrupted domain interactions would reduce structural compactness and expose hydrophobic patches, making this variant retained in the ER by the quality control system.

Taken together, the *in vitro* studies of purified proteins showed that: (1) most of the variants preserve the oligomeric state whereas the Q299H variant has a significantly smaller size than a wild type dimer; (2) three variants (R87C, A91T, and Q299H) exhibit lower α-helical contents; (3) the $\theta_{222}/\theta_{208}$ ratios of four variants (C64R, R87C, A91T, and Q299H) are significantly reduced and lower than one; and (4) the P193L variant exhibits significantly reduced thermal stability. In

sum, the substitutions in pZIP4-ECD, which are equivalent to the AE-causing mutations in hZIP4-ECD, lead to structural defects or decrease of thermal stability.

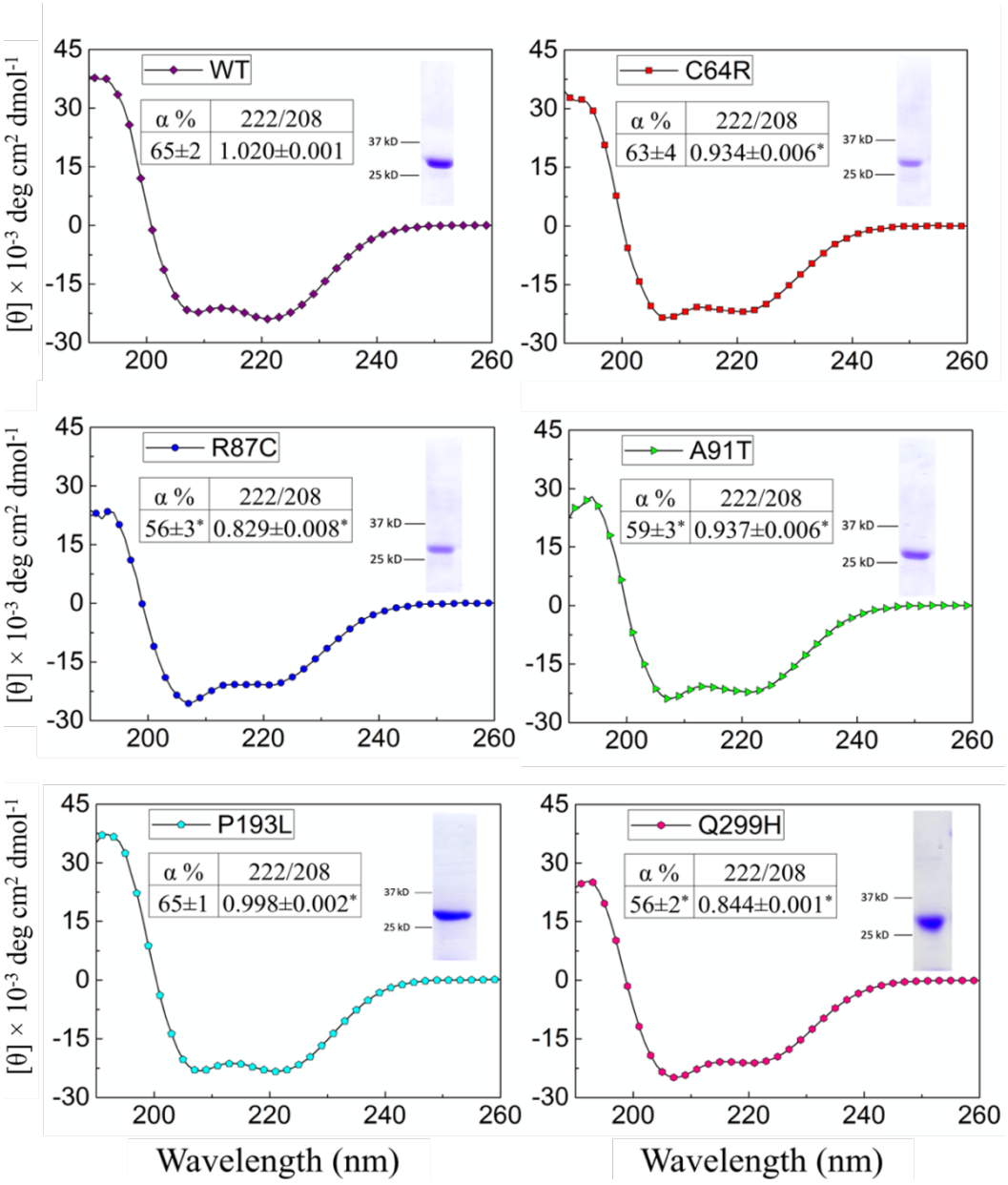

Figure 3.7. CD spectra of pZIP4-ECD and the variants.
For each protein, representative spectrum out of three repeats is shown. The α-helical content (α %) was estimated using the K2D3 server. 222/208 indicates the ratio of $\theta_{222}/\theta_{208}$. The SDS-PAGEs of purified protein are shown in the insets. Data are expressed as average ± standard deviation (n=3-5). *:P<0.05.

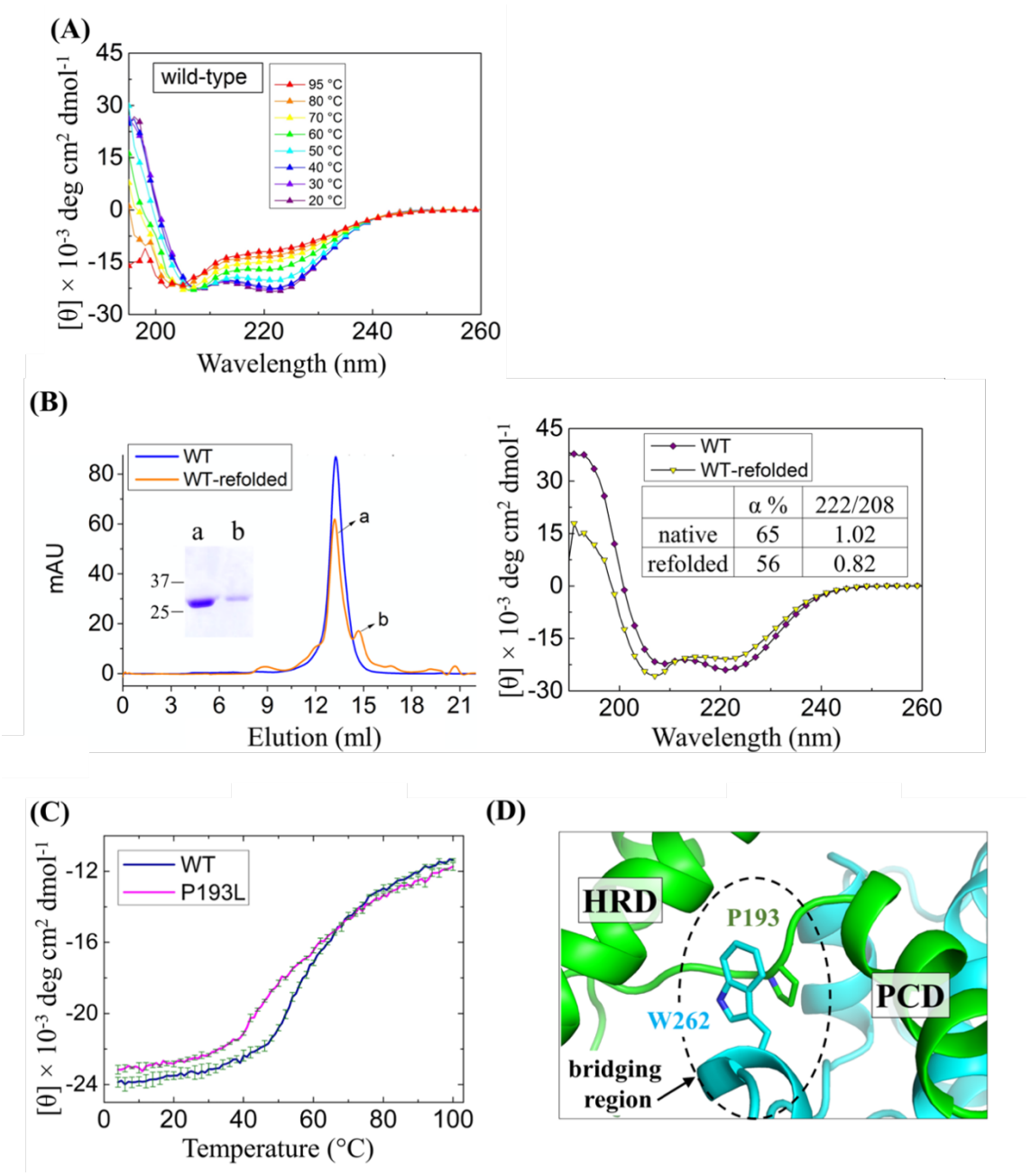

Figure 3.8. Thermal stability of the wild type pZIP4-ECD and the P193L variant.
Thermal stability of the wild type pZIP4-ECD and the P193L variant. (**A**) CD spectra of wild type pZIP4-ECD at different temperatures. At 95 °C, the α-helical content was estimated to be 20%. (**B**) Comparison of the native and the refolded pZIP4-ECD. *Left:* size-exclusion chromatography. Peaks a and b are dimer and monomer, respectively, of which SDS-PAGE is shown in the inset. *Right:* CD spectra with indicated α-helix contents and $\theta_{222}/\theta_{208}$ ratios. (**C**) Heat denaturation curves of the wild type pZIP4-ECD and the P193L variant. The error bars indicate standard deviations (n=3). (**D**) The interaction of P193 with W262 (PDB ID: 4X82). The two monomers are colored in green and cyan, respectively. The bridging region is indicated by the dashed oval.

3.5. DISCUSSION

As the ZIP family plays a central role in transition metal homeostasis and cell signaling (Jeong and Eide, 2013b), LOF mutations of human ZIPs cause severe syndromes, including AE which is the first genetic disorder discovered to be associated with the ZIP family (Küry et al., 2002; Wang et al., 2002). Some of the AE-causing mutations have been biochemically studied in mZIP4, a close homolog of hZIP4. Most of the missense mutations in the TMD of mZIP4 led to lower expression level, reduced cell surface expression and largely diminished zinc transport activity (Wang et al., 2004a). Mapping the mutations on the structural model of hZIP4 suggests that the involved residues appear to play key structural roles and as such the AE-causing mutations in the TMD would affect protein folding and/or stability (Zhang et al., 2017), leading to degradation by quality control mechanism in the ER (Marinko et al., 2019). The only characterized mutation in the ECD of mZIP4 is P200L, which is equivalent to P200L in hZIP4 (Wang et al., 2004a). The same mutation in hZIP4 was also reported in a recent study (Hoch et al., 2020). In this work, we characterized all the seven confirmed AE-causing mutations occurring in the ECD and found that they exhibited similar behavior when expressed in HEK293T cells – they were able to be expressed but barely detected at cell surface, which accounts for the total loss of zinc transport activity. The fact that the variants are immaturely glycosylated and aberrantly trapped in the ER strongly indicates intracellular mistrafficking. By biophysically studying the corresponding mutations in pZIP4-ECD, we demonstrated that the mutations led to structural defects or decreased thermal stability, which may account for mistrafficking and dysfunction of the AE-associated hZIP4 variants.

Protein misfolding and structural defects are known pathogenic mechanisms for dysfunction of membrane proteins caused by disease-associated mutations. A well-documented

case is the autosomal recessive disorder cystic fibrosis (CF) which is caused by LOF mutations of a chloride ion channel, cystic fibrosis transmembrane conductance regulator (CFTR). Notably, the most prevalent mutation (>90%) associated with CFTR is ΔF508, for which the residue F508 within the cytosolic nucleotide binding domain 1 (NBD1) is deleted (Cheng et al., 1990). The ΔF508 variant exhibited drastically reduced transport activity, immature glycosylation, reduced cell surface expression and accelerated clearance from plasma membrane (Lukacs and Verkman, 2012). The atomic resolution of cryo-EM structures of CFTR have shown that F508 is buried in a hydrophobic core (Liu et al., 2019, 2017) which mediates physical interactions of the NBD1 and the TMD, and biochemical/biophysical studies have indicated that the variant has defects in folding and structural compactness (Lukacs and Verkman, 2012). Remarkably, the AE-associated variants with single residue substituted in the ECD showed a similar behavior as the ΔF508 CFTR variant. As discussed in our previous report and also shown in **Figure 3.1**, the AE-causing mutations occur at the conserved residues in structured regions where they participate in disulfide bonds (C62R, C309Y), salt bridge (R95C), hydrogen bonds (N106K and Q303H), hydrophobic core (A99T), and inter-domain interactions (P200L). The extremely low yield for the D98K and C305Y variants already implies defects in folding and/or stability. With no surprise, the biophysical studies on pZIP4-ECD indicated that the tested five variants (C64R, R87C, A91T, P193L, and Q299H) have structural defects (lower α-helical content and reduced $\theta_{222}/\theta_{208}$ ratio) or decreased thermal stability (**Figures 3.7 and 3.8**). Strangely enough, wild type pZIP4-ECD or the variants turned out to be resistant to heat denaturation and seemingly not completely unfolded at 95 °C and/or 100 °C. Thereby, it is hard to argue about absolute T_ms of the variants in absence of

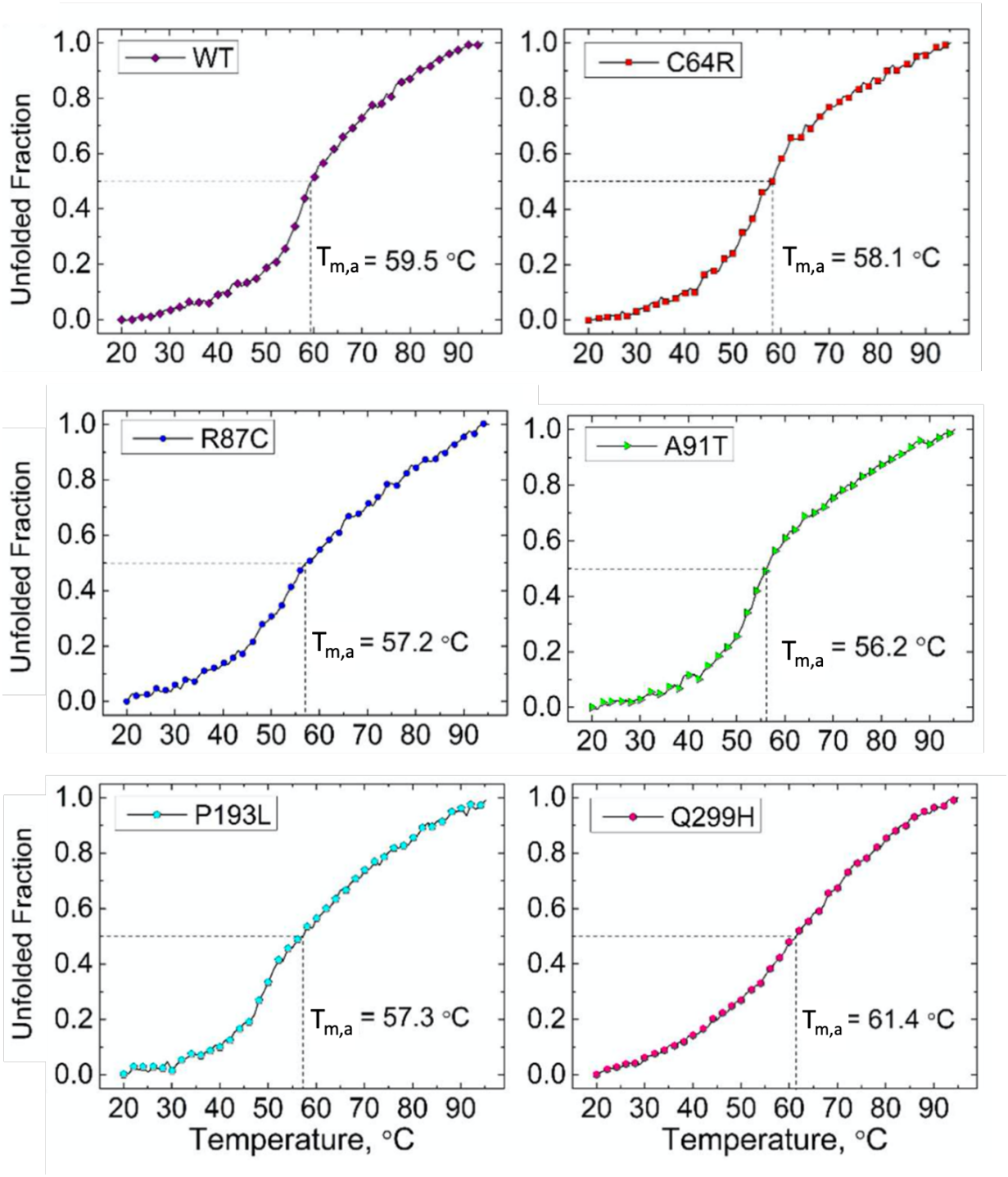

Figure 3.9. Heat denaturation of pZIP4-ECD and the variants.
Heat denaturation curves of the wild type pZIP4-ECD and the variants. The apparent melting temperature ($T_{m,a}$) was estimated on the denaturation curve where the unfolded fraction is 0.5.

visually clear plateau. Nevertheless, by plotting normalized $\Delta\theta_{222}$ against temperature, the apparent $T_{m,a}$, at which the unfolding process reaches 50% during heat denaturation, can be estimated. When compared to the $T_{m,a}$ of the wild type protein (59.5 °C), all the variants except for Q299H exhibited lowered $T_{m,a}$s, ranging from 56.2 °C to 58.1 °C (**Figure 3.9**). The unexpected high T_m for the Q299H variant (61.4 °C) is accompanied with a more flattened heat denaturation curve when compared to the sigmoid curves of the wild type or the other variants, which is implicative of impaired cooperativity and interaction network of the structural elements of this variant. In this work, as the biophysical studies were limited to isolated ECD, it is some uncertainty whether the mutations would similarly affect the full-length protein or whether the observed defects are severe enough to cause mistrafficking. Given the ECD is a functionally important accessory domain which may form extensive interactions with the TMD, it is possible that the seemingly modest structural changes may have profound effects on the full-length protein to alter intracellular trafficking.

We notice the discrepancy between our results and other reports on the P200L variant. It was shown that the P200L variant of mZIP4 was expressed in HEK293T cells with a cell surface level comparable to that of the wild type protein and a 70% decrease in zinc transport activity (Wang et al., 2004a). In contrast, the P200L variant of hZIP4 showed little surface expression and no detectable activity in this work (**Figures 3.2, 3.3 and 3.4**). As already mentioned in the mZIP4 study, nearly all the wild type mZIP4 was maturely glycosylated, whereas only 50%-70% of the P200L variant did so, suggesting that a significant amount of the variant was not properly processed. Notably, even for the wild type hZIP4, maturely glycosylated protein is no more than 50% (**Figure 3.2**). It is unclear why mZIP4 is more efficiently processed and traffic in a human cell line than hZIP4. One possibility would be that mZIP4 is intrinsically more stable than hZIP4

so that it has a better chance to fold correctly in the ER. It would also explain why the P200L variant of mZIP4 can still be presented at cell surface despite of folding defect evidenced by immature glycosylation. While this work was being conducted, we noticed a study reporting that the P200L variant of hZIP4 expressed in HEK293T cells was shown to have a normal zinc transport activity which was measured by using a small molecule zinc-responsive fluorescence dye (Hoch et al., 2020). It is unclear whether the discrepancy is due to different approaches used for tracing zinc transport. Radioactive ^{65}Zn based transport assay has been used to study transport kinetics of a variety of ZIPs, including hZIP4 (Chowanadisai et al., 2013; Gaither and Eide, 2001; Jeong et al., 2012, p. 13; Mao et al., 2007; Pinilla-Tenas et al., 2011; Wang et al., 2004a; T. Zhang et al., 2020; Zhang et al., 2019, 2017, 2016). Consistent with loss of zinc transport activity, the P200L variant of hZIP4 is shown to be barely expressed at cell surface. We detected cell surface expression levels of hZIP4 and its variants using two approaches following the previous mZIP4 study (Wang et al., 2004a) – Western blot for detecting cell surface bound anti-HA antibody and immunofluorescence imaging for visualizing fluorescence-labeled anti-HA antibody associated at cell surface. As shown in **Figures 3.4A** and **3.4B,** the results of both approaches consistently showed that the AE-associated variants, including the P200L variant, had much lower levels of cell surface expression than the wild type hZIP4. Co-localization experiment further revealed that the P200L variant is largely retained in the ER (**Figure 3.5**), which explains the lack of zinc transport activity of this variant.

After the discovery of the causal link between ZIP4 mutations and AE, disease-causing mutations have been reported in other human ZIPs. The LOF mutations of ZIP13 cause the SCD-EDS (Bin et al., 2014; Fukada et al., 2008; Jeong et al., 2012, p. 13), an autosomal recessive disorder characteristic of defects of connective tissues, bones, and teeth. It has been demonstrated

that both the missense mutation G64D and the deletion mutation ΔFLA (on the third transmembrane helix) drastically reduced stability and protein expression level in cells due to accelerated clearance through the ubiquitination dependent proteasome degradation pathway (Bin et al., 2014). Recently, inherited LOF mutations of ZIP8 and ZIP14, which are close homologs with broad substrate spectrum covering from the beneficial trace elements (zinc, iron, manganese) to the toxic cadmium, have been linked with severe failure of systemic manganese homeostasis (Boycott et al., 2015; Park et al., 2015). The disease-linked ZIP8 variants fail to transport Mn^{2+} because of abrogated cell surface expression and being aberrantly retained in the ER (Choi et al., 2018). Notably, these ZIP8 variants contain at least one substitution in the ECD, highlighting the importance of the ECD in ZIP8 intracellular trafficking. In this work and also in our previous report, we demonstrate that the mutations on the conserved residues in the ECD significantly affected ZIP4 intracellular trafficking (Zhang et al., 2016). Although the exact role of the ECD is still not fully clarified, these studies have suggested that correct folding and structural integrity of the ECD are required for normal intracellular trafficking of the ZIPs. Whether the ECD plays any active roles in folding, processing or trafficking of mammalian ZIPs would be interesting to investigate later. Given that AE and CF share a similar molecular pathogenic mechanism and that small molecule chemical chaperones have been successfully applied for CF treatment (Taylor-Cousar et al., 2017), developing AE-specific chemical chaperones may represent an alternative strategy to treat this rare disease. After all, life-time and high-dose zinc administration may cause imbalance of other trace elements, such as copper deficiency (Fischer et al., 1984; Hoogenraad et al., 1985).

3.6. CONCLUSION

In this work we studied implications of AE-disease causing mutations on hZIP4 transport function, folding, expression and localization in the HEK293T cells. To do so, we firstly investigated ZIP4 uptake activity by using radioactive Zn-65. Our results strongly indicated that AE-causing mutant variants' zinc uptake activities were no different from basal level transport of the cells transfected with the empty vector. To understand the reason for the lack of activity we further investigated protein expressions and post-translational modifications. Also, we monitored localization of the variants and compared to the wild type hZIP4 in terms of the cell surface and intracellular levels. Our results indicated that AE-causing mutant variants were associated with immature glycosylation and retained in the ER, explaining unpresented ZIP4 on the plasma membrane, which provides a clear interpretation for lacking zinc accumulation in the cells expressing the variants. Further, we attributed mistrafficking of the AE-associated variants to protein misfolding, structural perturbations and reduced thermal stability, based on biophysical characterization of the pZIP4-ECD variants.

In summary, this report establishes that AE-disease causing mutations lead to LOF of ZIP4 and deemed to be helpful for developing therapeutical AE treatment. As for further strategy, in my personal opinion, activity of isolated full-length AE-causing ECD mutant variants should be investigated in micellar system or with similar alternative method. If uptake ability of the protein is still preserved (theoretically transport machinery should be still intact), then tactics of external interference with the ER quality checking chaperones can be investigated to allow the misfolded proteins to relocate to the plasma membrane, by therapeutical companies.

3.7. ACKNOWLEDGMENTS

I thank Dr. Chi Zhang at Department of Biochemistry and Molecular Biology for contributing greatly to this project. I thank Dr. Dexin Sui at Department of Biochemistry and Molecular Biology for his help preparing constructs. I thank Mengxia Sun at Department of Chemistry for conducting the dynamic light scattering experiment. I thank Dr. Jian Hu at Departments of Biochemistry and Molecular Biology & Chemistry for supervising the project experiments and manuscript writing. I thank Dr. Jin He at Department of Biochemistry and Molecular Biology for access to fluorescence microscopy for initial sample inspection. I thank Dr. Melinda Frame at Center for Advanced Microscopy for providing assistance in Confocal experiments.

This work is supported by NIH GM115373 and GM129004 (to J.H.).

CHAPTER 4

CONCLUSIONS & PERSPECTIVES

Zinc is a trace nutrient essential for human health. Found in stable divalent cationic form, zinc ion functions as Lewis acid in catalysis and an irreplaceable cofactor for over 2000 zinger finger transcription factors directly involved in gene expression and regulation. Zinc deficiency may cause growth retardation, formation of lesions, alopecia, compromised immune function and cognitive impairment. Inherited form of severe zinc deficiency is known for causing the AE disease which is associated with dysfunction of ZIP4 primarily responsible for zinc uptake through the gastrointestinal system. AE is potentially lethal if not treated promptly. Currently treatment exclusively relies on extra oral zinc sulfate supplementation, and presumably zinc enters the body through low-affinity transporters and/or via paracellular routes. However, the adverse effects of high dose zinc administration should not be ignored.

ZIP4 is an integral protein with a TMD where transport machinery resides and a large ECD (Zhang et al., 2020, 2017). ZIP4-ECD was shown as an accessory domain which is required for optimal zinc uptake (Zhang et al., 2016). ZIP4-ECD forms a dimer where each monomer possesses two independent subdomains, HRD and PCD. PCD appears to be important for dimerization, however, function of HRD is unknown. Noteworthy to mention, deletion of HRD reduced activity by ~50%. By 2015 when I started this thesis work, the exact role of ZIP4-ECD in zinc transport has not been fully elucidated and the effects of AE-causing missense mutations on ZIP4 function has not been systematically studied.

This thesis project has taken tasks of untangling the role of ZIP4-ECD in zinc transport and molecular pathology of the ECD mutations leading to AE. To achieve the first task, we

characterized mammalian (human and black fruit bat) ZIP4-ECD by answering following questions:

- Does ZIP4-ECD bind to zinc?
- If it does, where is the binding site(s) and what is zinc binding affinity?
- Does zinc binding induce conformational change(s)?
- What is the functional role of zinc binding site/segment in transport?
- Can we deduce function of the whole ZIP4-ECD based on zinc binding abilities? *i.e.* a zinc sensor and/or zinc uptake facilitator.

In our investigations we found that ZIP4-ECD indeed binds to two zinc ions per protomer with averaged dissociation constant of 0.62 μM in the unstructured His-rich loop. Zinc binding to isolated pZIP4-ECD induced small local conformational change with no major secondary structure change observed. Our functional assays indicated that the His-rich loop plays a role in zinc transport, albeit to small extent. Based on these results we conclude that the His-rich loop of ZIP4-ECD may act as:

1. A chaperone facilitating zinc binding to the transport site in the TMD.
2. A zinc sensor allosterically regulating transporter's function.

To execute the second task, we prepared seven single mutation constructs in hZIP4 and begun with *in vivo* study by asking the question:

- How or to what extent do AE-causing mutations affect zinc uptake activity?

After finding out that the AE-causing variants nearly have null activity, we started looking for clues of misfolding such as loss N-glycosylation. Western-blot studies indicated that the variants cannot be maturely glycosylated despite total expression levels are comparable to the wild type. Then we asked:

- Where are the proteins located in cells?

To address this question, we utilized CLSM and confirmed that AE mutant variants cannot be found on the cell surface but detected them entrapped in the ER with much higher degree compared to the wild type protein. We further continued our investigation by asking:

- Do the variants impact and/or destabilize the protein structure? If they do, to what extent?

To elucidate this matter, we diverted our course to *in vitro* study by preparing seven single mutation constructs in pZIP4-ECD for *in vitro* biophysical studies. The variants had much lower yield compared to wild type protein, showing early glimpse of misfolding issue. By exploiting CD spectrometer, we found that secondary structure alterations and/or reduced thermal stability in which some variants more adverse than others.

In summary, the data support that AE-causing missense mutations do not affect protein expression in human cells but prevent proper trafficking to cell surface, leading to zinc uptake impediment. The altered biophysical properties caused by the mutations are likely responsible for the mistrafficking. These findings would be found helpful in AE treatment progression.

One of the main objectives of this work was to elucidate ZIP4-ECD function in zinc transport. We found that the flexible His-rich loop accommodates primary zinc binding sites which mediated by four conserved histidine residues in ZIP4-ECD. However, our the 4HS mutagenesis study in hZIP4 showed that zinc uptake activity reduced by ~20% which is a relatively small reduction when compared to deletion of HRD or ECD which cause ~50% and ~75% activity reduction, respectively. Considering the His-rich loop is the only zinc binding site in ZIP4-ECD, it would be interesting to see what the role of HRD in zinc transport is without directly interacting with zinc. Does it HRD interact with TMD? Obtaining full-length structure of ZIP4 would shed light to orientation of ECD relative to TMD and many other remaining questions such as what the

functional and structural importance of dimerization of ZIP4 in zinc transport are and how HRD fit into this?

Interestingly, the ECD of ZIP4 was found to be proteolytically cleaved from the transporter during prolonged zinc starvation in mice and the cleavage was inhibited by AE-causing mutations (Kambe and Andrews, 2009). This observation is quite intriguing because the ECD truncated hZIP4 demonstrated that ZIP4-ECD serves as zinc transport facilitator in HEK293 cells (Zhang et al., 2016) rather having inhibitory effects. These seemingly contradictory results raise many questions: Why would ZIP4 lose its ECD under zinc deficiency if ECD is required for optimal zinc transport? What is the mechanism of ECD removal and which protease(s) is recruited to cleave ZIP4 only under zinc-limiting conditions? Answering these questions would provide key insights into additional ZIP4 regulation mechanism.

In sum, characterization of ZIP family is still in a relative early stage and much work yet to be done. Also, we should bear in mind that not all human ZIP family members are being regulated in the same way even though they share some structural frame. Therefore, each ZIP member should be investigated separately to achieve fully understanding about the roles of ZIP members in human zinc homeostasis and diseases.

This work is dedicated to all those suffering from Acrodermatitis enteropathica and I sincerely wish may science community make their lives better.

BIBLIOGRAPHY

BIBLIOGRAPHY

Abu-Duhier, F., Pooranachandran, V., McDonagh, A.J.G., Messenger, A.G., Cooper-Knock, J., Bakri, Y., Heath, P.R., Tazi-Ahnini, R., 2018. Whole Genome Sequencing in an Acrodermatitis Enteropathica Family from the Middle East. *Dermatol Res Pract* 2018, 1284568. https://doi.org/10.1155/2018/1284568

Ackland, M.L., Michalczyk, A., 2006. Zinc deficiency and its inherited disorders -a review. *Genes Nutr* 1, 41–49. https://doi.org/10.1007/BF02829935

Acrodermatitis enteropathica | Genetic and Rare Diseases Information Center (GARD) – an NCATS Program [WWW Document], n.d. URL https://rarediseases.info.nih.gov/diseases/5723/acrodermatitis-enteropathica#ref_4641 (accessed 8.26.20).

Adlard, P.A., Parncutt, J.M., Finkelstein, D.I., Bush, A.I., 2010. Cognitive loss in zinc transporter-3 knock-out mice: a phenocopy for the synaptic and memory deficits of Alzheimer's disease? *The Journal of Neuroscience: The Official Journal of the Society for Neuroscience* 30, 1631–1636. https://doi.org/10.1523/JNEUROSCI.5255-09.2010

Adulcikas, J., Norouzi, S., Bretag, L., Sohal, S.S., Myers, S., 2018. The zinc transporter SLC39A7 (ZIP7) harbours a highly-conserved histidine-rich N-terminal region that potentially contributes to zinc homeostasis in the endoplasmic reticulum. *Comput Biol Med* 100, 196–202. https://doi.org/10.1016/j.compbiomed.2018.07.007

Aggett, P.J., Atherton, D.J., More, J., Davey, J., Delves, H.T., Harries, J.T., 1980. Symptomatic zinc deficiency in a breast-fed preterm infant. *Archives of Disease in Childhood* 55, 547–550. https://doi.org/10.1136/adc.55.7.547

Andrews, G.K., Wang, H., Dey, S.K., Palmiter, R.D., 2004. Mouse zinc transporter 1 gene provides an essential function during early embryonic development. *genesis* 40, 74–81. https://doi.org/10.1002/gene.20067

Antala, S., Ovchinnikov, S., Kamisetty, H., Baker, D., Dempski, R.E., 2015. Computation and Functional Studies Provide a Model for the Structure of the Zinc Transporter hZIP4. *J. Biol. Chem.* 290, 17796–17805. https://doi.org/10.1074/jbc.M114.617613

Aydemir, T.B., Liuzzi, J.P., McClellan, S., Cousins, R.J., 2009. Zinc transporter ZIP8 (SLC39A8) and zinc influence IFN-gamma expression in activated human T cells. *J Leukoc Biol* 86, 337–348. https://doi.org/10.1189/jlb.1208759

Bafaro, E., Liu, Y., Xu, Y., Dempski, R.E., 2017. The emerging role of zinc transporters in cellular homeostasis and cancer. *Signal Transduct Target Ther* 2, 17029. https://doi.org/10.1038/sigtrans.2017.29

Bafaro, E.M., Antala, S., Nguyen, T.-V., Dzul, S.P., Doyon, B., Stemmler, T.L., Dempski, R.E., 2015. The large intracellular loop of hZIP4 is an intrinsically disordered zinc binding domain. *Metallomics* 7, 1319–1330. https://doi.org/10.1039/C5MT00066A

Bafaro, E.M., Maciejewski, M.W., Hoch, J.C., Dempski, R.E., 2019. Concomitant disorder and high-affinity zinc binding in the human zinc- and iron-regulated transport protein 4 intracellular loop. *Protein Sci* 28, 868–880. https://doi.org/10.1002/pro.3591

Banci, L., Bertini, I., Ciofi-Baffoni, S., Finney, L.A., Outten, C.E., O'Halloran, T.V., 2002. A New Zinc–protein Coordination Site in Intracellular Metal Trafficking: Solution Structure of the Apo and Zn(II) forms of ZntA(46–118). *Journal of Molecular Biology* 323, 883–897. https://doi.org/10.1016/S0022-2836(02)01007-0

Banerjee, S., Wei, B., Bhattacharyya-Pakrasi, M., Pakrasi, H.B., Smith, T.J., 2003. Structural Determinants of Metal Specificity in the Zinc Transport Protein ZnuA from Synechocystis 6803. *Journal of Molecular Biology* 333, 1061–1069. https://doi.org/10.1016/j.jmb.2003.09.008

Barnes, P.M., Moynahan, E.J., 1973. Zinc deficiency in acrodermatitis enteropathica: multiple dietary intolerance treated with synthetic diet. *Proc R Soc Med* 66, 327–329.

Bauer, M.C., Nilsson, H., Thulin, E., Frohm, B., Malm, J., Linse, S., 2008. Zn2+ binding to human calbindin D28k and the role of histidine residues. *Protein Sci* 17, 760–767. https://doi.org/10.1110/ps.073381108

Berg, A.H., Rice, C.D., Rahman, M.S., Dong, J., Thomas, P., 2014. Identification and Characterization of Membrane Androgen Receptors in the ZIP9 Zinc Transporter Subfamily: I. Discovery in Female Atlantic Croaker and Evidence ZIP9 Mediates Testosterone-Induced Apoptosis of Ovarian Follicle Cells. *Endocrinology* 155, 4237–4249. https://doi.org/10.1210/en.2014-1198

Bhattacharya, P.T., Misra, S.R., Hussain, M., 2016. Nutritional Aspects of Essential Trace Elements in Oral Health and Disease: An Extensive Review. *Scientifica* (Cairo) 2016, 5464373. https://doi.org/10.1155/2016/5464373

Bin, B.-H., Fukada, T., Hosaka, T., Yamasaki, S., Ohashi, W., Hojyo, S., Miyai, T., Nishida, K., Yokoyama, S., Hirano, T., 2011. Biochemical Characterization of Human ZIP13 Protein. *J Biol Chem* 286, 40255–40265. https://doi.org/10.1074/jbc.M111.256784

Bin, B.-H., Hojyo, S., Hosaka, T., Bhin, J., Kano, H., Miyai, T., Ikeda, M., Kimura-Someya, T., Shirouzu, M., Cho, E.-G., Fukue, K., Kambe, T., Ohashi, W., Kim, K.-H., Seo, J., Choi, D.-H., Nam, Y.-J., Hwang, D., Fukunaka, A., Fujitani, Y., Yokoyama, S., Superti-Furga, A., Ikegawa, S., Lee, T.R., Fukada, T., 2014. Molecular pathogenesis of Spondylocheirodysplastic Ehlers-Danlos syndrome caused by mutant ZIP13 proteins. *EMBO Molecular Medicine* 6, 1028–1042. https://doi.org/10.15252/emmm.201303809

Bolte, S., Cordelières, F.P., 2006. A guided tour into subcellular colocalization analysis in light microscopy. *Journal of Microscopy* 224, 213–232. https://doi.org/10.1111/j.1365-2818.2006.01706.x

Bosomworth, H.J., Thornton, J.K., Coneyworth, L.J., Ford, D., Valentine, R.A., 2012. Efflux function, tissue-specific expression and intracellular trafficking of the Zn transporter ZnT10 indicate roles in adult Zn homeostasis. *Metallomics: Integrated Biometal Science* 4, 771–779. https://doi.org/10.1039/c2mt20088k

Boycott, K.M., Beaulieu, C.L., Kernohan, K.D., Gebril, O.H., Mhanni, A., Chudley, A.E., Redl, D., Qin, W., Hampson, S., Küry, S., Tetreault, M., Puffenberger, E.G., Scott, J.N., Bezieau, S., Reis, A., Uebe, S., Schumacher, J., Hegele, R.A., McLeod, D.R., Gálvez-Peralta, M., Majewski, J., Ramaekers, V.T., Nebert, D.W., Innes, A.M., Parboosingh, J.S., Abou Jamra, R., 2015. Autosomal-Recessive Intellectual Disability with Cerebellar Atrophy Syndrome Caused by Mutation of the Manganese and Zinc Transporter Gene SLC39A8. *The American Journal of Human Genetics* 97, 886–893. https://doi.org/10.1016/j.ajhg.2015.11.002

Brocks, A., Reid, H., Glazer, G., 1977. Acute intravenous zinc poisoning. *Br Med J* 1, 1390–1391. https://doi.org/10.1136/bmj.1.6073.1390

Cao, J., Bobo, J.A., Liuzzi, J.P., Cousins, R.J., 2001. Effects of intracellular zinc depletion on metallothionein and ZIP2 transporter expression and apoptosis. *J Leukoc Biol* 70, 559–566.

Chakrabarti, P., 1990. Geometry of interaction of metal ions with histidine residues in protein structures. *Protein Eng Des Sel* 4, 57–63. https://doi.org/10.1093/protein/4.1.57

Chan, K.L., Bakman, I., Marts, A.R., Batir, Y., Dowd, T.L., Tierney, D.L., Gibney, B.R., 2014. Characterization of the Zn(II) binding properties of the human Wilms' tumor suppressor protein C-terminal zinc finger peptide. *Inorg Chem* 53, 6309–6320. https://doi.org/10.1021/ic500862b

Chao, Y., Fu, D., 2004. Kinetic Study of the Antiport Mechanism of an Escherichia coli Zinc Transporter, ZitB. *J. Biol. Chem.* 279, 12043–12050. https://doi.org/10.1074/jbc.M313510200

Cheng, S.H., Gregory, R.J., Marshall, J., Paul, S., Souza, D.W., White, G.A., O'Riordan, C.R., Smith, A.E., 1990. Defective intracellular transport and processing of CFTR is the molecular basis of most cystic fibrosis. *Cell* 63, 827–834. https://doi.org/10.1016/0092-8674(90)90148-8

Chimienti, F., Devergnas, S., Favier, A., Seve, M., 2004. Identification and Cloning of a β-Cell–Specific Zinc Transporter, ZnT-8, Localized Into Insulin Secretory Granules. *Diabetes* 53, 2330–2337. https://doi.org/10.2337/diabetes.53.9.2330

Choi, E.-K., Nguyen, T.-T., Gupta, N., Iwase, S., Seo, Y.A., 2018. Functional analysis of SLC39A8 mutations and their implications for manganese deficiency and mitochondrial disorders. *Scientific Reports* 8, 3163. https://doi.org/10.1038/s41598-018-21464-0

Chowanadisai, W., Graham, D.M., Keen, C.L., Rucker, R.B., Messerli, M.A., 2013. Neurulation and neurite extension require the zinc transporter ZIP12 (slc39a12). *PNAS* 110, 9903–9908. https://doi.org/10.1073/pnas.1222142110

Chowanadisai, W., Lönnerdal, B., Kelleher, S.L., 2008. Zip6 (LIV-1) regulates zinc uptake in neuroblastoma cells under resting but not depolarizing conditions. *Brain Research* 1199, 10–19. https://doi.org/10.1016/j.brainres.2008.01.015

Chowanadisai, W., Lönnerdal, B., Kelleher, S.L., 2006. Identification of a mutation in SLC30A2 (ZnT-2) in women with low milk zinc concentration that results in transient neonatal zinc deficiency. *J. Biol. Chem.* 281, 39699–39707. https://doi.org/10.1074/jbc.M605821200

Christianson, D.W., 1991. Structural biology of zinc. *Advances in Protein Chemistry* 42, 281–355. https://doi.org/10.1016/s0065-3233(08)60538-0

Chun, H., Korolnek, T., Lee, C.-J., Coyne, H.J., Winge, D.R., Kim, B.-E., Petris, M.J., 2019. An extracellular histidine-containing motif in the zinc transporter ZIP4 plays a role in zinc sensing and zinc-induced endocytosis in mammalian cells. *J. Biol. Chem.* 294, 2815–2826. https://doi.org/10.1074/jbc.RA118.005203

Cole, T.B., Wenzel, H.J., Kafer, K.E., Schwartzkroin, P.A., Palmiter, R.D., 1999. Elimination of zinc from synaptic vesicles in the intact mouse brain by disruption of the ZnT3 gene. *Proc Natl Acad Sci* U S A 96, 1716–1721.

Coleman, J.E., 1998. Zinc enzymes. *Current Opinion in Chemical Biology* 2, 222–234. https://doi.org/10.1016/S1367-5931(98)80064-1

Costello, L.C., Franklin, R.B., 2006. The clinical relevance of the metabolism of prostate cancer; zinc and tumor suppression: connecting the dots. *Mol Cancer* 5, 17. https://doi.org/10.1186/1476-4598-5-17

Costello, L.C., Levy, B.A., Desouki, M.M., Zou, J., Bagasra, O., Johnson, L.A., Hanna, N., Franklin, R.B., 2011. Decreased zinc and downregulation of ZIP3 zinc uptake transporter in the development of pancreatic adenocarcinoma. *Cancer Biol.* Ther. 12, 297–303. https://doi.org/10.4161/cbt.12.4.16356

Cotton, F.A., Wilkinson, G., 1988. *Advanced Inorganic Chemistry Comprehensive* Text by Albert Cotton Wilkinson [WWW Document]. URL (accessed 10.4.20).

Coudray, N., Valvo, S., Hu, M., Lasala, R., Kim, C., Vink, M., Zhou, M., Provasi, D., Filizola, M., Tao, J., Fang, J., Penczek, P.A., Ubarretxena-Belandia, I., Stokes, D.L., 2013.

Inward-facing conformation of the zinc transporter YiiP revealed by cryoelectron microscopy. *PNAS* 110, 2140–2145. https://doi.org/10.1073/pnas.1215455110

Coyle, P., Philcox, J.C., Carey, L.C., Rofe, A.M., 2002. Metallothionein: the multipurpose protein. *Cell. Mol. Life Sci.* 59, 627–647. https://doi.org/10.1007/s00018-002-8454-2

Cp, K., L, H., 2002. ZnT7, a novel mammalian zinc transporter, accumulates zinc in the Golgi apparatus. *J Biol Chem* 278, 4096–4102. https://doi.org/10.1074/jbc.m207644200

Dalton, T.P., He, L., Wang, B., Miller, M.L., Jin, L., Stringer, K.F., Chang, X., Baxter, C.S., Nebert, D.W., 2005. Identification of mouse SLC39A8 as the transporter responsible for cadmium-induced toxicity in the testis. *Proc Natl Acad Sci* U S A 102, 3401–3406. https://doi.org/10.1073/pnas.0406085102

Dermatitis in children with disturbances of the general condition and the absorption of food elements: Brandt, T.: Acta dermat.-venereol. 17: 513, 1936, 1936. *Journal of Allergy* 8, 110. https://doi.org/10.1016/S0021-8707(36)90158-2

Desouki, M.M., Geradts, J., Milon, B., Franklin, R.B., Costello, L.C., 2007. hZip2 and hZip3 zinc transporters are down regulated in human prostate adenocarcinomatous glands. *Molecular Cancer* 6, 37. https://doi.org/10.1186/1476-4598-6-37

Dodson, G., Steiner, D., 1998. The role of assembly in insulin's biosynthesis. *Curr. Opin. Struct. Biol.* 8, 189–194. https://doi.org/10.1016/s0959-440x(98)80037-7

Drinker, K.R., 1926. The Significance of Zinc in the Living Organism. [WWW Document]. URL (accessed 9.30.20).

Dubeaux, G., Neveu, J., Zelazny, E., Vert, G., 2018. Metal Sensing by the IRT1 Transporter-Receptor Orchestrates Its Own Degradation and Plant Metal Nutrition. *Molecular Cell* 69, 953-964.e5. https://doi.org/10.1016/j.molcel.2018.02.009

Dufner-Beattie, J., Huang, Z.L., Geiser, J., Xu, W., Andrews, G.K., 2006. Mouse ZIP1 and ZIP3 genes together are essential for adaptation to dietary zinc deficiency during pregnancy. *genesis* 44, 239–251. https://doi.org/10.1002/dvg.20211

Dufner-Beattie, J., Huang, Z.L., Geiser, J., Xu, W., Andrews, G.K., 2005. Generation and Characterization of Mice Lacking the Zinc Uptake Transporter ZIP3. *Mol Cell Biol* 25, 5607–5615. https://doi.org/10.1128/MCB.25.13.5607-5615.2005

Dufner-Beattie, J., Kuo, Y.-M., Gitschier, J., Andrews, G.K., 2004. The Adaptive Response to Dietary Zinc in Mice Involves the Differential Cellular Localization and Zinc Regulation of the Zinc Transporters ZIP4 and ZIP5. *J. Biol. Chem.* 279, 49082–49090. https://doi.org/10.1074/jbc.M409962200

Dufner-Beattie, J., Wang, F., Kuo, Y.-M., Gitschier, J., Eide, D., Andrews, G.K., 2003. The acrodermatitis enteropathica gene ZIP4 encodes a tissue-specific, zinc-regulated zinc transporter in mice. *J. Biol. Chem.* 278, 33474–33481. https://doi.org/10.1074/jbc.M305000200

Dufner-Beattie, J., Weaver, B.P., Geiser, J., Bilgen, M., Larson, M., Xu, W., Andrews, G.K., 2007. The mouse acrodermatitis enteropathica gene Slc39a4 (Zip4) is essential for early development and heterozygosity causes hypersensitivity to zinc deficiency. *Hum. Mol. Genet.* 16, 1391–1399. https://doi.org/10.1093/hmg/ddm088

Eide, D., Broderius, M., Fett, J., Guerinot, M.L., 1996. A novel iron-regulated metal transporter from plants identified by functional expression in yeast. *Proc Natl Acad Sci* U S A 93, 5624–5628.

Eide, D.J., 2020. Transcription factors and transporters in zinc homeostasis: lessons learned from fungi. *Critical Reviews in Biochemistry and Molecular Biology* 55, 88–110. https://doi.org/10.1080/10409238.2020.1742092

Emdin, S.O., Dodson, G.G., Cutfield, J.M., Cutfield, S.M., 1980. Role of zinc in insulin biosynthesis. Some possible zinc-insulin interactions in the pancreatic B-cell. *Diabetologia* 19, 174–182. https://doi.org/10.1007/BF00275265

Falcón-Pérez, J.M., Dell'Angelica, E.C., 2007. Zinc transporter 2 (SLC30A2) can suppress the vesicular zinc defect of adaptor protein 3-depleted fibroblasts by promoting zinc accumulation in lysosomes. *Experimental Cell Research* 313, 1473–1483. https://doi.org/10.1016/j.yexcr.2007.02.006

Fischer, P.W., Giroux, A., L'Abbé, M.R., 1984. Effect of zinc supplementation on copper status in adult man. *Am J Clin Nutr* 40, 743–746. https://doi.org/10.1093/ajcn/40.4.743

Franklin, R.B., Ma, J., Zou, J., Guan, Z., Kukoyi, B.I., Feng, P., Costello, L.C., 2003. Human ZIP1 is a major zinc uptake transporter for the accumulation of zinc in prostate cells. *J Inorg Biochem* 96, 435–442.

Franz, M.C., Pujol-Giménez, J., Montalbetti, N., Fernandez-Tenorio, M., DeGrado, T.R., Niggli, E., Romero, M.F., Hediger, M.A., 2018. Reassessment of the Transport Mechanism of the Human Zinc Transporter SLC39A2. *Biochemistry* 57, 3976–3986. https://doi.org/10.1021/acs.biochem.8b00511

Franz, M.-C., Simonin, A., Graeter, S., Hediger, M.A., Kovacs, G., 2014. Development of the First Fluorescence Screening Assay for the SLC39A2 Zinc Transporter. *J Biomol Screen* 19, 909–916. https://doi.org/10.1177/1087057114526781

Fujishiro, H., Yano, Y., Takada, Y., Tanihara, M., Himeno, S., 2012. Roles of ZIP8, ZIP14, and DMT1 in transport of cadmium and manganese in mouse kidney proximal tubule cells. *Metallomics* 4, 700–708. https://doi.org/10.1039/C2MT20024D

Fukada, T., Civic, N., Furuichi, T., Shimoda, S., Mishima, K., Higashiyama, H., Idaira, Y., Asada, Y., Kitamura, H., Yamasaki, S., Hojyo, S., Nakayama, M., Ohara, O., Koseki, H., Dos Santos, H.G., Bonafe, L., Ha-Vinh, R., Zankl, A., Unger, S., Kraenzlin, M.E., Beckmann, J.S., Saito, I., Rivolta, C., Ikegawa, S., Superti-Furga, A., Hirano, T., 2008. The zinc transporter SLC39A13/ZIP13 is required for connective tissue development; its involvement in BMP/TGF-beta signaling pathways. *PLoS One* 3, e3642. https://doi.org/10.1371/journal.pone.0003642

Fukunaka, A., Suzuki, T., Kurokawa, Y., Yamazaki, T., Fujiwara, N., Ishihara, K., Migaki, H., Okumura, K., Masuda, S., Yamaguchi-Iwai, Y., Nagao, M., Kambe, T., 2009. Demonstration and Characterization of the Heterodimerization of ZnT5 and ZnT6 in the Early Secretory Pathway. *J Biol Chem* 284, 30798–30806. https://doi.org/10.1074/jbc.M109.026435

Gaither, L.A., Eide, D.J., 2001. The Human ZIP1 Transporter Mediates Zinc Uptake in Human K562 Erythroleukemia Cells. *J. Biol. Chem.* 276, 22258–22264. https://doi.org/10.1074/jbc.M101772200

Gaither, L.A., Eide, D.J., 2000. Functional expression of the human hZIP2 zinc transporter. *J. Biol. Chem.* 275, 5560–5564. https://doi.org/10.1074/jbc.275.8.5560

Galkin, A., Li, Z., Li, L., Kulakova, L., Pal, L.R., Dunaway-Mariano, D., Herzberg, O., 2009. Structural Insights into the Substrate Binding and Stereoselectivity of Giardia Fructose-1,6-bisphosphate Aldolase,. *Biochemistry* 48, 3186–3196. https://doi.org/10.1021/bi9001166

Ganss, B., Jheon, A., 2004. Zinc Finger Transcription Factors in Skeletal Development. *Critical Reviews in Oral Biology & Medicine* 15, 282–297. https://doi.org/10.1177/154411130401500504

Gao, J., Zhao, N., Knutson, M.D., Enns, C.A., 2008. The hereditary hemochromatosis protein, HFE, inhibits iron uptake via down-regulation of Zip14 in HepG2 cells. *J. Biol. Chem.* 283, 21462–21468. https://doi.org/10.1074/jbc.M803150200

Geiser, J., De Lisle, R.C., Andrews, G.K., 2013. The zinc transporter Zip5 (Slc39a5) regulates intestinal zinc excretion and protects the pancreas against zinc toxicity. *PLoS ONE* 8, e82149. https://doi.org/10.1371/journal.pone.0082149

Geiser, J., Venken, K.J.T., Lisle, R.C.D., Andrews, G.K., 2012. A Mouse Model of Acrodermatitis Enteropathica: Loss of Intestine Zinc Transporter ZIP4 (Slc39a4) Disrupts the Stem Cell Niche and Intestine Integrity. *PLOS Genetics* 8, e1002766. https://doi.org/10.1371/journal.pgen.1002766

Giedroc, D.P., Chen, X., Apuy, J.L., 2001. Metal response element (MRE)-binding transcription factor-1 (MTF-1): structure, function, and regulation. *Antioxid. Redox Signal.* 3, 577–596. https://doi.org/10.1089/15230860152542943

Girijashanker, K., He, L., Soleimani, M., Reed, J.M., Li, H., Liu, Z., Wang, B., Dalton, T.P., Nebert, D.W., 2008. Slc39a14 gene encodes ZIP14, a metal/bicarbonate symporter: similarities to the ZIP8 transporter. *Mol Pharmacol* 73, 1413–1423. https://doi.org/10.1124/mol.107.043588

Gitan, R.S., Eide, D.J., 2000. Zinc-regulated ubiquitin conjugation signals endocytosis of the yeast ZRT1 zinc transporter. *Biochem J* 346 Pt 2, 329–336.

Gitan, R.S., Luo, H., Rodgers, J., Broderius, M., Eide, D., 1998. Zinc-induced Inactivation of the Yeast ZRT1 Zinc Transporter Occurs through Endocytosis and Vacuolar Degradation. J. *Biol. Chem.* 273, 28617–28624. https://doi.org/10.1074/jbc.273.44.28617

Giunta, C., Elçioglu, N.H., Albrecht, B., Eich, G., Chambaz, C., Janecke, A.R., Yeowell, H., Weis, M., Eyre, D.R., Kraenzlin, M., Steinmann, B., 2008. Spondylocheiro dysplastic form of the Ehlers-Danlos syndrome--an autosomal-recessive entity caused by mutations in the zinc transporter gene SLC39A13. *Am J Hum Genet* 82, 1290–1305. https://doi.org/10.1016/j.ajhg.2008.05.001

Greenfield, N.J., 2006. Using circular dichroism collected as a function of temperature to determine the thermodynamics of protein unfolding and binding interactions. *Nat Protoc* 1, 2527–2535. https://doi.org/10.1038/nprot.2006.204

Gregory, D.S., Martin, A.C., Cheetham, J.C., Rees, A.R., 1993. The prediction and characterization of metal binding sites in proteins. *Protein Eng.* 6, 29–35. https://doi.org/10.1093/protein/6.1.29

Grotz, N., Fox, T., Connolly, E., Park, W., Guerinot, M.L., Eide, D., 1998. Identification of a family of zinc transporter genes from Arabidopsis that respond to zinc deficiency. *Proc Natl Acad Sci* U S A 95, 7220–7224.

Günes, C., Heuchel, R., Georgiev, O., Müller, K.H., Lichtlen, P., Blüthmann, H., Marino, S., Aguzzi, A., Schaffner, W., 1998. Embryonic lethality and liver degeneration in mice lacking the metal-responsive transcriptional activator MTF-1. *EMBO J.* 17, 2846–2854. https://doi.org/10.1093/emboj/17.10.2846

Guo, H., Jin, X., Zhu, T., Wang, T., Tong, P., Tian, L., Peng, Y., Sun, L., Wan, A., Chen, J., Liu, Y., Li, Ying, Tian, Q., Xia, L., Zhang, L., Pan, Y., Lu, L., Liu, Q., Shen, L., Li, Yunping, Xiong, W., Li, J., Tang, B., Feng, Y., Zhang, X., Zhang, Z., Pan, Q., Hu, Z., Xia, K., 2014. SLC39A5 mutations interfering with the BMP/TGF-β pathway in non-syndromic high myopia. *Journal of Medical Genetics* 51, 518–525. https://doi.org/10.1136/jmedgenet-2014-102351

Guo, L., Lichten, L.A., Ryu, M.-S., Liuzzi, J.P., Wang, F., Cousins, R.J., 2010. STAT5-glucocorticoid receptor interaction and MTF-1 regulate the expression of ZnT2 (Slc30a2) in pancreatic acinar cells. *PNAS* 107, 2818–2823. https://doi.org/10.1073/pnas.0914941107

Gupta, S., Chai, J., Cheng, J., D'Mello, R., Chance, M.R., Fu, D., 2014. Visualizing the kinetic power stroke that drives proton-coupled zinc(II) transport. *Nature* 512, 101–104. https://doi.org/10.1038/nature13382

Gyulkhandanyan, A.V., Lu, H., Lee, S.C., Bhattacharjee, A., Wijesekara, N., Fox, J.E.M., MacDonald, P.E., Chimienti, F., Dai, F.F., Wheeler, M.B., 2008. Investigation of Transport Mechanisms and Regulation of Intracellular Zn2+ in Pancreatic α-Cells. *J. Biol. Chem.* 283, 10184–10197. https://doi.org/10.1074/jbc.M707005200

Haase, H., Rink, L., 2014. Zinc signals and immune function. *Biofactors* 40, 27–40. https://doi.org/10.1002/biof.1114

Hambidge, K.M., Hambidge, C., Jacobs, M., Baum, J.D., 1972. Low levels of zinc in hair, anorexia, poor growth, and hypogeusia in children. *Pediatr Res* 6, 868–874. https://doi.org/10.1203/00006450-197212000-00003

Haney, C.J., Grass, G., Franke, S., Rensing, C., 2005. New developments in the understanding of the cation diffusion facilitator family. *J IND MICROBIOL BIOTECHNOL* 32, 215–226. https://doi.org/10.1007/s10295-005-0224-3

Hara, T., Takeda, T., Takagishi, T., Fukue, K., Kambe, T., Fukada, T., 2017. Physiological roles of zinc transporters: molecular and genetic importance in zinc homeostasis. *J Physiol Sci* 67, 283–301. https://doi.org/10.1007/s12576-017-0521-4

Hardy, A.B., Prentice, K.J., Froese, S., Liu, Y., Andrews, G.K., Wheeler, M.B., 2015. Zip4 Mediated Zinc Influx Stimulates Insulin Secretion in Pancreatic Beta Cells. PLOS ONE 10, e0119136. https://doi.org/10.1371/journal.pone.0119136

Hardyman, J.E.J., Tyson, J., Jackson, K.A., Aldridge, C., Cockell, S.J., Wakeling, L.A., Valentine, R.A., Ford, D., 2016. Zinc sensing by metal-responsive transcription factor 1 (MTF1) controls metallothionein and ZnT1 expression to buffer the sensitivity of the transcriptome response to zinc. *Metallomics: Integrated Biometal Science* 8, 337–343. https://doi.org/10.1039/c5mt00305a

He, L., Girijashanker, K., Dalton, T.P., Reed, J., Li, H., Soleimani, M., Nebert, D.W., 2006. ZIP8, member of the solute-carrier-39 (SLC39) metal-transporter family: characterization of transporter properties. *Mol Pharmacol* 70, 171–180. https://doi.org/10.1124/mol.106.024521

Hirano, T., Murakami, M., Fukada, T., Nishida, K., Yamasaki, S., Suzuki, T., 2008. Roles of zinc and zinc signaling in immunity: zinc as an intracellular signaling molecule. *Adv. Immunol.* 97, 149–176. https://doi.org/10.1016/S0065-2776(08)00003-5

Hoch, E., Levy, M., Hershfinkel, M., Sekler, I., 2020. Elucidating the H+ Coupled Zn2+ Transport Mechanism of ZIP4; Implications in Acrodermatitis Enteropathica.

International Journal of Molecular Sciences 21, 734. https://doi.org/10.3390/ijms21030734

Hoch, E., Lin, W., Chai, J., Hershfinkel, M., Fu, D., Sekler, I., 2012. Histidine pairing at the metal transport site of mammalian ZnT transporters controls Zn2+ over Cd2+ selectivity. *Proc. Natl. Acad. Sci.* U.S.A. 109, 7202–7207. https://doi.org/10.1073/pnas.1200362109

Hogstrand, C., Kille, P., Ackland, M.L., Hiscox, S., Taylor, K.M., 2013. A mechanism for epithelial-mesenchymal transition and anoikis resistance in breast cancer triggered by zinc channel ZIP6 and STAT3 (signal transducer and activator of transcription 3). *Biochem J* 455, 229–237. https://doi.org/10.1042/BJ20130483

Hogstrand, C., Kille, P., Nicholson, R.I., Taylor, K.M., 2009. Zinc transporters and cancer: a potential role for ZIP7 as a hub for tyrosine kinase activation. *Trends Mol Med* 15, 101–111. https://doi.org/10.1016/j.molmed.2009.01.004

Hojyo, S., Fukada, T., Shimoda, S., Ohashi, W., Bin, B.-H., Koseki, H., Hirano, T., 2011. The zinc transporter SLC39A14/ZIP14 controls G-protein coupled receptor-mediated signaling required for systemic growth. *PLoS One* 6, e18059. https://doi.org/10.1371/journal.pone.0018059

Hoogenraad, T.U., Dekker, A.W., Van Den Hamer, C.J.A., 1985. Copper responsive anemia, induced by oral zinc therapy in a patient with acrodermatitis enteropathica. *Science of The Total Environment, Trace Elements, Human Health and Hair Analysis* 42, 37–43. https://doi.org/10.1016/0048-9697(85)90005-1

Huang, L., Kirschke, C.P., Gitschier, J., 2002. Functional characterization of a novel mammalian zinc transporter, ZnT6. *The Journal of Biological Chemistry* 277, 26389–26395. https://doi.org/10.1074/jbc.M200462200

Huang, L., Kirschke, C.P., Lay, Y.-A.E., Levy, L.B., Lamirande, D.E., Zhang, P.H., 2012. Znt7-null mice are more susceptible to diet-induced glucose intolerance and insulin resistance. *The Journal of Biological Chemistry* 287, 33883–33896. https://doi.org/10.1074/jbc.M111.309666

Huang, L., Kirschke, C.P., Zhang, Y., 2006. Decreased intracellular zinc in human tumorigenic prostate epithelial cells: a possible role in prostate cancer progression. *Cancer Cell Int* 6, 10. https://doi.org/10.1186/1475-2867-6-10

Huang, L., Kirschke, C.P., Zhang, Y., Yu, Y.Y., 2005. The ZIP7 gene (Slc39a7) encodes a zinc transporter involved in zinc homeostasis of the Golgi apparatus. *J Biol Chem* 280, 15456–15463. https://doi.org/10.1074/jbc.M412188200

Huang, L., Tepaamorndech, S., 2013. The SLC30 family of zinc transporters - a review of current understanding of their biological and pathophysiological roles. *Mol. Aspects Med.* 34, 548–560. https://doi.org/10.1016/j.mam.2012.05.008

Huang, L., Yu, Y.Y., Kirschke, C.P., Gertz, E.R., Lloyd, K.K.C., 2007. Znt7 (Slc30a7)-deficient mice display reduced body zinc status and body fat accumulation. *The Journal of Biological Chemistry* 282, 37053–37063. https://doi.org/10.1074/jbc.M706631200

Huheey, J.E., Keiter, E.A., Keiter, R.L., 1993. Inorganic chemistry: principles of structure and reactivity. HarperCollins College Publishers, New York, NY.

Jenkitkasemwong, S., Wang, C.-Y., Mackenzie, B., Knutson, M.D., 2012. Physiologic implications of metal-ion transport by ZIP14 and ZIP8. *Biometals* 25, 643–655. https://doi.org/10.1007/s10534-012-9526-x

Jeong, J., Eide, D., 2013a. The SLC39 family of zinc transporters. *Molecular Aspects of Medicine*.

Jeong, J., Eide, D.J., 2013b. The SLC39 family of zinc transporters. *Mol Aspects Med* 34, 612–619. https://doi.org/10.1016/j.mam.2012.05.011

Jeong, J., Walker, J.M., Wang, F., Park, J.G., Palmer, A.E., Giunta, C., Rohrbach, M., Steinmann, B., Eide, D.J., 2012. Promotion of vesicular zinc efflux by ZIP13 and its implications for spondylocheiro dysplastic Ehlers-Danlos syndrome. *Proc Natl Acad Sci U S A* 109, E3530-3538. https://doi.org/10.1073/pnas.1211775110

Juárez-Rebollar, D., Rios, C., Nava-Ruíz, C., Méndez-Armenta, M., 2017. Metallothionein in Brain Disorders. *Oxid Med Cell Longev* 2017, 5828056. https://doi.org/10.1155/2017/5828056

Jung, A.G., Mathony, U.A., Behre, B., Küry, S., Schmitt, S., Zouboulis, C.C., Lippert, U., 2011. Acrodermatitis enteropathica: an uncommon differential diagnosis in childhood – first description of a new sequence variant. *JDDG: Journal der Deutschen Dermatologischen Gesellschaft* 9, 999–1002. https://doi.org/10.1111/j.1610-0387.2011.07742.x

Kägi, J.H.R., Kojima, Y., 1987. Chemistry and Biochemistry of Metallothionein, in: Kägi, Jeremias H. R., Kojima, Yutaka (Eds.), Metallothionein II: Proceedings of the «Second International Meeting on Metallothionein and Other Low Molecular Weight Metalbinding Proteins», Zürich, August 21–24, 1985, *Experientia Supplementum*. *Birkhäuser, Basel*, pp. 25–61. https://doi.org/10.1007/978-3-0348-6784-9_3

Kambe, T., Andrews, G.K., 2009. Novel proteolytic processing of the ectodomain of the zinc transporter ZIP4 (SLC39A4) during zinc deficiency is inhibited by acrodermatitis enteropathica mutations. *Mol. Cell. Biol.* 29, 129–139. https://doi.org/10.1128/MCB.00963-08

Kambe, T., Geiser, J., Lahner, B., Salt, D.E., Andrews, G.K., 2008. Slc39a1 to 3 (Subfamily II) Zip Genes in Mice have Unique Cell-Specific Functions during Adaptation to Zinc Deficiency. *Am J Physiol Regul Integr Comp Physiol* 294, R1474–R1481. https://doi.org/10.1152/ajpregu.00130.2008

Kambe, T., Hashimoto, A., Fujimoto, S., 2014. Current understanding of ZIP and ZnT zinc transporters in human health and diseases. *Cellular and Molecular Life Sciences*. https://doi.org/10.1007/s00018-014-1617-0

Kambe, T., Suzuki, T., Nagao, M., Yamaguchi-Iwai, Y., 2006. Sequence Similarity and Functional Relationship Among Eukaryotic ZIP and CDF Transporters. *Genomics, Proteomics & Bioinformatics* 4, 1–9. https://doi.org/10.1016/S1672-0229(06)60010-7

Kambe, T., Tsuji, T., Hashimoto, A., Itsumura, N., 2015. The Physiological, Biochemical, and Molecular Roles of Zinc Transporters in Zinc Homeostasis and Metabolism. *Physiological Reviews* 95, 749–784. https://doi.org/10.1152/physrev.00035.2014

Kambe, T., Yamaguchi-Iwai, Y., Sasaki, R., Nagao, M., 2004. Overview of mammalian zinc transporters. *CMLS, Cell. Mol. Life Sci.* 61, 49–68. https://doi.org/10.1007/s00018-003-3148-y

Kamizono, A., Nishizawa, M., Teranishi, Y., Murata, K., Kimura, A., 1989. Identification of a gene conferring resistance to zinc and cadmium ions in the yeast Saccharomyces cerevisiae. *Molec. Gen. Genet.* 219, 161–167. https://doi.org/10.1007/BF00261172

Kasana, S., Din, J., Maret, W., 2015. Genetic causes and gene–nutrient interactions in mammalian zinc deficiencies: acrodermatitis enteropathica and transient neonatal zinc deficiency as examples. *J Trace Elem Med Biol* 29, 47–62. https://doi.org/10.1016/j.jtemb.2014.10.003

Kawachi, M., Kobae, Y., Mimura, T., Maeshima, M., 2008. Deletion of a Histidine-rich Loop of AtMTP1, a Vacuolar Zn2+/H+ Antiporter of Arabidopsis thaliana, Stimulates the Transport Activity. *J. Biol. Chem.* 283, 8374–8383. https://doi.org/10.1074/jbc.M707646200

Keilin, D., Mann, T., 1939. Carbonic Anhydrase. *Nature* 144, 442–443. https://doi.org/10.1038/144442b0

Kelleher, S.L., Lönnerdal, B., 2005. Zip3 plays a major role in zinc uptake into mammary epithelial cells and is regulated by prolactin. *Am. J. Physiol., Cell Physiol.* 288, C1042-1047. https://doi.org/10.1152/ajpcell.00471.2004

Kelleher, S.L., Lönnerdal, B., 2003. Zn Transporter Levels and Localization Change Throughout Lactation in Rat Mammary Gland and Are Regulated by Zn in Mammary Cells. *The Journal of Nutrition* 133, 3378–3385. https://doi.org/10.1093/jn/133.11.3378

Kelleher, S.L., Velasquez, V., Croxford, T.P., McCormick, N.H., Lopez, V., MacDavid, J., 2012. Mapping the zinc-transporting system in mammary cells: molecular analysis reveals a phenotype-dependent zinc-transporting network during lactation. *J Cell Physiol* 227, 1761–1770. https://doi.org/10.1002/jcp.22900

Kerkeb, L., Mukherjee, I., Chatterjee, I., Lahner, B., Salt, D.E., Connolly, E.L., 2008. Iron-Induced Turnover of the Arabidopsis IRON-REGULATED TRANSPORTER1 Metal Transporter Requires Lysine Residues. *Plant Physiol* 146, 1964–1973. https://doi.org/10.1104/pp.107.113282

Kim, B.-E., Wang, F., Dufner-Beattie, J., Andrews, G.K., Eide, D.J., Petris, M.J., 2004. Zn2+-stimulated endocytosis of the mZIP4 zinc transporter regulates its location at the plasma membrane. *J. Biol. Chem.* 279, 4523–4530. https://doi.org/10.1074/jbc.M310799200

Kimura, T., Itoh, N., Andrews, G.K., 2009. Mechanisms of Heavy Metal Sensing by Metal Response Element-binding Transcription Factor-1. *Journal of Health Science* 55, 484–494. https://doi.org/10.1248/jhs.55.484

Kimura, T., Kambe, T., 2016. The Functions of Metallothionein and ZIP and ZnT Transporters: An Overview and Perspective. *International Journal of Molecular Sciences* 17, 336. https://doi.org/10.3390/ijms17030336

Kitamura, H., Morikawa, H., Kamon, H., Iguchi, M., Hojyo, S., Fukada, T., Yamashita, S., Kaisho, T., Akira, S., Murakami, M., Hirano, T., 2006. Toll-like receptor-mediated regulation of zinc homeostasis influences dendritic cell function. *Nat. Immunol.* 7, 971–977. https://doi.org/10.1038/ni1373

Klug, A., 2010. The discovery of zinc fingers and their applications in gene regulation and genome manipulation. *Annu. Rev. Biochem.* 79, 213–231. https://doi.org/10.1146/annurev-biochem-010909-095056

Kong, B.Y., Duncan, F.E., Que, E.L., Kim, A.M., O'Halloran, T.V., Woodruff, T.K., 2014. Maternally-derived zinc transporters ZIP6 and ZIP10 drive the mammalian oocyte-to-egg transition. *Mol Hum Reprod* 20, 1077–1089. https://doi.org/10.1093/molehr/gau066

Krężel, A., Maret, W., 2007. Dual Nanomolar and Picomolar Zn(II) Binding Properties of Metallothionein. *J. Am. Chem. Soc.* 129, 10911–10921. https://doi.org/10.1021/ja071979s

Küry, S., Dréno, B., Bézieau, S., Giraudet, S., Kharfi, M., Kamoun, R., Moisan, J.-P., 2002. Identification of SLC39A4 , a gene involved in acrodermatitis enteropathica. *Nat Genet* 31, 239–240. https://doi.org/10.1038/ng913

Küry, S., Kharfi, M., Blouin, E., Schmitt, S., Bézieau, S., 2016. Clinical utility gene card for: acrodermatitis enteropathica – update 2015. European *Journal of Human Genetics* 24, 779–779. https://doi.org/10.1038/ejhg.2015.203

Küry, S., Kharfi, M., Kamoun, R., Taïeb, A., Mallet, E., Baudon, J.-J., Glastre, C., Michel, B., Sebag, F., Brooks, D., Schuster, V., Scoul, C., Dréno, B., Bézieau, S., Moisan, J.-P., 2003. Mutation spectrum of human SLC39A4 in a panel of patients with acrodermatitis enteropathica. *Human Mutation* 22, 337–338. https://doi.org/10.1002/humu.9178

Langmade, S.J., Ravindra, R., Daniels, P.J., Andrews, G.K., 2000. The transcription factor MTF-1 mediates metal regulation of the mouse ZnT1 gene. *J. Biol. Chem.* 275, 34803–34809. https://doi.org/10.1074/jbc.M007339200

Lee, M.G., Hong, K.T., Kim, J.J., 1990. Transient symptomatic zinc deficiency in a full-term breast-fed infant. *J Am Acad Dermatol* 23, 375–379. https://doi.org/10.1016/0190-9622(90)70226-8

Lee, S., 2018. Critical Role of Zinc as Either an Antioxidant or a Prooxidant in Cellular Systems. *Oxidative Medicine and Cellular Longevity* 2018, 1–11. https://doi.org/10.1155/2018/9156285

Legardinier, S., Raguénès-Nicol, C., Tascon, C., Rocher, C., Hardy, S., Hubert, J.-F., Le Rumeur, E., 2009. Mapping of the Lipid-Binding and Stability Properties of the Central Rod Domain of Human Dystrophin. *Journal of Molecular Biology* 389, 546–558. https://doi.org/10.1016/j.jmb.2009.04.025

Lemaire, K., Ravier, M.A., Schraenen, A., Creemers, J.W.M., Van de Plas, R., Granvik, M., Van Lommel, L., Waelkens, E., Chimienti, F., Rutter, G.A., Gilon, P., in't Veld, P.A., Schuit, F.C., 2009. Insulin crystallization depends on zinc transporter ZnT8 expression, but is not required for normal glucose homeostasis in mice. *Proceedings of the National Academy of Sciences of the United States of America* 106, 14872–14877. https://doi.org/10.1073/pnas.0906587106

Li, M., Zhang, Y., Bharadwaj, U., Zhai, Q.J., Ahern, C.H., Fisher, W.E., Brunicardi, F.C., Logsdon, C.D., Chen, C., Yao, Q., 2009. Down-regulation of ZIP4 by RNA interference inhibits pancreatic cancer growth and increases the survival of nude mice with pancreatic cancer xenografts. *Clin. Cancer Res.* 15, 5993–6001. https://doi.org/10.1158/1078-0432.CCR-09-0557

Li, M., Zhang, Y., Liu, Z., Bharadwaj, U., Wang, H., Wang, X., Zhang, S., Liuzzi, J.P., Chang, S.-M., Cousins, R.J., Fisher, W.E., Brunicardi, F.C., Logsdon, C.D., Chen, C., Yao, Q., 2007. Aberrant expression of zinc transporter ZIP4 (SLC39A4) significantly contributes to human pancreatic cancer pathogenesis and progression. *Proc. Natl. Acad. Sci.* U.S.A. 104, 18636–18641. https://doi.org/10.1073/pnas.0709307104

Lichten, L.A., Cousins, R.J., 2009. Mammalian zinc transporters: nutritional and physiologic regulation. *Annual Review of Nutrition* 29, 153–176. https://doi.org/10.1146/annurev-nutr-033009-083312

Lichtlen, P., Schaffner, W., 2001. Putting its fingers on stressful situations: the heavy metal-regulatory transcription factor MTF-1. *BioEssays* 23, 1010–1017. https://doi.org/10.1002/bies.1146

Lin, W., Chai, J., Love, J., Fu, D., 2010. Selective electrodiffusion of zinc ions in a Zrt-, Irt-like protein, ZIPB. *J Biol Chem* 285, 39013–39020. https://doi.org/10.1074/jbc.M110.180620

Lin, Y., Chen, Y., Wang, Y., Yang, J., Zhu, V.F., Liu, Y., Cui, X., Chen, L., Yan, W., Jiang, T., Hergenroeder, G.W., Fletcher, S.A., Levine, J.M., Kim, D.H., Tandon, N., Zhu, J.-J., Li, M., 2013. ZIP4 is a novel molecular marker for glioma. *Neuro Oncol* 15, 1008–1016. https://doi.org/10.1093/neuonc/not042

Liu, F., Zhang, Z., Csanády, L., Gadsby, D.C., Chen, J., 2017. Molecular Structure of the Human CFTR Ion Channel. *Cell* 169, 85-95.e8. https://doi.org/10.1016/j.cell.2017.02.024

Liu, F., Zhang, Z., Levit, A., Levring, J., Touhara, K.K., Shoichet, B.K., Chen, J., 2019. Structural identification of a hotspot on CFTR for potentiation. *Science* 364, 1184–1188. https://doi.org/10.1126/science.aaw7611

Liu, M.-J., Bao, S., Gálvez-Peralta, M., Pyle, C.J., Rudawsky, A.C., Pavlovicz, R.E., Killilea, D.W., Li, C., Nebert, D.W., Wewers, M.D., Knoell, D.L., 2013. ZIP8 regulates host defense through zinc-mediated inhibition of NF-κB. *Cell Rep* 3, 386–400. https://doi.org/10.1016/j.celrep.2013.01.009

Liu, Y., Batchuluun, B., Ho, L., Zhu, D., Prentice, K.J., Bhattacharjee, A., Zhang, M., Pourasgari, F., Hardy, A.B., Taylor, K.M., Gaisano, H., Dai, F.F., Wheeler, M.B., 2015. Characterization of Zinc Influx Transporters (ZIPs) in Pancreatic β Cells. *J Biol Chem* 290, 18757–18769. https://doi.org/10.1074/jbc.M115.640524

Liu, Z., Li, H., Soleimani, M., Girijashanker, K., Reed, J.M., He, L., Dalton, T.P., Nebert, D.W., 2008. Cd2+ versus Zn2+ uptake by the ZIP8 HCO3--dependent symporter: kinetics, electrogenicity and trafficking. *Biochem Biophys Res Commun* 365, 814–820. https://doi.org/10.1016/j.bbrc.2007.11.067

Liuzzi, J.P., Bobo, J.A., Cui, L., McMahon, R.J., Cousins, R.J., 2003. Zinc transporters 1, 2 and 4 are differentially expressed and localized in rats during pregnancy and lactation. *The Journal of Nutrition* 133, 342–351. https://doi.org/10.1093/jn/133.2.342

Liuzzi, J.P., Cousins, R.J., 2004. Mammalian zinc transporters. *Annu. Rev. Nutr.* 24, 151–172. https://doi.org/10.1146/annurev.nutr.24.012003.132402

Liuzzi, J.P., Guo, L., Chang, S.-M., Cousins, R.J., 2009. Krüppel-like factor 4 regulates adaptive expression of the zinc transporter Zip4 in mouse small intestine. *Am. J. Physiol. Gastrointest. Liver Physiol.* 296, G517-523. https://doi.org/10.1152/ajpgi.90568.2008

Lopez-Redondo, M.L., Coudray, N., Zhang, Z., Alexopoulos, J., Stokes, D.L., 2018. Structural basis for the alternating access mechanism of the cation diffusion facilitator YiiP. *PNAS* 115, 3042–3047. https://doi.org/10.1073/pnas.1715051115

Louis-Jeune, C., Andrade-Navarro, M.A., Perez-Iratxeta, C., 2012. Prediction of protein secondary structure from circular dichroism using theoretically derived spectra. *Proteins: Structure, Function, and Bioinformatics* 80, 374–381. https://doi.org/10.1002/prot.23188

Lovejoy, B., Cleasby, A., Hassell, A.M., Longley, K., Luther, M.A., Weigl, D., McGeehan, G., McElroy, A.B., Drewry, D., Lambert, M.H., Et, A., 1994. Structure of the catalytic domain of fibroblast collagenase complexed with an inhibitor. *Science* 263, 375–377. https://doi.org/10.1126/science.8278810

Lu, M., Chai, J., Fu, D., 2009. Structural Basis for Auto-regulation of the Zinc Transporter YiiP. *Nat Struct Mol Biol* 16, 1063–1067. https://doi.org/10.1038/nsmb.1662

Lu, M., Fu, D., 2007. Structure of the zinc transporter YiiP. *Science* 317, 1746–1748. https://doi.org/10.1126/science.1143748

Lukacs, G.L., Verkman, A.S., 2012. CFTR: folding, misfolding and correcting the ΔF508 conformational defect. *Trends in Molecular Medicine* 18, 81–91. https://doi.org/10.1016/j.molmed.2011.10.003

Lutz, R.E., 1926. The Normal Occurrence of Zinc in Biologic Materials: a Review of the Literature, and a Study of the Normal Distribution of Zinc in the Rat, Cat, and Man. *Journal of Industrial Hygiene* 8, 177–207.

Mao, X., Kim, B.-E., Wang, F., Eide, D.J., Petris, M.J., 2007. A Histidine-rich Cluster Mediates the Ubiquitination and Degradation of the Human Zinc Transporter, hZIP4, and Protects against Zinc Cytotoxicity. *J. Biol. Chem.* 282, 6992–7000. https://doi.org/10.1074/jbc.M610552200

Maret, W., 2013. Zinc biochemistry: from a single zinc enzyme to a key element of life. *Adv Nutr* 4, 82–91. https://doi.org/10.3945/an.112.003038

Maret, W., 2000. The function of zinc metallothionein: a link between cellular zinc and redox state. *J. Nutr.* 130, 1455S–8S. https://doi.org/10.1093/jn/130.5.1455S

Maret, W., Li, Y., 2009. Coordination Dynamics of Zinc in Proteins. *Chem. Rev.* 109, 4682–4707. https://doi.org/10.1021/cr800556u

Marinko, J.T., Huang, H., Penn, W.D., Capra, J.A., Schlebach, J.P., Sanders, C.R., 2019. Folding and Misfolding of Human Membrane Proteins in Health and Disease: From Single Molecules to Cellular Proteostasis. *Chem Rev* 119, 5537–5606. https://doi.org/10.1021/acs.chemrev.8b00532

Martin, A.B., Aydemir, T.B., Guthrie, G.J., Samuelson, D.A., Chang, S.-M., Cousins, R.J., 2013. Gastric and colonic zinc transporter ZIP11 (Slc39a11) in mice responds to dietary zinc and exhibits nuclear localization. *J Nutr* 143, 1882–1888. https://doi.org/10.3945/jn.113.184457

Matsuura, W., Yamazaki, T., Yamaguchi-iwai, Y., Masuda, S., Nagao, M., Andrews, G.K., Kambe, T., 2009. Slc39a9 (ZIP9) Regulates Zinc Homeostasis in the Secretory Pathway:

Characterization of the ZIP Subfamily I Protein in Vertebrate Cells. *Bioscience, Biotechnology, and Biochemistry* 73, 1142–1148. https://doi.org/10.1271/bbb.80910

Maverakis, E., Fung, M.A., Lynch, P.J., Draznin, M., Michael, D.J., Ruben, B., Fazel, N., 2007. Acrodermatitis enteropathica and an overview of zinc metabolism. *Journal of the American Academy of Dermatology* 56, 116–124. https://doi.org/10.1016/j.jaad.2006.08.015

McCall, K.A., Huang, C., Fierke, C.A., 2000. Function and Mechanism of Zinc Metalloenzymes. *J Nutr* 130, 1437S-1446S. https://doi.org/10.1093/jn/130.5.1437S

McCormick, N.H., Hennigar, S.R., Kiselyov, K., Kelleher, S.L., 2014. The biology of zinc transport in mammary epithelial cells: implications for mammary gland development, lactation, and involution. *J Mammary Gland Biol Neoplasia* 19, 59–71. https://doi.org/10.1007/s10911-013-9314-4

McCormick, N.H., Kelleher, S.L., 2012. ZnT4 provides zinc to zinc-dependent proteins in the trans-Golgi network critical for cell function and Zn export in mammary epithelial cells. *American Journal of Physiology. Cell Physiology* 303, C291-297. https://doi.org/10.1152/ajpcell.00443.2011

McMahon, R.J., Cousins, R.J., 1998. Regulation of the zinc transporter ZnT-1 by dietary zinc. *PNAS* 95, 4841–4846. https://doi.org/10.1073/pnas.95.9.4841

Miles, A.T., Hawksworth, G.M., Beattie, J.H., Rodilla, V., 2000. Induction, Regulation, Degradation, and Biological Significance of Mammalian Metallothioneins. Critical *Reviews in Biochemistry and Molecular Biology* 35, 35–70. https://doi.org/10.1080/10409230091169168

Miller, J., McLachlan, A.D., Klug, A., 1985. Repetitive zinc-binding domains in the protein transcription factor IIIA from Xenopus oocytes. *EMBO J.* 4, 1609–1614.

Milon, B., Dhermy, D., Pountney, D., Bourgeois, M., Beaumont, C., 2001. Differential subcellular localization of hZip1 in adherent and non-adherent cells. *FEBS Letters* 507, 241–246. https://doi.org/10.1016/S0014-5793(01)02950-7

Milon, B., Wu, Q., Zou, J., Costello, L.C., Franklin, R.B., 2006. Histidine residues in the region between transmembrane domains III and IV of hZip1 are required for zinc transport across the plasma membrane in PC-3 cells. *Biochim Biophys Acta* 1758, 1696–1701. https://doi.org/10.1016/j.bbamem.2006.06.005

Mitra, B., Sharma, R., 2001. The Cysteine-Rich Amino-Terminal Domain of ZntA, a Pb(II)/Zn(II)/Cd(II)-Translocating ATPase from Escherichia coli, Is Not Essential for Its Function. *Biochemistry* 40, 7694–7699. https://doi.org/10.1021/bi010576g

Moynahan, E.J., 1974. Letter: Acrodermatitis enteropathica: a lethal inherited human zinc-deficiency disorder. *Lancet* 2, 399–400. https://doi.org/10.1016/s0140-6736(74)91772-3

Moynahan, E.J., Barnes, P.M., 1973. Zinc deficiency and a synthetic diet for lactose intolerance. *Lancet* 1, 676–677. https://doi.org/10.1016/s0140-6736(73)92253-8

Nakano, A., Nakano, H., Toyomaki, Y., Hanada, K., Nomura, K., 2003. Novel SLC39A4 Mutations in Acrodermatitis Enteropathica. *J Invest Dermatol* 120, 963–966. https://doi.org/10.1046/j.1523-1747.2003.12243.x

Nebert, D.W., Gálvez-Peralta, M., Hay, E.B., Li, H., Johansson, E., Yin, C., Wang, B., He, L., Soleimani, M., 2012. ZIP14 and ZIP8 zinc/bicarbonate symporters in Xenopus oocytes: characterization of metal uptake and inhibition. *Metallomics* 4, 1218–1225. https://doi.org/10.1039/c2mt20177a

Nishida, S., Mizuno, T., Obata, H., 2008. Involvement of histidine-rich domain of ZIP family transporter TjZNT1 in metal ion specificity. *Plant Physiol Biochem* 46, 601–606. https://doi.org/10.1016/j.plaphy.2008.02.011

Nutrition, W.E.C. on T.E. in H., Organization, W.H., 1973. Trace elements in human nutrition: report of a WHO expert committee [meeting held in Geneva from 9 to 17 April 1973]. *World Health Organization*.

Ohana, E., Hoch, E., Keasar, C., Kambe, T., Yifrach, O., Hershfinkel, M., Sekler, I., 2009. Identification of the Zn2+ binding site and mode of operation of a mammalian Zn2+ transporter. *J. Biol. Chem.* 284, 17677–17686. https://doi.org/10.1074/jbc.M109.007203

Ohana, E., Sekler, I., Kaisman, T., Kahn, N., Cove, J., Silverman, W.F., Amsterdam, A., Hershfinkel, M., 2006. Silencing of ZnT-1 expression enhances heavy metal influx and toxicity. *J. Mol. Med.* 84, 753–763. https://doi.org/10.1007/s00109-006-0062-4

Palmiter, R.D., Cole, T.B., Quaife, C.J., Findley, S.D., 1996. ZnT-3, a putative transporter of zinc into synaptic vesicles. *PNAS* 93, 14934–14939. https://doi.org/10.1073/pnas.93.25.14934

Palmiter, R.D., Findley, S.D., 1995. Cloning and functional characterization of a mammalian zinc transporter that confers resistance to zinc. *EMBO J* 14, 639–649.

Palmiter, R.D., Huang, L., 2004. Efflux and compartmentalization of zinc by members of the SLC30 family of solute carriers. *Pflugers Arch.* 447, 744–751. https://doi.org/10.1007/s00424-003-1070-7

Park, J.H., Hogrebe, M., Grüneberg, M., DuChesne, I., von der Heiden, A.L., Reunert, J., Schlingmann, K.P., Boycott, K.M., Beaulieu, C.L., Mhanni, A.A., Innes, A.M., Hörtnagel, K., Biskup, S., Gleixner, E.M., 2015. SLC39A8 Deficiency: A Disorder of

Manganese Transport and Glycosylation. *The American Journal of Human Genetics* 97, 894–903. https://doi.org/10.1016/j.ajhg.2015.11.003

Pavletich, N.P., Pabo, C.O., 1991. Zinc finger-DNA recognition: crystal structure of a Zif268-DNA complex at 2.1 A. *Science* 252, 809–817. https://doi.org/10.1126/science.2028256

Pelmenschikov, V., Siegbahn, P.E.M., 2002. Catalytic Mechanism of Matrix Metalloproteinases: Two-Layered ONIOM Study. *Inorg. Chem.* 41, 5659–5666. https://doi.org/10.1021/ic0255656

Penny, M.E., 2013. Zinc supplementation in public health. *Ann. Nutr. Metab.* 62 Suppl 1, 31–42. https://doi.org/10.1159/000348263

Perafán-Riveros, C., França, L.F.S., Alves, A.C.F., Sanches, J.A., 2002. Acrodermatitis Enteropathica: Case Report and Review of the Literature. *Pediatric Dermatology* 19, 426–431. https://doi.org/10.1046/j.1525-1470.2002.00200.x

Pérez-Clausell, J., Danscher, G., 1985. Intravesicular localization of zinc in rat telencephalic boutons. A histochemical study. *Brain Res.* 337, 91–98. https://doi.org/10.1016/0006-8993(85)91612-9

Petrarca, P., Ammendola, S., Pasquali, P., Battistoni, A., 2010. The Zur-Regulated ZinT Protein Is an Auxiliary Component of the High-Affinity ZnuABC Zinc Transporter That Facilitates Metal Recruitment during Severe Zinc Shortage. *Journal of Bacteriology* 192, 1553–1564. https://doi.org/10.1128/JB.01310-09

Pinilla-Tenas, J.J., Sparkman, B.K., Shawki, A., Illing, A.C., Mitchell, C.J., Zhao, N., Liuzzi, J.P., Cousins, R.J., Knutson, M.D., Mackenzie, B., 2011. Zip14 is a complex broad-scope metal-ion transporter whose functional properties support roles in the cellular uptake of zinc and nontransferrin-bound iron. *Am J Physiol Cell Physiol* 301, C862–C871. https://doi.org/10.1152/ajpcell.00479.2010

Pound, L.D., Sarkar, S.A., Benninger, R.K.P., Wang, Y., Suwanichkul, A., Shadoan, M.K., Printz, R.L., Oeser, J.K., Lee, C.E., Piston, D.W., McGuinness, O.P., Hutton, J.C., Powell, D.R., O'Brien, R.M., 2009. Deletion of the mouse Slc30a8 gene encoding zinc transporter-8 results in impaired insulin secretion. *The Biochemical Journal* 421, 371–376. https://doi.org/10.1042/BJ20090530

Prasad, A.S., 2012. Discovery of human zinc deficiency: 50 years later. *Journal of Trace Elements in Medicine and Biology*, IX ISTERH Conference. Trace elements in health and disease: Essentiality, toxicity 26, 66–69. https://doi.org/10.1016/j.jtemb.2012.04.004

Prasad, A.S., 2003. Zinc deficiency. *BMJ* 326, 409–410.

Qian, J., Xu, K., Yoo, J., Chen, T.T., Andrews, G., Noebels, J.L., 2011. Knockout of Zn Transporters Zip-1 and Zip-3 Attenuates Seizure-Induced CA1 *Neurodegeneration*. *J. Neurosci*. 31, 97–104. https://doi.org/10.1523/JNEUROSCI.5162-10.2011

Raulin, J., 1869. Etudes chimiques sur la vegetation. *Ann Sci Nat Bot Biol Veg*. https://doi.org/11:92–299

Rink, L., 2011. Zinc in Human Health. *IOS Press*, Amsterdam, NETHERLANDS, THE.

Roohani, N., Hurrell, R., Kelishadi, R., Schulin, R., 2013. Zinc and its importance for human health: An integrative review. *J Res Med Sci* 18, 144–157.

Saxena, R., Voight, B.F., Lyssenko, V., Burtt, N.P., Bakker, P.I.W. de, Chen, H., Roix, J.J., Kathiresan, S., Hirschhorn, J.N., Daly, M.J., Hughes, T.E., Groop, L., Altshuler, D., Almgren, P., Florez, J.C., Meyer, J., Ardlie, K., Boström, K.B., Isomaa, B., Lettre, G., Lindblad, U., Lyon, H.N., Melander, O., Newton-Cheh, C., Nilsson, P., Orho-Melander, M., Råstam, L., Speliotes, E.K., Taskinen, M.-R., Tuomi, T., Guiducci, C., Berglund, A., Carlson, J., Gianniny, L., Hackett, R., Hall, L., Holmkvist, J., Laurila, E., Sjögren, M., Sterner, M., Surti, A., Svensson, Margareta, Svensson, Malin, Tewhey, R., Blumenstiel, B., Parkin, M., DeFelice, M., Barry, R., Brodeur, W., Camarata, J., Chia, N., Fava, M., Gibbons, J., Handsaker, B., Healy, C., Nguyen, K., Gates, C., Sougnez, C., Gage, D., Nizzari, M., Gabriel, S.B., Chirn, G.-W., Ma, Q., Parikh, H., Richardson, D., Ricke, D., Purcell, S., 2007. Genome-Wide Association Analysis Identifies Loci for Type 2 Diabetes and Triglyceride Levels. *Science* 316, 1331–1336. https://doi.org/10.1126/science.1142358

Schmitt, S., Küry, S., Giraud, M., Dréno, B., Kharfi, M., Bézieau, S., 2009. An update on mutations of the SLC39A4 gene in acrodermatitis enteropathica. *Hum. Mutat*. 30, 926–933. https://doi.org/10.1002/humu.20988

Schmitt-Ulms, G., Ehsani, S., Watts, J.C., Westaway, D., Wille, H., 2009. Evolutionary Descent of Prion Genes from the ZIP Family of Metal Ion Transporters. *PLOS ONE* 4, e7208. https://doi.org/10.1371/journal.pone.0007208

Scott, L.J., Mohlke, K.L., Bonnycastle, L.L., Willer, C.J., Li, Y., Duren, W.L., Erdos, M.R., Stringham, H.M., Chines, P.S., Jackson, A.U., Prokunina-Olsson, L., Ding, C.-J., Swift, A.J., Narisu, N., Hu, T., Pruim, R., Xiao, R., Li, X.-Y., Conneely, K.N., Riebow, N.L., Sprau, A.G., Tong, M., White, P.P., Hetrick, K.N., Barnhart, M.W., Bark, C.W., Goldstein, J.L., Watkins, L., Xiang, F., Saramies, J., Buchanan, T.A., Watanabe, R.M., Valle, T.T., Kinnunen, L., Abecasis, G.R., Pugh, E.W., Doheny, K.F., Bergman, R.N., Tuomilehto, J., Collins, F.S., Boehnke, M., 2007. A genome-wide association study of type 2 diabetes in Finns detects multiple susceptibility variants. *Science* 316, 1341–1345. https://doi.org/10.1126/science.1142382

Seo, Y.A., Lopez, V., Kelleher, S.L., 2011. A histidine-rich motif mediates mitochondrial localization of ZnT2 to modulate mitochondrial function. *American Journal of*

Physiology. *Cell Physiology* 300, C1479-1489. https://doi.org/10.1152/ajpcell.00420.2010

Shrimpton, R., Gross, R., Darnton-Hill, I., Young, M., 2005. Zinc deficiency: what are the most appropriate interventions? *BMJ* 330, 347–349. https://doi.org/10.1136/bmj.330.7487.347

Shusterman, E., Beharier, O., Shiri, L., Zarivach, R., Etzion, Y., Campbell, C.R., Lee, I.-H., Okabayashi, K., Dinudom, A., Cook, D.I., Katz, A., Moran, A., 2014. ZnT-1 extrudes zinc from mammalian cells functioning as a Zn(2+)/H(+) exchanger. *Metallomics* 6, 1656–1663. https://doi.org/10.1039/c4mt00108g

Siegel, R.L., Miller, K.D., Jemal, A., 2020. Cancer statistics, 2020. CA: *A Cancer Journal for Clinicians* 70, 7–30. https://doi.org/10.3322/caac.21590

Sladek, R., Rocheleau, G., Rung, J., Dina, C., Shen, L., Serre, D., Boutin, P., Vincent, D., Belisle, A., Hadjadj, S., Balkau, B., Heude, B., Charpentier, G., Hudson, T.J., Montpetit, A., Pshezhetsky, A.V., Prentki, M., Posner, B.I., Balding, D.J., Meyre, D., Polychronakos, C., Froguel, P., 2007. A genome-wide association study identifies novel risk loci for type 2 diabetes. *Nature* 445, 881–885. https://doi.org/10.1038/nature05616

Spiro, R.G., 2002. Protein glycosylation: nature, distribution, enzymatic formation, and disease implications of glycopeptide bonds. *Glycobiology* 12, 43R-56R. https://doi.org/10.1093/glycob/12.4.43R

Stuart, G.W., Searle, P.F., Palmiter, R.D., 1985. Identification of multiple metal regulatory elements in mouse metallothionein-I promoter by assaying synthetic sequences. *Nature* 317, 828–831. https://doi.org/10.1038/317828a0

Suzuki, T., Ishihara, K., Migaki, H., Matsuura, W., Kohda, A., Okumura, K., Nagao, M., Yamaguchi-Iwai, Y., Kambe, T., 2005. Zinc transporters, ZnT5 and ZnT7, are required for the activation of alkaline phosphatases, zinc-requiring enzymes that are glycosylphosphatidylinositol-anchored to the cytoplasmic membrane. *The Journal of Biological Chemistry* 280, 637–643. https://doi.org/10.1074/jbc.M411247200

Takatani-Nakase, T., Matsui, C., Maeda, S., Kawahara, S., Takahashi, K., 2014. High Glucose Level Promotes Migration Behavior of Breast Cancer Cells through Zinc and Its Transporters. *PLOS ONE* 9, e90136. https://doi.org/10.1371/journal.pone.0090136

Tanaka, N., Kawachi, M., Fujiwara, T., Maeshima, M., 2013. Zinc-binding and structural properties of the histidine-rich loop of Arabidopsis thaliana vacuolar membrane zinc transporter MTP1. *FEBS Open Bio* 3, 218–224. https://doi.org/10.1016/j.fob.2013.04.004

Taniguchi, M., Fukunaka, A., Hagihara, M., Watanabe, K., Kamino, S., Kambe, T., Enomoto, S., Hiromura, M., 2013. Essential Role of the Zinc Transporter ZIP9/SLC39A9 in Regulating the Activations of Akt and Erk in B-Cell Receptor Signaling Pathway in DT40 Cells. *PLOS ONE* 8, e58022. https://doi.org/10.1371/journal.pone.0058022

Taylor, K.M., Vichova, P., Jordan, N., Hiscox, S., Hendley, R., Nicholson, R.I., 2008. ZIP7-mediated intracellular zinc transport contributes to aberrant growth factor signaling in antihormone-resistant breast cancer Cells. *Endocrinology* 149, 4912–4920. https://doi.org/10.1210/en.2008-0351

Taylor-Cousar, J.L., Munck, A., McKone, E.F., van der Ent, C.K., Moeller, A., Simard, C., Wang, L.T., Ingenito, E.P., McKee, C., Lu, Y., Lekstrom-Himes, J., Elborn, J.S., 2017. Tezacaftor–Ivacaftor in Patients with Cystic Fibrosis Homozygous for Phe508del. *New England Journal of Medicine* 377, 2013–2023. https://doi.org/10.1056/NEJMoa1709846

Tb, C., Ca, R., Hj, W., Pa, S., Rd, P., 2000. Seizures and neuronal damage in mice lacking vesicular zinc. *Epilepsy Res* 39, 153–169. https://doi.org/10.1016/s0920-1211(99)00121-7

Thirumoorthy, N., Shyam Sunder, A., Manisenthil Kumar, K., Senthil Kumar, M., Ganesh, G., Chatterjee, M., 2011. A review of metallothionein isoforms and their role in pathophysiology. *World J Surg Oncol* 9, 54. https://doi.org/10.1186/1477-7819-9-54

Thomas, P., Pang, Y., Dong, J., Berg, A.H., 2014. Identification and characterization of membrane androgen receptors in the ZIP9 zinc transporter subfamily: II. Role of human ZIP9 in testosterone-induced prostate and breast cancer cell apoptosis. *Endocrinology* 155, 4250–4265. https://doi.org/10.1210/en.2014-1201

Tóth, K., 2011. Zinc in neurotransmission. *Annu. Rev. Nutr.* 31, 139–153. https://doi.org/10.1146/annurev-nutr-072610-145218

Vallee, B.L., Auld, D.S., 1993. New perspective on zinc biochemistry: Cocatalytic sites in multi-zinc enzymes. *Biochemistry* 32, 6493–6500. https://doi.org/10.1021/bi00077a001

Vallee, B.L., Auld, D.S., 1992a. Functional zinc-binding motifs in enzymes and DNA-binding proteins. *Faraday Discuss.* 93, 47–65. https://doi.org/10.1039/FD9929300047

Vallee, B.L., Auld, D.S., 1992b. Active zinc binding sites of zinc metalloenzymes. *Matrix Suppl* 1, 5–19.

Vallee, B.L., Coleman, J.E., Auld, D.S., 1991. Zinc fingers, zinc clusters, and zinc twists in DNA-binding protein domains. *PNAS* 88, 999–1003. https://doi.org/10.1073/pnas.88.3.999

Vallee, B.L., Neurath, H., 1955. Carboxypeptidase, a zinc metalloenzyme. *J. Biol. Chem.* 217, 253–261.

Van Wouwe, J.P., 1995. Clinical and laboratory assessment of zinc deficiency in Dutch children. *Biol Trace Elem Res* 49, 211–225. https://doi.org/10.1007/BF02788969

Vedani, A., Huhta, D.W., 1990. A new force field for modeling metalloproteins. *J. Am. Chem. Soc.* 112, 4759–4767. https://doi.org/10.1021/ja00168a021

Walravens, P.A., Krebs, N.F., Hambidge, K.M., 1983. Linear growth of low income preschool children receiving a zinc supplement. *Am J Clin Nutr* 38, 195–201. https://doi.org/10.1093/ajcn/38.2.195

Wang, F., Kim, B.-E., Dufner-Beattie, J., Petris, M.J., Andrews, G., Eide, D.J., 2004a. Acrodermatitis enteropathica mutations affect transport activity, localization and zinc-responsive trafficking of the mouse ZIP4 zinc transporter. *Hum Mol Genet* 13, 563–571. https://doi.org/10.1093/hmg/ddh049

Wang, F., Kim, B.-E., Petris, M.J., Eide, D.J., 2004b. The mammalian Zip5 protein is a zinc transporter that localizes to the basolateral surface of polarized cells. *J Biol Chem* 279, 51433–51441. https://doi.org/10.1074/jbc.M408361200

Wang, K., Pugh, E.W., Griffen, S., Doheny, K.F., Mostafa, W.Z., al-Aboosi, M.M., el-Shanti, H., Gitschier, J., 2001. Homozygosity mapping places the acrodermatitis enteropathica gene on chromosomal region 8q24.3. *Am. J. Hum.* Genet. 68, 1055–1060. https://doi.org/10.1086/319514

Wang, K., Zhou, B., Kuo, Y.-M., Zemansky, J., Gitschier, J., 2002. A Novel Member of a Zinc Transporter Family Is Defective in Acrodermatitis Enteropathica. *The American Journal of Human Genetics* 71, 66–73. https://doi.org/10.1086/341125

Wang, S., Xue, L., Guo, Z.-P., Wang, L., Yang, Y., 2008. A novel SLC39A4 gene mutation in the family of an acrodermatitis enteropathica patient with an unusual presentation. *British Journal of Dermatology* 159, 976–978. https://doi.org/10.1111/j.1365-2133.2008.08777.x

Waterhouse, A., Bertoni, M., Bienert, S., Studer, G., Tauriello, G., Gumienny, R., Heer, F.T., de Beer, T.A.P., Rempfer, C., Bordoli, L., Lepore, R., Schwede, T., 2018. SWISS-MODEL: homology modelling of protein structures and complexes. *Nucleic Acids Res* 46, W296–W303. https://doi.org/10.1093/nar/gky427

Weaver, B.P., Dufner-Beattie, J., Kambe, T., Andrews, G.K., 2007. Novel zinc-responsive post-transcriptional mechanisms reciprocally regulate expression of the mouse Slc39a4 and Slc39a5 zinc transporters (Zip4 and Zip5). *Biol. Chem.* 388, 1301–1312. https://doi.org/10.1515/BC.2007.149

Whitfield, D.R., Vallortigara, J., Alghamdi, A., Howlett, D., Hortobágyi, T., Johnson, M., Attems, J., Newhouse, S., Ballard, C., Thomas, A.J., O'Brien, J.T., Aarsland, D., Francis, P.T., 2014. Assessment of ZnT3 and PSD95 protein levels in Lewy body dementias and Alzheimer's disease: association with cognitive impairment. *Neurobiology of Aging 35,* 2836–2844. https://doi.org/10.1016/j.neurobiolaging.2014.06.015

Wijesekara, N., Dai, F.F., Hardy, A.B., Giglou, P.R., Bhattacharjee, A., Koshkin, V., Chimienti, F., Gaisano, H.Y., Rutter, G.A., Wheeler, M.B., 2010. Beta cell-specific Znt8 deletion in mice causes marked defects in insulin processing, crystallisation and secretion. *Diabetologia* 53, 1656–1668. https://doi.org/10.1007/s00125-010-1733-9

Yamasaki, S., Sakata-Sogawa, K., Hasegawa, A., Suzuki, T., Kabu, K., Sato, E., Kurosaki, T., Yamashita, S., Tokunaga, M., Nishida, K., Hirano, T., 2007. Zinc is a novel intracellular second messenger. *J. Cell Biol.* 177, 637–645. https://doi.org/10.1083/jcb.200702081

Yamashita, M.M., Wesson, L., Eisenman, G., Eisenberg, D., 1990. Where metal ions bind in proteins. *PNAS* 87, 5648–5652. https://doi.org/10.1073/pnas.87.15.5648

Yang, J., Zhang, Y., Cui, X., Yao, W., Yu, X., Cen, P., Hodges, S.E., Fisher, W.E., Brunicardi, F.C., Chen, C., Yao, Q., Li, M., 2013. Gene profile identifies zinc transporters differentially expressed in normal human organs and human pancreatic cancer. *Curr. Mol. Med.* 13, 401–409.

Yuzbasiyan-Gurkan, V., Grider, A., Nostrant, T., Cousins, R.J., Brewer, G.J., 1992. Treatment of Wilson's disease with zinc: X. Intestinal metallothionein induction. *J Lab Clin Med* 120, 380–386.

Zalewski, P.D., Millard, S.H., Forbes, I.J., Kapaniris, O., Slavotinek, A., Betts, W.H., Ward, A.D., Lincoln, S.F., Mahadevan, I., 1994. Video image analysis of labile zinc in viable pancreatic islet cells using a specific fluorescent probe for zinc. *J. Histochem. Cytochem.* 42, 877–884. https://doi.org/10.1177/42.7.8014471

Zhang, C., Sui, D., Zhang, T., Hu, J., 2020. Molecular Basis of Zinc-Dependent Endocytosis of Human ZIP4 Transceptor. *Cell Reports* 31, 107582. https://doi.org/10.1016/j.celrep.2020.107582

Zhang, T., Kuliyev, E., Sui, D., Hu, J., 2019. The histidine-rich loop in the extracellular domain of ZIP4 binds zinc and plays a role in zinc transport. *Biochem J* 476, 1791–1803. https://doi.org/10.1042/BCJ20190108

Zhang, T., Liu, J., Fellner, M., Zhang, C., Sui, D., Hu, J., 2017. Crystal structures of a ZIP zinc transporter reveal a binuclear metal center in the transport pathway. *Science Advances* 3, e1700344. https://doi.org/10.1126/sciadv.1700344

Zhang, T., Sui, D., Hu, J., 2016. Structural insights of ZIP4 extracellular domain critical for optimal zinc transport. *Nat Commun 7*. https://doi.org/10.1038/ncomms11979

Zhang, T., Sui, D., Zhang, C., Cole, L., Hu, J., 2020. Asymmetric functions of a binuclear metal center within the transport pathway of a human zinc transporter ZIP4. *The FASEB Journal* 34, 237–247. https://doi.org/10.1096/fj.201902043R

Zhao, H., Eide, D., 1996a. The yeast ZRT1 gene encodes the zinc transporter protein of a high-affinity uptake system induced by zinc limitation. *PNAS* 93, 2454–2458. https://doi.org/10.1073/pnas.93.6.2454

Zhao, H., Eide, D., 1996b. The ZRT2 gene encodes the low affinity zinc transporter in Saccharomyces cerevisiae. *J. Biol. Chem.* 271, 23203–23210. https://doi.org/10.1074/jbc.271.38.23203

Zheng, D., Feeney, G.P., Kille, P., Hogstrand, C., 2008. Regulation of ZIP and ZnT zinc transporters in zebrafish gill: zinc repression of ZIP10 transcription by an intronic MRE cluster. *Physiol. Genomics* 34, 205–214. https://doi.org/10.1152/physiolgenomics.90206.2008

Zhong, W., Yang, C., Zhu, L., Huang, Y.-Q., Chen, Y.-F., 2020. Analysis of the relationship between the mutation site of the SLC39A4 gene and acrodermatitis enteropathica by reporting a rare Chinese twin: a case report and review of the literature. *BMC Pediatr* 20, 34. https://doi.org/10.1186/s12887-020-1942-4

Zhou, N.E., Kay, C.M., Hodges, R.S., 1992. Synthetic model proteins. Positional effects of interchain hydrophobic interactions on stability of two-stranded alpha-helical coiled-coils. *J. Biol. Chem.* 267, 2664–2670.